NOVEL METHODS OF CARDIAC RISK ASSESSMENT IN PATIENTS WITH CHRONIC KIDNEY DISEASE AND RENAL TRANSPLANT RECIPIENTS

Dr Ranjit J Shah, FRACP

School of Medicine

Flinders University

Submitted in fulfilment of the requirements of the degree of

Doctor of Philosophy

July 2020

DECLARATION

This work contains no material which has been accepted for the award of any other degree or diploma in any university or other tertiary institution and, to the best of my knowledge and belief, contains no material previously published or written by another person, except where due reference has been made in the text.

I give consent to this copy of my thesis, when deposited in the University Library, being available for loan and photocopying, subject to the provisions of the Copyright Act 1968.

I also give permission for the digital version of my thesis to be made available on the web, via the University's digital research repository, the Library catalogue, the Australasian Digital Theses Program and also through web search engines.

Dr Ranjit Shah

July 2020

TABLE OF CONTENTS

ACKNOWLEDGEMENTS

Over the course of my PhD, I have been fortunate to receive support from many people. I am profoundly grateful to each of these. I must make particular mention of some that have been an integral support over the last 4 years.

Firstly, to my principal supervisor, Prof Joseph Selvanayagam, I extend my sincerest gratitude for his guidance and mentorship. He has been an inspiration, who leads by example and has provided leadership and support over the course of my PhD. Prof Jonathan Gleadle and A/Prof Gaetano Nucifora, who are my co-supervisors, always provided motivation and encouragement. I thank Prof Richard Woodman for being the most wonderful statistic mentor. I thank Dr Susie Parnham for her initial help with understanding of the project when I started my PhD studies. I have been privileged during my thesis to work with Prof Randall Faull and Prof Arduino Mangoni and hope to continue to build relationships with them in the future.

A special mention should be made for Dr Karthigesh Sree Raman and Dr Rebecca Perry who have been great friends and have provided help and support when needed over the course of my PhD. I appreciate their generosity with their time and their encouragement during the last four years. Many thanks to Dr Sara Tommasi for the help with the biochemical analysis of the serum samples.

To my colleagues during my PhD, I am thankful for the experiences I have shared with you, and without your support, this work would not have been possible. I have worked with many individuals but must single out a few. I thank Angela Walls, Craig Bradbrook, Emma Smith, Cherie Raven and Charlotte Wigley for the MRI scanning.

Thank you, Jan Roesler, for helping with the bookings and Zach Liang, for making preliminary phone calls for contacting some of the research participants. Special thanks to Jane McKinnon, Dr Sau Lee, Serene Wong, Hazel Morrison, Tonia Bromley, Jonathon Foote, Madiha Saiedi, and Dr Rajiv Ananthakrishna for their friendship and support.

Lastly, I thank my wife, Dr Sonia Shah, who has provided unwavering support in everything that I have done (and not done), whom I have always found beside me during the tough times in the course of my PhD and without whom this would not have been possible. A very special thanks to my children, Eric and Jessica, who remind me about what is most important in life. And finally, I would like to thank my parents who, since my early days, have always encouraged me to be an independent thinker and have been proud of everything that I have done.

ABSTRACT

Cardiovascular disease is the major cause of death in the chronic kidney disease (CKD) population. Coronary artery disease (CAD) in CKD is often asymptomatic, with multi-vessel ischaemia, and carries a poor prognosis. Although the risk of death is reduced with renal transplantation, cardiovascular disease is still one of the major causes of death post-transplant with mechanisms not well defined.

Despite the high prevalence of CAD, current functional cardiac investigations to assess inducible myocardial ischaemia in CKD population are suboptimal and may lead to significant adverse effects. Multi-modality cardiovascular magnetic resonance (CMR) imaging has emerged as a non-invasive clinical tool to assess cardiomyopathy, infarction and viability and myocardial perfusion, without risk of radiation. Stress CMR potentially detects inducible myocardial ischaemia from both epicardial and microvascular CAD. The use of gadolinium contrast is, however, contraindicated in the CKD population. Using Oxygen-sensitive CMR (OS-CMR) it has previously been shown that CKD patients have reduced myocardial oxygenation response to stress. Furthermore, the reduced OS-CMR signal intensity in the CKD population could be related to the declining renal function.

The aims of this thesis are to 1) to investigate the prognostic utility of OS-CMR imaging and feature tracking CMR (FT-CMR) derived myocardial deformation in asymptomatic CKD patients with and without diabetes mellitus and 2) utilise other novel Gadolinium-free CMR techniques and serum biochemical markers to assess coronary artery disease in the CKD population as a measure of ischaemia.

Chapter 3 shows that the blunted myocardial oxygenation response to stress and abnormal myocardial deformation in patients with CKD without known coronary artery disease is an independent predictor of adverse events.

Chapter 4 examines the diagnostic ability of CMR stress T1 mapping technique to detect coronary artery disease in CKD patients with and without CAD. In this chapter, it is demonstrated that in patients with CKD, stress T1 response is impaired and may be able to differentiate between remote, ischaemic and infarcted segments.

Chapter 5 compares the ability of OS-CMR imaging and Stress CMR T1 mapping in the diagnosis of myocardial ischaemia in patients with CKD. This study shows that in patients with CKD, stress T1 response may be a more accurate method of diagnosing myocardial ischaemia than stress OS-CMR response.

The study in chapter 6 investigates the association between Paraventricular Adipose Tissue (PVAT) and CKD. In this chapter, there was a trend seen for the PVAT volume to be increased in patients with CKD when compared to participants without CKD. However, this increased PVAT volume did not seem to be an independent predictor of adverse events in the small population that was studied.

Chapter 7 demonstrates that there is a significant association between plasma Asymmetric Dimethylarginine (ADMA) and Stress T1 response in CKD patients. However, Δ OS-CMR SI was not significantly associated with circulating ADMA or HMA levels.

The studies in this thesis were done in relatively small number of patients and need to be confirmed with larger, multi-centre studies. Nonetheless these studies do achieve in demonstrating the utility of novel methods of cardiac risk assessment in

the very high-risk group of CKD patients. These studies will also help in further understand the complex pathogenetic mechanisms that lead to the higher CVD risk in CKD patients.

PEER REVIEWED JOURNAL PUBLICATIONS

1. **Shah R**, Raman K, Walls A, Woodman R, Faull R, Gleadle JM, Selvanayagam JB. *Gadolinium Free Cardiovascular Magnetic Resonance (CMR) Stress T1 mapping in patients with Chronic Kidney Disease (CKD).* JACC Cardiovasc. Imaging. 2019 Jun 7. pii: S1936-878X(19)30442-5.

2. **Shah R**, Parnham S, Liang Z, Perry R, Bradbrook C, Smith E, Faull R, Woodman R, Nucifora G, Gleadle JM, Selvanayagam JB. *Prognostic Utility of Oxygen-Sensitive Cardiovascular Magnetic Resonance imaging in Diabetic and Non-Diabetic Chronic Kidney Disease (CKD) Patients with no known coronary artery disease*. JACC Cardiovasc Imaging. 2019 Jun;12(6):1107-1109.

3. **Shah R**, Patil S, Woodman R, Faull R, Gleadle JM, Selvanayagam JB. *Ventricular Pericardial Fat Content in Chronic Kidney Disease Patients.* Manuscript in preparation.

4. **Shah R**, Tommasi S, Faull R, Woodman R, Gleadle JM, Mangoni A, Selvanayagam JB. *Arginine Metabolites as Biomarkers of Myocardial Ischaemia, Assessed with Cardiac Magnetic Resonance Imaging in Chronic Kidney Disease.* Manuscript in preparation.

PEER REVIEWED ABSTRACTS

Oral Presentations

1. **Shah R**, Parnham S, Liang Z, Nucifora G, Sree Raman K, Woodman R, Gleadle GM, Selvanayagam JB. *Prognostic Utility of Blood Oxygen Level Dependent (BOLD) Cardiovascular Magnetic Resonance (CMR) Imaging in Asymptomatic Chronic Kidney Disease (CKD) Patients with and without Diabetes Mellitus*. Presented at CMR 2018, (Barcelona, Spain).

2. Parnham S, **Shah R**, Gleadle J, Ganesan A, Woodman R, De-Pasquale C, Selvanayagam J. *Blood Oxygen Level Dependent (BOLD) Cardiovascular Magnetic Resonance (CMR) as Predictor of Cardiac Prognosis in Asymptomatic Chronic Kidney Disease (CKD) Patients*. Presented at the SCMR 2017, (Washington D.C, USA).

Poster Presentations

1. **Shah R**, Raman K, Walls A, Woodman R, Faull R, Gleadle JM, Selvanayagam JB. *Gadolinium Free Cardiovascular Magnetic Resonance (CMR) Stress T1 mapping in patients with Chronic Kidney Disease (CKD).* Accepted presentation at ESC ASIA with APSC and AFC 2019 (Singapore).

2. **Shah R**, Raman K, Walls A, Woodman R, Faull R, Gleadle JM, Selvanayagam JB. *Gadolinium Free Cardiovascular Magnetic Resonance (CMR) Stress T1 mapping in patients with Chronic Kidney Disease (CKD).* Poster presentation at CSANZ 2019 (Adelaide).

3. **Shah R**, Parnham S, Nucifora G, Liang Z, Sree Raman K, Woodman R, Gleadle GM, Selvanayagam JB. *Prognostic Utility of Blood Oxygen Level Dependent (BOLD) Cardiovascular Magnetic Resonance (CMR) Imaging in Asymptomatic Chronic Kidney Disease (CKD) Patients with and without Diabetes Mellitus.* European Heart Journal, Volume 39, Issue suppl_1, 1 August 2018, ehy563.P3430. Poster Presentation at the ESC 2018 (Munich, Germany).

4. **Shah R**, Parnham R, Parnham S, Nucifora G, Liang Z, Sree Raman K, Woodman R, Gleadle GM, Selvanayagam JB. *Prognostic Utility of Blood Oxygen Level Dependent (BOLD) Cardiovascular Magnetic Resonance (CMR) Imaging in Asymptomatic Chronic Kidney Disease (CKD) Patients with and without Diabetes Mellitus.* Heart, Lung and Circulation, Volume 27, Supplement 2, S266. Poster Presentation at the CSANZ 2018 (Brisbane, Australia).

LIST OF ABBREVIATIONS

1.5 T	1.5 Tesla
3 T	3 Tesla
7 T	7 Tesla
ΔOS-CMR	Change in Oxygen Sensitive Cardiovascular Magnetic Resonance (%)
ΔT1	Change in T1 relaxation time (%)
Ac-ADMA	Acetylated Asymmetric Dimethylarginine
Ac-SDMA	Acetylated Symmetric Dimethylarginine
ACE	Angiotensinogen Converting Enzyme
ADMA	Asymmetric Dimethylarginine
AFD	Anderson-Fabry Disease
AHA	American Heart Association
AMI	Acute Myocardial Infarction
AS	Aortic Stenosis
BMI	Body Mass Index (kg/m)
BOLD	Blood Oxygen Level Dependent
CAD	Coronary Artery Disease
CFR	Coronary Flow Reserve
CKD	Chronic Kidney Disease
c-LDL	Carbamylated Low Density Lipoprotein
CMR	Cardiovascular Magnetic Resonance
CO_2	Carbon Dioxide

CRP	C-Reactive Protein
CVD	Cardiovascular Disease
DCM	Dilated Cardiomyopathy
DDAH-1	Dimethylarginine Dimethylaminohydrolase-1
DDAH-2	Dimethylarginine Dimethylaminohydrolase-2
DM	Diabetes Mellitus
DNA	Deoxyribonucleic Acid
DSE	Dobutamine Stress Echocardiogram
EC	Endothelial Cell
ECG	Electrocardiogram
ECV	Extra-Cellular Volume
eGFR	estimated Glomerular Filtration Rate (mL/min/1.73 m²)
ESE	Exercise Stress Echocardiogram
ESRD	End Stage Renal Disease
EST	Exercise Stress Test
FFR	Fractional Flow Reserve
FT	Feature Tracking
GLS	Global Longitudinal Strain
HCM	Hypertrophic Cardiomyopathy
HD	Haemodialysis
HF	Heart Failure
HMA	Homoarginine
HOCl	Hypochlorous Acid
HT	Hypertension
IL-6	Interleukin-6

LAD	Left Anterior Descending artery
LCx	Left Circumflex artery
LDL	Low Density Lipoprotein
LGE	Late Gadolinium Enhancement
LNMMA	L-N-Monomethyl arginine
LV	Left Ventricle
LVEF	Left Ventricular Ejection Fraction (%)
LVH	Left Ventricular Hypertrophy
LVMi	Left Ventricular Mass Indexed to body surface area (g/ m^2)
MAE	Major Adverse Events
MBF	Myocardial Blood Flow
MBV	Myocardial Blood Volume
MCP-1	Monocyte Chemoattractant Protein-1
mCRP	Monomeric C-Reactive Protein
MD	Mechanical Dispersion (milliseconds)
MI	Myocardial Infarction
MOLLI	Modified Look Locker Inversion Recovery
MPO	Myeloperoxidase
MPS	Myocardial Perfusion Scan
mRNA	Messenger Ribonucleic Acid
NO	Nitric Oxide
NOS	Nitric Oxide Synthetase
NSF	Nephrogenic Systemic Fibrosis
OS-CMR	Oxygen Sensitive Cardiovascular Magnetic Resonance
Ox-LDL	Oxidised Low-Density Lipoprotein

PAI-1	Plasminogen Activator Inhibitor-1
pCRP	Pentameric C-Reactive Protein
PD	Peritoneal Dialysis
PET	Positron Emission Tomography
PRMTs	Protein Methyltransferases
PTH	Parathormone
PVAT	Paraventricular Adipose Tissue
RCA	Right Coronary Artery
RNS	Reactive Nitrogen Species
RRT	Renal Replacement Therapy
RT	Renal Transplant
RVEF	Right Ventricular Ejection Fraction (%)
SDMA	Symmetric Dimethylarginine
ShMOLLI	Shortened Modified Look Locker Inversion Recovery
SI	Signal Intensity
SNR	Signal:Noise Ratio
SSFP	Steady State Free Precession
T1	T1 Relaxation Time (milliseconds)
T2	T2 Relaxation Time (milliseconds)
T2DM	Type 2 Diabetes Mellitus
TNF-∝	Tumour Necrosis Factor - Alpha
TSH	Thyroid Stimulating Hormone
TTC	Tako-Tsubo Cardiomyopathy
VA	Ventricular Arrhythmias
ΔSI	Change in Signal Intensity (%)

CHAPTER 1: INTRODUCTION

With significant medical advancements made in the past few decades the number of patients with severe kidney disease requiring renal replacement therapy (RRT) is rising (1). Cardiovascular disease (CVD) is common in CKD and it is estimated that 25-47% patients with severe CKD have congestive heart failure, ischaemic cardiomyopathy or ventricular hypertrophy (2-4). Coronary artery disease (CAD) is often multi-vessel and causes silent or asymptomatic myocardial ischaemia in CKD patients (5, 6). Chapter 1 explores the challenges of currently available diagnostic tests for assessment of CAD in patients with CKD. Furthermore, some novel methods of assessment of CAD in this very high-risk group of patients are also discussed.

1.1 Clinical Problem

CKD is common in Australia and the number of patients requiring RRT in Australia and New Zealand is rising (Figure 1.1).

Figure 1.1: New Patients on Renal Replacement Therapy – Australia and New Zealand

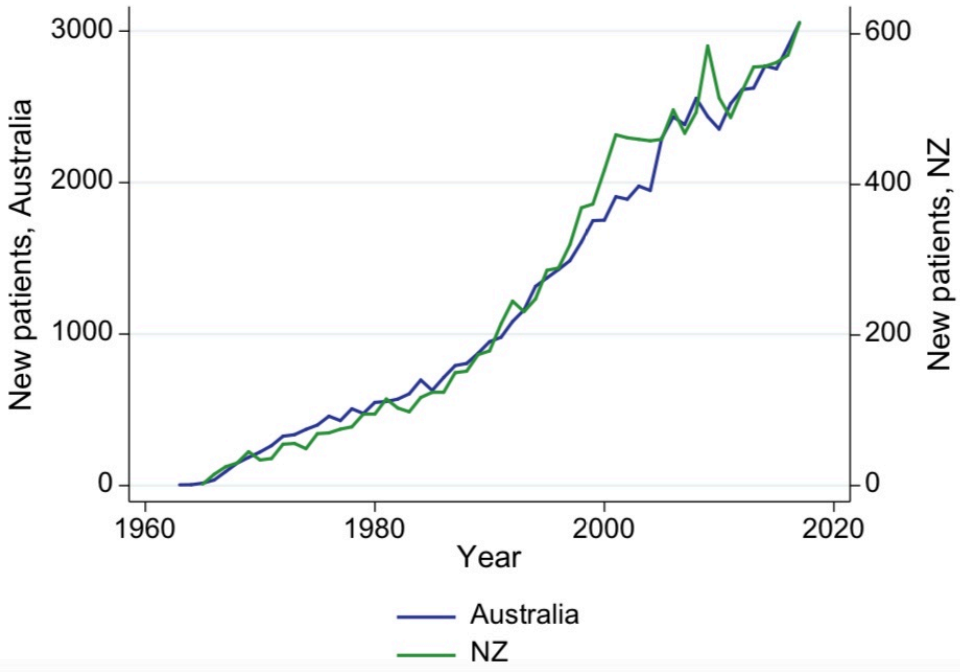

In 2017 there were 3056 new patients on RRT, with an overall incidence rate of 124 per million population CKD is common in Australia (1). This rate has continued a long trend of increasing RRT incidence. In New Zealand there were 615 new patients (128 per million population). The number of prevalent patients in each country also continues to climb; in Australia at the end of 2017 there were 24738 (1006 per million population) patients receiving RRT, and in New Zealand there were 4658 (972 per million population). There were 11,687 functioning renal transplant patients with 1,109 new transplants reported in 2017. There were 2,077 deaths reported in this group of patients in 2017, of which 1,858 were on dialysis and 219 patients were renal transplant recipients. Type 2 diabetes mellitus, glomerulonephritis, hypertension

and polycystic kidney disease accounted for the majority of all new diagnosed cases of ESRD (1).

CVD is the most common cause of mortality and morbidity in people with CKD (7, 8) and is about 10 – 30 times higher in the CKD cohort when compared to the non-CKD population, despite stratification for diabetes (9). The mortality rate of people with CKD worldwide is approximately 20% annually, and CVD accounts for 50% of these deaths (8, 10, 11). Decreasing renal function has been shown to be associated with increased risk of death (7, 12) and increased severity of cardiac disease (13-15). Coronary artery disease is highly prevalent in the CKD population (16) and is present even in early renal disease (13, 17) and in young CKD patients (18).

CKD patients have both traditional and non-traditional cardiac risk factors (Table 1.1).

Table 1.1 Cardiovascular Risk Factors in the Chronic Kidney Disease Population

Traditional Risk Factors	**Non-Traditional Risk Factors**
Diabetes	Left ventricular hypertrophy
Hypertension	Fluid overload
Dyslipidemia	Uraemia
Smoking	Anaemia
Age	Disorders of vitamin D, calcium and phosphate
Family History of Ischaemic Heart Disease	Hyperparathyroidism
	Inflammatory state
	Proteinuria nephrotic state

Painless myocardial ischaemia occurs more commonly in the CKD patients compared to individuals with normal renal function, and is associated with a higher mortality rate in CKD patients (19). Epicardial and/or microvascular coronary disease

is often present in this population (20, 21) and can cause silent or asymptomatic myocardial ischaemia (5, 6). Both microvascular and epicardial coronary diseases are associated with a higher major adverse cardiac event rate (6, 22).

Asymptomatic epicardial CAD has been detected even in people with early stage CKD (23) and is associated with a higher major adverse cardiac event rate compared to those without CAD (6). While the coronary plaque characteristics in patients with CKD showed no difference in the prevalence of high-risk plaque compared to the group without CKD (20), Kawai et al. showed that patients with mild CKD had a higher prevalence of severe epicardial CAD compared to those without CKD, thus, suggesting that the problem relates to coronary stenosis rather than plaque stability.

Ischemia-driven angiogenesis and myocardial capillary supply are clearly reduced in experimental models of uraemia (24, 25). However, relatively few human studies have investigated microvascular function in CKD. Several autopsy studies have demonstrated a reduction in myocardial capillary supply in humans with CKD or end-stage renal disease (26, 27), but the cohorts were small, and the representativeness of individuals undergoing post-mortem examination for the overall CKD population is unclear. Microvascular CAD has been shown to occur early in the CKD population (28). In a study of mild to moderate CKD patients without diabetes or uncontrolled hypertension using positron emission tomography (PET) imaging it was found that the CKD cohort had decreased coronary flow reserve (CFR, defined as the ratio of peak to resting flow) compared to controls (21). Another study utilizing PET imaging found that stages 1-4 CKD were associated with progressive deteriorations in CFR without further changes in stage 5 or dialysis dependant CKD (29). This may suggest that the cause of microvascular dysfunction in CKD patients is associated with CKD

rather than associated with the effects of dialysis. Previous studies that have demonstrated that abnormal myocardial perfusion scintigraphy in CKD patients was associated with higher incidence of cardiac events and mortality (30-36). Furthermore, myocardial perfusion PET derived CFR has been shown to be strongly associated with cardiovascular risk regardless of CKD severity (29). The prevalence of microvascular coronary artery dysfunction in the asymptomatic CKD patients and its association with adverse events has not been studied.

The prevalence of left ventricular hypertrophy (LVH) in the CKD population is 75% (37) and increases with progressive decline of renal function (38). It may contribute to ischaemia due to microvascular disease and has been shown to be an independent predictor of survival and cardiovascular events in dialysis patients (39).

Although renal transplantation significantly improves survival, CVD is still one of the most frequent causes of death post-transplant and accounts for 35-50% of all-cause mortality (Figure 1.2) (40). It is the most frequent cause of death in renal transplant recipients worldwide (40). The annual risk of CVD event in renal transplant recipients is 3.5 to 5%, which is 50 times higher than the general population (41).

Figure 1.2: Mortality while on Renal Replacement Therapy – Australia 2007-2016

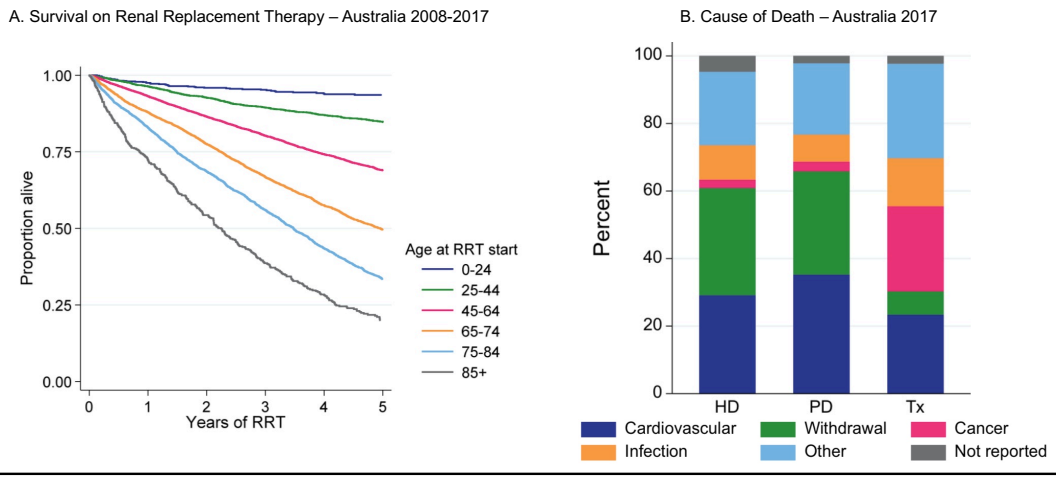

In Australia malignancy has surpassed CVD as the leading cause of mortality in the post renal transplant populations (42). The age of ESRD patients undergoing transplantation is increasing and may partly account for CVD mortality (43).

The mechanism of CVD in renal transplant population is not well defined. Nanmoku et al. studied 64 people in the “Elderly Group” with mean age 63.2 ± 3.4 years and 500 people in the “Young Group” with mean age 37.4 ± 13.5 years and showed that the main cause of graft loss in the “Elderly Group” was sudden death with a functioning graft due to heart failure (43). There is a suggestion that both ischaemic heart disease and congestive heart failure occur in the first few years post renal transplant (44).Another study, however, found ventricular arrhythmia had a high prevalence in the first few months post renal transplant (45). The presence of coronary artery calcification was shown to be a risk factor for arrhythmia in this study.

In addition to the traditional cardiac risk factors, renal transplant recipients have additional risk factors related to the immunosuppressive therapy. Prednisolone is well known to be atherogenic and increases the risk of developing diabetes mellitus, obesity, hypertension and hypercholesterolaemia (46). Mycophenolate is associated with bone marrow suppression and diarrhoea (47), thus may cause anaemia and electrolytes imbalance, which may contribute to myocardial ischaemia, increased risk of arrhythmia and cardiac failure (48). Cyclosporine is associated with development of post-transplant hypercholesterolaemia and diabetes mellitus (49). It also causes nephrotoxicity and vasoconstriction of the renal afferent arteriole (50, 51) and may also cause coronary vasospasm. The administration of calcium channel blocker can prevent the arteriolar vasoconstriction (52). Post renal transplant LVH in the absence of hypertension was shown to be cyclosporine-related (53). Although it is preferred to

cyclosporine (54-58), tacrolimus is associated with post-transplant hypercholesterolaemia and diabetes mellitus (59), which increases the risk of developing CAD. Marked LVH has been reported in children on tacrolimus (60). Sirolimus use is associated with lower risk of post-transplant malignancy (61-63) and nephrotoxicity compared to calcineurin inhibitors (64), thus may be associated with less CVD post transplantation. Everolimus is also an mTOR inhibitor (65) with similar side effects to sirolimus (66).

1.2 Non-invasive Methods of Assessment of Coronary Artery Disease: Strategies and Current Evidence

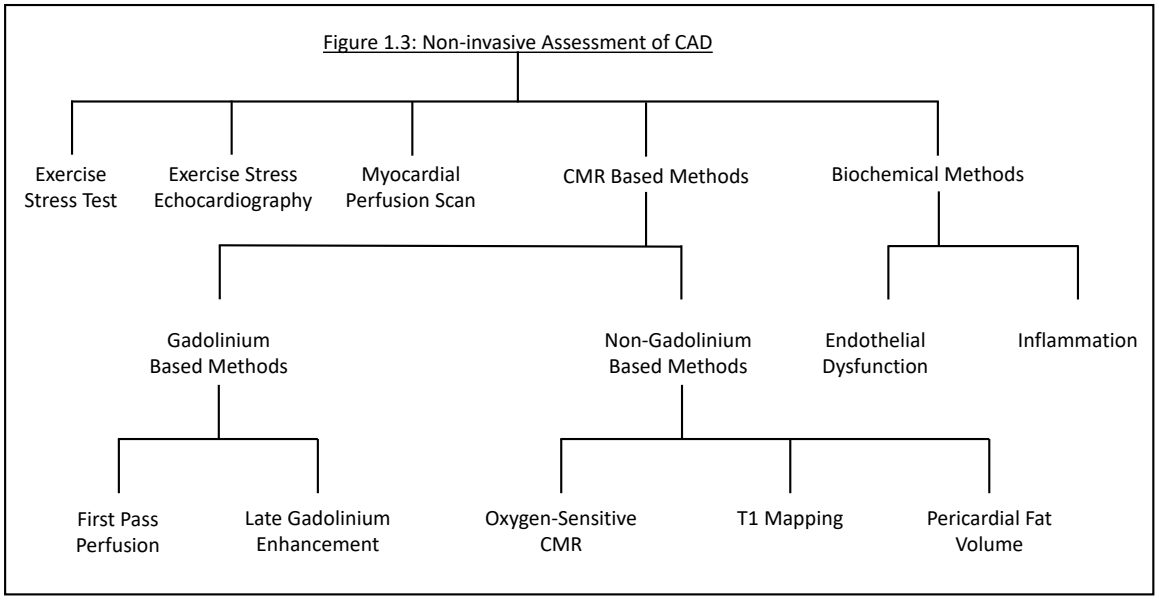

1.2.1 Exercise Stress ECG

In patients with normal renal function, exercise stress test (EST) with ECG has a low to moderate sensitivity and specificity, 68 ± 16 % and 77 ± 17 % respectively, even when adequate exercise capacity and 85% heart rate is achieved (67). EST is further limited in the advanced CKD population with poor sensitivity of 36% (68) (especially

those undergoing dialysis), as deconditioning leads to reduced exercise capacity (69). Deconditioning can be due to vascular, neurological or musculoskeletal comorbidities and the catabolic/cachectic metabolic state associated with CKD. CKD patients have also been shown to have impaired heart rate response to exercise (70), and the frequently abnormal baseline ECG in CKD patients (often secondary to hypertension) hampers the interpretation of standard stress testing.

1.2.2 Exercise/Dobutamine Stress Echocardiography

Exercise stress echocardiography (ESE) has a sensitivity ranging between 71% and 97% and a specificity ranging between 64% and 90% (71). It is better than the standard stress ECG in ruling in CAD (Positive likelihood ratio ESE 7.94 versus EST 3.57) and ruling out CAD (Negative likelihood ratio ESE 0.19 versus EST 0.38) (72). The accuracy of ESE in CKD population is reduced due to the same reasons as mentioned for EST above. Furthermore, as this technique detects inducible myocardial ischaemia based on detection of wall motion abnormalities, it does not detect minor epicardial CAD or microvascular disease.

A systematic review in of 11 Dobutamine Stress Echocardiogram (DSE) studies with 690 potential renal transplant recipients found that DSE had a moderate sensitivity of 80% (confidence interval 64-90) in detecting inducible myocardial ischaemia in renal transplant candidates (73). Most patients with advanced CKD have a blunted chronotropic response, and thus do not achieve 85% maximal predicted heart rate despite the use of atropine (74). Furthermore, in LVH the thick myocardium and small intracavitary volume obscures the detection of wall motion abnormalities at stress.

Abnormal DSE results in CKD patients have been associated with poorer prognosis for cardiac events and overall mortality (68, 75-77). Negative stress

echocardiography results, on the other hand, have been shown to be associated with low incidence of major adverse cardiac events (74).

Blunted chronotropic response with exercise in CKD population may relate to poorer overall cardiac prognosis. A 2012 meta-analysis of 11,542 patients showed that submaximal age-predicted heart rate (<85% maximum heart rate) in the setting of normal ESE and DSE had higher cardiovascular risk than those who achieved >85% maximal predicted heart rate (78).

1.2.3 Myocardial Perfusion Scintigraphy (MPS)

Exercise and pharmacological MPS have sensitivity of 87% and 89%, and specificity of 73% and 75%, respectively, in detecting >50% coronary artery stenosis in patients without advanced CKD (79). Exercise Myocardial Perfusion Scintigraphy (MPS) in the advanced CKD population has the same limitation as EST and ESE, i.e. related to the inadequate exercise performance and chronotropic incompetence (80). MPS radiation may increase the risk of malignancy in the renal transplant population who is already at high risk of cancer.

A systematic review in 2011 showed that MPS has a sensitivity of 69% (confidence interval 48-85) and specificity of 77% (confidence interval 59-89) in diagnosing inducible myocardial ischaemia in the pre-renal transplant population (73). MPS has high false negative result in detecting ischaemia in people with significant triple vessel CAD, as in the CKD population, because of homogeneous tracer uptake due to ‘balanced ischaemia’ (81, 82).

Normal myocardial perfusion measured by single-photon emission computed tomography (SPECT) may not be associated with excellent prognosis in CKD

population unlike the normal population (83, 84), perhaps due to the high false negative result from balanced ischaemia. A recent systematic review in 2015 showed that although functional cardiac stress investigations were as good as coronary angiography in predicting major adverse cardiac events, a substantial number of potential kidney transplant recipients with negative results still experienced adverse cardiac events (85). Hakeem et al. showed that patients with CKD with normal MPS still had a three times higher cardiac death rate than those with normal MPS and no CKD (84). In addition, concurrent reduced coronary flow reserve and left ventricular hypertrophy may play a role. Fukushima et al. reported CKD patients with normal clinical myocardial perfusion by PET scan had reduced global myocardial flow reserve, which implied an underlying microvascular dysfunction in this population (86) that could explain the poorer prognosis. Increased baseline myocardial blood flow and peripheral endothelial dysfunction in CKD patients have been suggested by Koivuviita et al. (87).

Nonetheless, abnormal MPS results in CKD patients have been shown to be associated with higher incidence of cardiac events and mortality (30-36). A meta-analysis of 12 studies of pre-renal transplant patients showed that the presence of reversible defects of inducible myocardial ischaemia was associated with sixfold increased risk of myocardial infarction and almost fourfold risk of cardiac death (88). In this study, the presence of fixed defects was associated with a nearly fivefold increased risk of cardiac death. Joki et al. suggested that myocardial perfusion abnormalities significantly predicted cardiac events in CKD patients independently of eGFR and left ventricular ejection fraction (30). Among 2967 patients with CKD, the incidence of major adverse cardiac events at one year was 1.0%, 3.9%, 5.9%, and 7.3% for normal, mild, moderate, and severe summed stress score, respectively (32).

Al-Mallah et al. demonstrated an interaction between renal function and the magnitude of perfusion deficit assessed by stress MPS in patients with moderate and severe CKD in the presence of abnormal MPS (34).

Blunted heart rate response in CKD patients during stress myocardial perfusion imaging has been reported to be associated with increased mortality (89-91).

1.2.4 Cardiovascular Magnetic Resonance (CMR)

1.2.4.1 Gadolinium Based Method of Assessment of Myocardial Ischaemia

1.2.4.1.1 First Pass Perfusion

Stress perfusion CMR provides comprehensive assessment of inducible myocardial ischaemia with high spatial resolution. During adenosine pharmacological vasodilatation, myocardial areas supplied by normal coronary arteries show a three- to five-fold increase of blood flow, whereas no or minimal change is found downstream of severely diseased arteries because arteriolar beds are already maximally vasodilated (92, 93). Such areas therefore show lower peak enhancement with delayed uptake of the contrast, and thus appear dark (or hypointense) compared to the adjacent normal myocardium (93). Stress perfusion CMR has high spatial resolution (< 3 mm) allowing the identification of very small perfusion defects in sub-endocardium (94). Because of its high resolution and lack of ionising radiation, it has increasingly become a very attractive non-invasive cardiac imaging modality for people with suspected myocardial ischaemia, especially those with poor echocardiographic windows.

Stress perfusion CMR is highly sensitive for detection of CAD with moderate specificity. Two meta-analyses have analysed the diagnostic performance of stress perfusion CMR. A meta-analysis in 2010 demonstrated a stress CMR sensitivity of 89% (95% CI: 88-91%), and a specificity of 80% (95% CI: 78-83%) (95). Adenosine stress perfusion CMR had better sensitivity than with dipyridamole (90% (88-92%) versus 86% (80-90%), p= 0.022), and a tendency to a better specificity (81% (78-84%) versus 77% (71-82%), p= 0.065) (95). An earlier meta-analysis in 2007 with 14 datasets (754 patients) using stress-induced wall motion abnormalities imaging and 24 dataset (1,516 patients) using perfusion imaging demonstrated a sensitivity of 83% (95% confidence interval 79-88%) and specificity of 86% (95% confidence interval 0.81 to 0.91) with disease prevalence of 71% and sensitivity of 91% and specificity of 81% with lower disease prevalence of 57% (96). Thus, stress perfusion CMR is highly sensitive for detection of CAD but its specificity remains moderate.

1.2.4.1.2 Assessment of Myocardial Infarction/Replacement Fibrosis

Late gadolinium enhancement (LGE) CMR administers relatively inert extracellular gadolinium T1 contrast during gradient-echo inversion recovery imaging (97). To optimise the contrast between gadolinium-enhanced infarcted myocardium and normal tissue, an inversion-recovery sequence is used (98). An inversion time is chosen at the zero (null) point for normal myocardium, which appears black due to low signal. The infarcted or fibrotic tissue appears bright (hyperenhanced) because of reduced clearance and increased volume of distribution of gadolinium (99).

LGE CMR is useful in detecting myocardial infarction and viability and to distinguish ischaemic from non-ischaemic cardiomyopathy. LGE is a transmural or a subendocardial pattern in myocardial infarction, due to the course of the coronary

arteries from the epicardium to the endocardium (100). LGE CMR has a high specificity 98% for the detection of myocardial infarction (101). The infarct size determined on CMR LGE in animal models was highly correlated with histopathology (102).

The presence of myocardial fibrosis detected by late gadolinium hyperenhancement (LGE) has been shown to correlate with prognosis. A recent meta-analysis (103) showed that LGE was strongly associated with all-cause mortality HR 2.96 (95%CI: 2.37-3.70, p<0.001), cardiovascular mortality HR 3.27 (95% CI: 2.05-5.22, p< 0.001), ventricular arrhythmia and sudden cardiac death HR 3.76 (95% CI: 3.14-4.52, p< 0.001), and major adverse cardiovascular events HR 3.24 (95% CI: 2.32-4.52, p< 0.001). In subgroup analyses, LGE was associated with all-cause mortality and cardiovascular mortality in both LVEF ≤ 35% and LVEF N 35% patients (p< 0.001 all endpoints), as well as in nonischemic and ischemic cardiomyopathy.

LGE CMR utility is limited in advanced CKD patients due to potential risk of NSF as outlined above, which manifests as hardening of skin and internal organs resembling scleroderma which is potentially fatal. The incidence of NSF in people with normal renal function is zero and in CKD patients ranging from 0.26% to 8.8% (104, 105). There has been no proven therapy for NSF. American College of Radiology 2015 recommended gadolinium precautions in patients with eGFR <40 mL/min/1.73 m^2. An in vitro experiment by Bose, et al. in CKD mice suggested a possible iron chelator deferiprone in preventing NSF (106).

1.2.4.2 Gadolinium-Free Methods of Assessment of Myocardial Ischaemia

1.2.4.2.1 Oxygen-Sensitive CMR (OS-CMR)

Coronary artery stenosis initially leads to a mismatch between myocardial oxygen demand and supply, particularly during stress. This in turn leads to post-stenotic capillary recruitment and elevated levels of de-oxyhaemoglobin in these vessels. OS-CMR, also known as Blood Oxygen Level Dependent (BOLD) CMR, differentiates areas containing high levels of de-oxyhaemoglobin from remote normal myocardium, and therefore is able to demonstrate myocardium subtended by coronary artery stenoses. T2/T2* signal is lower from tissue with a high de-oxyhaemoglobin content. And the reason why OS-CMR is particularly useful in coronary disease is that these changes in oxygenation occur very early in the so-called ischaemic cascade, much earlier than the patient gets chest pain or ECG changes (Figure 1.4). Furthermore, direct quantification of cardiac tissue de-oxygenation is possible, which may be a superior parameter for myocardial ischaemia.

Figure 1.4: The Ischaemic Cascade: Progressive myocardial oxygen supply–demand mismatch leads to a sequence of events, starting with myocardial perfusion abnormalities and followed sequentially by metabolic alterations, wall motion abnormalities, ECG changes, and angina.

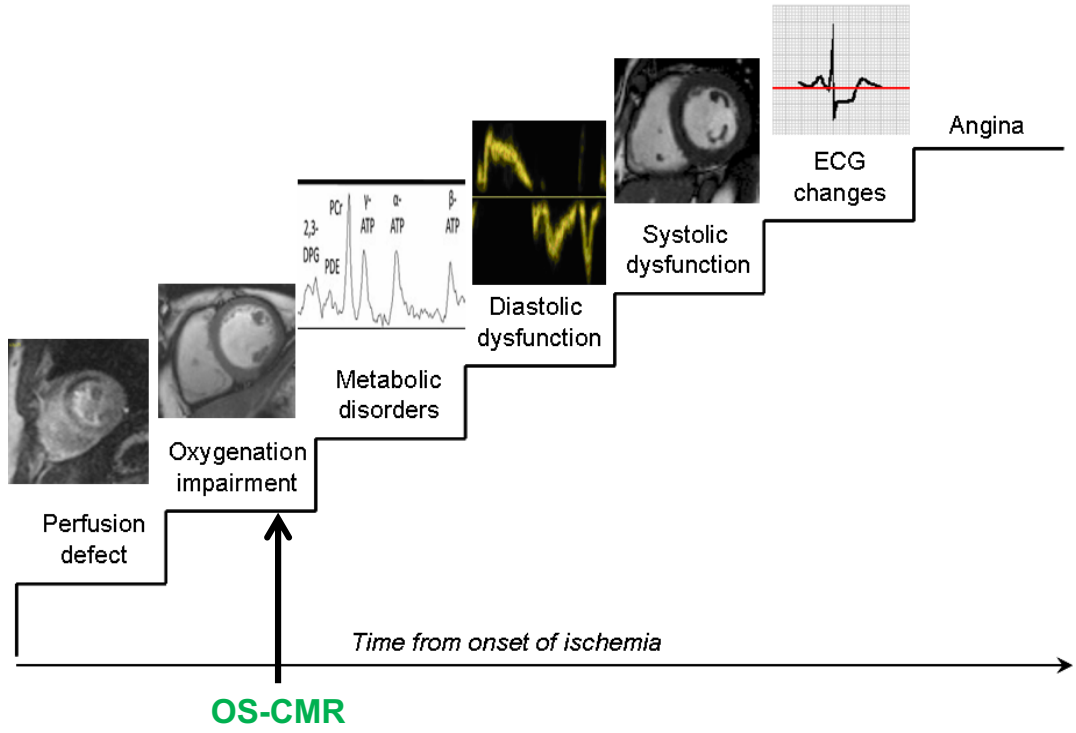

OS-CMR has been validated in human and animal models with promising results (107-117). OS-CMR has been utilised in several human studies to assess myocardial oxygenation as a measure of ischaemia with promising benefits (107, 108, 118-122), namely in syndrome X, hypertensive patients, patients with CAD, hypertrophic cardiomyopathy and aortic stenosis. It detects both epicardial and microvascular CAD without the use of potentially toxic contrast. OS-CMR accuracy in detecting significant CAD has been evaluated, overall with moderately good sensitivity and specificity.

Figure 1.5: The interplay between coronary microvasculature, dipyridamole and the OS-CMR effect. A, Under rest conditions on a fraction of capillaries are open. B, The effect of dipyridamole which is by increasing coronary dilatation hence recruiting the dormant coronary capillaries. C, in stenotic conditions the autoregulatory mechanisms causes relaxation of the capillaries to maintain adequate perfusion at rest. D, As such there are not further coronary vasodilation when dipyridamole is used. Modified from Wacker et al (121).

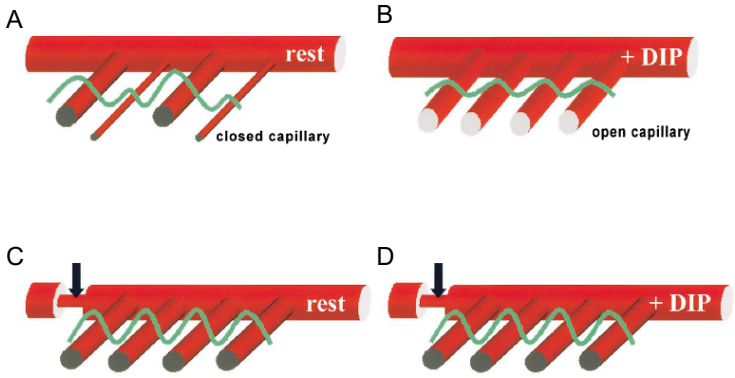

The first OS-CMR study in coronary artery disease was by Wacker et al. 1999 (123), at the time using T2* measurements using a segmented gradient echo pulse sequence with ten echoes under pharmacological stress with dipyridamole. Later, in 2003, they concluded that in regions associated with the stenotic artery, T2* was significantly lower than in residual myocardium ($p < 0.01$) (120). Friedrich et al. 2003 studied 25 patients with stress-induced angina using OS-CMR T2*- sensitive echo planar imaging sequence before and during adenosine in a single-slice approach, comparing with quantitative angiography and adenosine thallium SPECT (121). They observed that a mean signal intensity decrease during adenosine was related to coronary stenoses >75%. According to this study, the OS-CMR signal intensity increase cut-off value of 1.2% had a sensitivity of 88% and a specificity of 47% to correctly classify severe stenoses. However, all these studies were undertaken using 1.5T, which is fundamentally limited by the relatively small difference in T2* between normal and de-oxygenated myocardial regions (43 ± 21%).

At 3T, the blood and extra-vascular tissue T2* is much more sensitive to differences in oxygenation levels, consequently increasing the contrast compared to 1.5T. This boost in contrast is accompanied by an increased SNR at 3T, which makes cardiac OS-CMR imaging considerably more robust. The first study at 3T validating the OS-CMR technique against PET in patients with known single or double vessel coronary disease was reported in 2010 (119). This showed regional myocardial perfusion and oxygenation are dissociated in a significant proportion of patients, indicating that in patients with CAD reduced perfusion does not always lead to deoxygenation.

Manka et al. 2010 studied 46 patients (34 men; age 65 ± 9 years) with suspected or known coronary artery disease who underwent adenosine OS-CMR at 3T prior to clinically indicated invasive coronary angiography (124). Significant stenosis was defined as a coronary artery with ≧50% luminal narrowing. Coronary angiography demonstrated significant CAD in 23 patients. OS-CMR at rest revealed significantly lower T2* values for ischaemic segments (26.7 ± 11.6 ms) compared to normal (31.9 ±11.9 ms; $p < 0.0001$) and non-ischaemic segments (31.2 ± 12.2 ms; $p = 0.0003$) [133]. Under adenosine stress T2* values increased significantly in normal segments only (37.2 ± 14.7 ms; $p < 0.0001$). This study was confirmed by a prospective study by Arnold, et al. 2012 comparing quantitative OS-CMR to coronary angiography, in which a significant CAD was defined as the presence of at least 1 stenosis of ≧50% diameter in any of the main epicardial coronary arteries or their branches with a diameter of ≧ 2 mm (125). OS-CMR has an accuracy of 84%, a sensitivity of 92% and a specificity of 72%. Their study also suggested that hypertension increased the likelihood of abnormal OS-CMR response, however not diabetes mellitus, hypercholesterolaemia or myocardial scarring.

Figure 1.6 Demonstration of non-linear BOLD signal intensity change in response to hyperemic myocardial blood flow (MBF). Modified from Arnold et al (123)

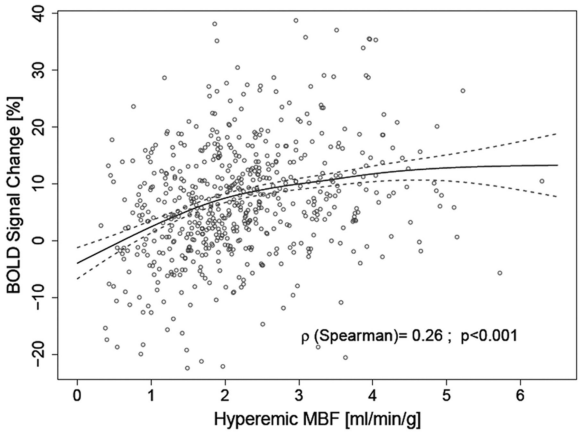

Walcher et al. 2012 further researched the diagnostic accuracy of OS-CMR compared to invasive FFR, current gold standard for measuring haemodynamically significant coronary artery lesion (126). They scanned 36 patients at 1.5T and performed FFR in all patients. An FFR ≦0.8 was regarded to indicate a significant coronary lesion. They found that relative OS-CMR signal intensity increase was significantly lower in myocardial segments supplied by coronary arteries with an FFR ≦0.8 compared with segments with an FFR >0.8 (1.1 ± 0.2 versus 1.5 ± 0.2; p<0.0001) [135]. The OS-CMR sensitivity and specificity compared to FFR ≦0.8 were 88.2% and 89.5%, respectively (126).

It is recognised that the interplay between myocardial ischaemia, perfusion, and oxygenation in the setting of CAD is complex and that myocardial oxygenation and perfusion may become dissociated. McCommis et al. 2010 compared CMR and PET imaging at rest and during dipyridamole vasodilation or dobutamine stress in canines to induce a wide range of changes in cardiac perfusion and oxygenation (112). CMR first-pass perfusion imaging was performed to quantify myocardial blood flow and volume and OS-CMR technique was used to determine the myocardial oxygen

extraction fraction during pharmacological hyperaemia. (15)O-water and (11)C-acetate were used to measure myocardial blood flow and myocardial oxygen consumption, respectively, by PET. They found that CMR results correlated with PET values for myocardial blood flow (r^2=0.79, p<0.001), myocardial oxygen consumption (r^2=0.74, p<0.001), and oxygen extraction fraction (r^2=0.66, p<0.01) (112). The Karamitsos et al. study referred to above found that 40% of myocardial segments with stress myocardial blood flow below the cut-off of 2.45 mL/min/g did not show deoxygenation (119). It is tempting to speculate that the normal oxygenation measurements seen in these segments with impaired perfusion indicate the absence of true ischaemia in these territories despite reduced regional blood flow. Arnold et al. studied the correlation between adenosine stress perfusion CMR and adenosine OS-CMR and also confirmed that oxygenation and perfusion were not strongly correlated (r= -0.26) (125).

A recent study assessed the utility of OS-CMR in advanced CKD patients with no known cardiac disease when compared to healthy and hypertensive controls **(127)**. Fifty-three subjects (23 subjects with CKD, 10 Renal Transplant (RT) recipients, 10 hypertensive (HT) controls, and 10 normal controls without known coronary artery disease) underwent CMR scanning. All groups had cine and OS-CMR at 3 T. The RT and HT groups also had late gadolinium CMR to assess infarction/replacement fibrosis. The CKD group underwent 2-dimensional echocardiography strain analysis as surrogate for interstitial fibrosis. Myocardial oxygenation was measured at rest and under stress with adenosine (140 μg/kg per minute) using OS-CMR signal intensity. Diabetes mellitus and hypertension were similar between CKD, RT, and HT groups. The mean OS-CMR signal intensity change was significantly lower in the CKD and RT groups compared to HT controls and normal controls (-0.89 ± 10.63% in CKD

versus 5.66 ± 7.87% in RT versus 15.54 ± 9.58% in HT controls versus 16.19 ± 11.11% in normal controls, $p < 0.001$) (Figure 1.7A). Further, the impairment in the stress OS-CMR signal is associated with the degree of renal dysfunction (Figure 1.7B). Left ventricular mass index and left ventricular septal wall diameter were similar between the CKD pre-dialysis, RT, and HT groups. None of the CKD patients had impaired global longitudinal strain and none of the RT group had late gadolinium hyperenhancement.

Figure 1.7: A, Myocardial oxygen response to stress in CKD (dialysis and pre-dialysis), renal transplant, hypertensive and normal volunteers. B, Association between myocardial oxygenation and eGFR. Modified from Parnham et al (125)

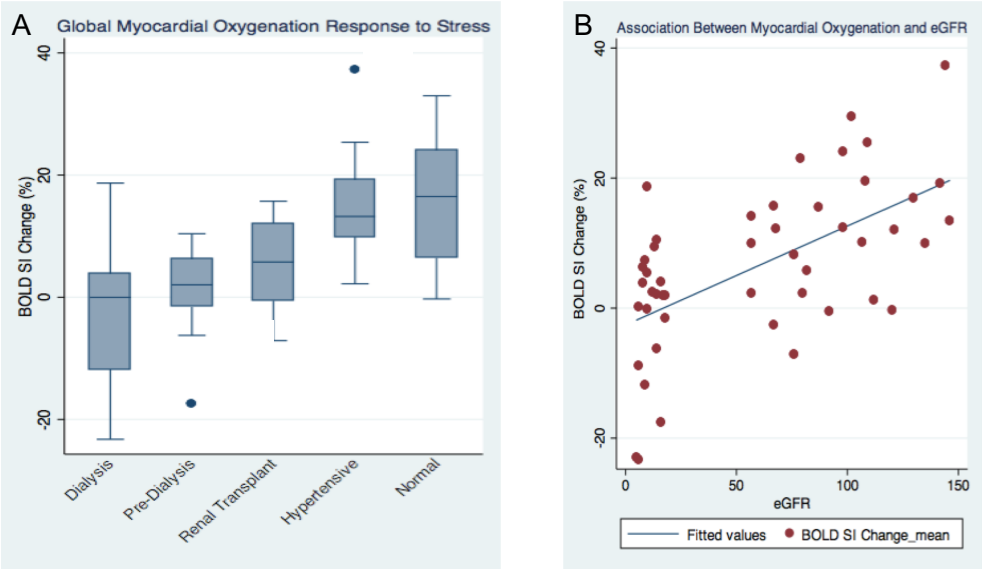

OS-CMR images have several limitations, namely, low signal to noise ratio (SNR), long acquisition times and off resonance artefacts that may mimic deoxygenation even at 3T (125). Even higher field strength (7T) magnets with corresponding increases in SNR will overcome these problems but clinical availability is likely to be limited. Novel means of coronary vasodilation, including CO_2 retention rather than IV Adenosine also offers promise.

In conclusion, OS-CMR potentially offers an attractive option for non-invasive ischaemia detection, given it does not use exogenous contrast, making it especially useful in cases where Gadolinium chelates are contraindicated (e.g. advanced CKD and ESRD). However, at present, only one (mid-ventricular) slice can be interrogated, limiting its sensitivity. It is hence unlikely to replace first pass perfusion as the preferred CMR method for ischaemia assessment in most patients, unless improvements in signal-noise can be made. OS-CMR nevertheless adds value in providing new insights into states of myocardial hibernation, hypertrophy, and diseases of the coronary macro- and micro-vasculature. A greater pathophysiological understanding of the underlying disease processes might enable the development of new therapies aimed at symptom relief and reducing disease progression.

1.2.4.2.2 Stress/Rest T1 Mapping

T1 relaxation time, spin-lattice relaxation time, or simply T1, describes the exponential recovery of the longitudinal component of magnetization back towards its thermal equilibrium. T1 is prolonged by increased water content and, importantly, depends on blood T1 through its partial volume. The measured T1 is determined by intrinsic tissue properties, and the extrinsic environment, including surrounding structure and milieu, as well as software and hardware used to measure T1. Each tissue type, such as myocardium, has a specific range of normal T1 values, deviation from which is indicative of disease.

In vivo mapping of the myocardial T1 relaxation time has recently attained wide clinical validation of its potential utility. Its values are characteristically increased and decreased in certain myocardial diseases.

Table 1.2 Causes of increased and reduced T1 values	
Increased T1 values	**Decreased T1 values**
Increased myocardial water content – AMI, TTC, oedema, myocarditis	Lipid deposition – AFD
Increased fibrosis and ECV – DCM, HCM, AS	Iron deposition – Cardiac siderosis
HCM, AS Protein deposition – Amyloid	

By measuring and displaying T1 relaxation times pixel by pixel, native T1 mapping provides a quantitative biomarker of intracellular and extracellular environments of the myocardium without the need for intravenous contrast agents. Common T1 mapping sequences used for cardiac T1 mapping are inversion recovery techniques (128-131), saturation recovery techniques (132), and mixed hybrid approaches (133).

The general design of T1 mapping sequences includes delivery of a pre-pulse and acquisition of multiple T1-weighted images to allow fitting of these signals to an exponential recovery curve. Modified Look-Locker inversion recovery (MOLLI) uses electrocardiographic (ECG) gating to target a designated phase of the cardiac cycle, and then repeating the inversion experiments after a carefully optimized delay time to obtain adequate information to fit a single exponential T1 recovery curve over 17-heartbeat-long breathold. The shortened modified Look-Locker inversion recovery (ShMOLLI) is similar to MOLLI but can acquire information over a shortened 9 breathold sequence as is heart rate independent.

T1 mapping is highly reproducible with tight normal ranges **(129, 134)**, capable of diagnosing a variety of cardiac diseases **(129, 135-141)**. Local validation should be performed as T1 values are sensitive to hardware and software used.

Myocardial Blood Volume (MBV) is composed of intramyocardial vessels ≤200 microns (90% are capillaries), i.e., capacitance vessels in both micro and macro circulation. Myocardial blood volume (MBV) constitutes ~10% of the total myocardial volume at rest (142) and may increase two-fold during coronary vasodilatory stress (111, 143). MBV may relate better to cardiomyocyte metabolism by reflecting changes in myocardial oxygen consumption, which is a more reliable marker of cellular ischemia. Therefore, stress/rest MBV determination may be a more complete assessment of ischemia than MBF (via perfusion imaging) alone.

Increased myocardial T1 values act as a surrogate for increased myocardial water; hence coronary vasodilatation, which increases MBV, is expected to prolong T1 and allow detection of microvascular and myocardial blood volume changes during ischemia. In chronic coronary artery disease (CAD), accurate detection of ischemia is important because targeted revascularization improves clinical outcomes. T1 mapping using cardiac magnetic resonance (CMR) is highly sensitive to changes in myocardial water content, including MBV.

In healthy individuals with normal myocardium and coronary arteries, there is significant coronary vasodilatory reserve, which can be interrogated by administration of adenosine vasodilatory stress **(92)**. Since native blood T1 is much longer than native myocardial T1, blood T1 is expected to increase the measured myocardial T1 through its partial volume effects **(134)**. This has been shown in normal volunteers who exhibit a 6% increase in myocardial T1 with narrow normal ranges during adenosine vasodilator stress, using the heart rate-independent ShMOLLI method (6.2 ± 0.5% at 1.5 T; 6.3 ± 1.1% at 3 T).

Recent studies have shown that T1 mapping, when used with a vasodilator stress, can distinguish between normal, ischaemic, infarcted and remote myocardium without the need for gadolinium contrast agents **(144)**.

Figure 1.8: (A) During adenosine stress, T1 increased significantly in normal and remote myocardial segments, whereas this was relatively unchanged in ischemic and infarcted segments. (B) T1 reactivity (δT1) was significantly lower in the remote myocardial segments compared with normal segments and was completely abolished in ischemic and infarcted myocardial segments. Modified from Liu et al (143)
All data indicate mean ± 1 SD. *p < 0.05.

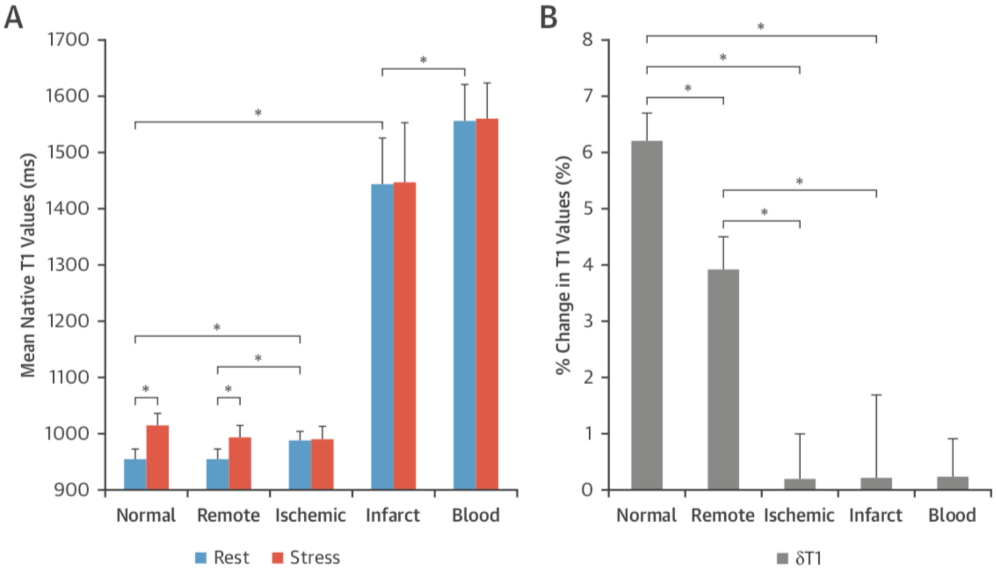

Normal myocardium in controls (normal wall motion, MPRI, no LGE) showed normal resting T1 (954 ± 19 ms at 1.5-T; 1,189 ± 34 ms at 3.0-T) and significant positive T1 reactivity during adenosine stress compared to baseline (6.2 ± 0.5% at 1.5-T; 6.3 ± 1.1% at 3.0-T; all $p < 0.0001$). Infarcted myocardium showed the highest resting T1 of all tissue classes (1,442 ± 84 ms), without significant T1 reactivity (0.2 ± 1.5%). Ischemic myocardium showed elevated resting T1 compared to normal (987 ± 17 ms; $p < 0.001$) without significant T1 reactivity (0.2 ± 0.8%). Remote myocardium, although having comparable resting T1 to normal (955 ± 17 ms; $p = 0.92$), showed blunted T1 reactivity (3.9 ± 0.6%; $p < 0.001$).

This method has subsequently been validated against invasive coronary measures for the accurate detection and differentiation between epicardial coronary artery disease and microvascular dysfunction **(145)**. Myocardium downstream of nonobstructive coronary arteries with microvascular dysfunction showed less-blunted T1 reactivity (ΔT1 = 3.0 $\pm$ 0.9%). A ΔT1 of 1.5% accurately detected obstructive CAD (sensitivity: 93%; specificity: 95%; $p < 0.001$), whereas a less-blunted ΔT1 of 4.0% accurately detected microvascular dysfunction (area under the receiver-operating characteristic curve: 0.95 $\pm$ 0.03; sensitivity: 94%; specificity: 94%: $p < 0.001$).

Stress and rest T1 mapping is a novel technique with potential to assess ischaemia, coronary vasodilatory reserve, and the health of the micro-coronary circulation, without the need for Gadolinium based contrast agents. This technique may also be of specific use in the chronic kidney disease population where both epicardial coronary artery disease and microvascular dysfunction are common and use of gadolinium-based contrast agents is not preferred.

1.2.4.2.3 Periventricular Fat Volume Assessment

Cardiovascular disease is the largest cause of death in the world, and coronary artery disease (CAD) makes up the greatest proportion of those deaths. Excess adiposity has been associated with increased cardiovascular risk (146). Possible mechanisms include alterations in body weight homeostasis, insulin resistance, lipids, blood pressure, coagulation, fibrinolysis and inflammation, leading to endothelial dysfunction and atherosclerosis (147).

More important than the total amount of adipose tissue is the location of adipose tissue. There is general agreement that central (trunk and abdomen), as opposed to

peripheral (hips and thighs) adipose tissue confers the most cardio-metabolic risk and therefore waist-to-hip ratio is a better predictor of cardiovascular disease than Body Mass Index (BMI) **(148-150)**. However, this measurement of general obesity is not always associated with increased cardiovascular risk **(151)** as some people with abnormal waist-to-hip ratio may have a low cardiovascular risk and vice versa. Therefore, a regional fat content with a more accurate risk prediction capability is warranted.

Epicardial fat is the adipose tissue that directly surrounds the heart (between the myocardium and visceral layer of pericardium) and is in direct contact with the coronary vasculature. Pericardial fat is located on the external surface of the parietal pericardium. Although close in proximity, these two fat depots are very different. Epicardial fat is brown fat and develops from splanchnopleuric mesoderm and gets its blood supply from the coronary arteries while pericardial fat develops from the primitive thoracic mesenchyme and gets its blood supply from the non-coronary arteries **(152)**. In adults, epicardial fat commonly exists in the atrioventricular and interventricular grooves, whereas in juveniles it is found around the atrial free wall and two atrial appendages **(152, 153)**. Cardiovascular magnetic resonance (CMR) imaging has been validated for the measurement of epicardial and pericardial fat volume **(154, 155)** and is considered the most accurate method for this purpose.

<u>Physiological functions of epicardial fat include</u>:

1) Mechanical – cushion around the coronary arteries

2) Metabolic – supply free fatty acids to the myocardium (main energy source of myocardium)

3) Thermogenic – protects heart against hypothermia

4) Protective secreting factors - Under normal physiological conditions, epicardial adipose produces anti-inflammatory cytokines, such as adiponectin and adrenomedullin, to exert its cardioprotective functions (156, 157). Adiponectin has antidiabetic, antiatherogenic, antioxidative, and anti-inflammatory properties (156, 158). Adrenomedullin is produced in a variety of organs including the kidneys, lungs, and heart, and it exerts many cardioprotective actions including vasodilation, natriuresis, anti-apoptosis, and stimulation of nitric oxide production (158).

Epicardial fat is biologically active and may play a central role in the association between obesity and cardiovascular disease. In obesity epicardial fat volume increases and it becomes hypoxic and dysfunctional **(159)**, resulting in a shift in its metabolic profile. Adipokines can have both endocrine and paracrine functions that influence the development of cardiovascular disease, and in particular CAD (*McLean DS, Stillman AE. Epicardial adipose tissue as a cardiovascular risk marker. Clin Lipidol 2009;4:55-62*). Elevated IL-6, TNF-α, MCP-1 and decreased adiponectin have been correlated with the development of atherosclerosis **(160)**. Increased epicardial fat leads to additional mass on both ventricles that can increase the work demands on the heart and result in left ventricular hypertrophy **(161)**. Moreover, epicardial fat thickness is positively correlated with myocardial lipid content and may affect cardiomyocyte function **(162)**. Epicardial fat has been implicated in coronary artery disease **(148, 163-182)**, atrial fibrillation **(183, 184)** and adverse cardiovascular outcomes **(185-187)**.

Increased epicardial fat is associated with the more traditional metabolic risk factors such as BMI, dyslipidemia, impaired fasting glucose, Type 2 Diabetes Mellitus (T2DM) and hypertension. CKD is often the result of one or more of the above risk factors (188). Furthermore, obesity is common amongst patients with moderate-severe CKD (189, 190). Patients with chronic kidney disease (CKD) exhibit an increased incidence of cardiovascular disease (CVD), and cardiovascular mortality is about 10 – 30 times higher when compared to the non-CKD population, despite stratification for diabetes (9). Although renal transplantation significantly improves survival, CVD is still one of the most frequent causes of death post-transplant and accounts for 35-50% of all-cause mortality (40). Given the high risk of CAD in CKD patients and the complex relationship between the metrics of body adiposity and CAD, studies looking at epicardial fat in CKD would be relevant.

Epicardial fat thickness is significantly greater in patients on hemodialysis compared with healthy controls and positively correlated with hemodialysis duration (191, 192). Furthermore, echocardiographically assessed epicardial fat tissue thickness has been shown to correlate with oxidant biomarkers in CKD and CKD disease progression (193). In another study, it was seen that in stage 3-5 pre-dialysis CKD patients, coronary calcification and IL-6 were predictors of epicardial fat thickness (194). Thus, inflammation, as also seen with increased epicardial fat, could be a possible link between the pathogenesis of CAD and chronic kidney disease. Increased epicardial fat volume in patients with chronic kidney disease (stages 3–5, pre-dialysis) is associated with an increased risk of cardiovascular events independently of visceral (abdominal) fat (195).

In the general population, obesity is associated with increased cardiovascular risk and decreased survival. In the CKD population, however, the relationship between excess adiposity and cardiovascular risk is complex. In the CKD population, observational studies have reported contradictory findings about the association between obesity and mortality. Previous studies of people on hemodialysis have suggested an 'obesity paradox', where being obese is protective against all-cause and cardiovascular mortality (196, 197). Other studies have reported a U- or J-shaped association between obesity measured by BMI and mortality, with a higher risk of death in underweight and morbidly obese categories compared with normal weight (198, 199). In a recent metanalysis, it was shown that, in hemodialysis patients, for every 1 kg/m^2 increase in BMI, there was a 3% and 4% decrease in risk of all cause death and cardiovascular-related mortality, respectively (200). In CKD stages 3-5, the reduction in risk for all-cause mortality per kg/m^2 rise in BMI was 1% (200). It is not known if this paradox relationship seen with BMI extends to the paracardiac fat content in the CKD population.

Epicardial fat is often very difficult to distinguish from pericardial fat on CMR cine images. Paracardial fat refers to the combination of epicardial and pericardial fat and denotes the total amount of fat surrounding the heart. This is much easier to measure. In this thesis, Periventricular Adipose Tissue (PVAT) is defined as the paraventricular fat that surrounds the ventricles. As described above, most of the paracardial fat in adults is located in the interventricular groove, atrio-ventricular groove and the ventricles. Therefore, PVAT should account for almost all the paracardial adipose tissue.

1.2.5 Biochemical Methods

1.2.5.1 Markers of Endothelial Dysfunction

Although traditional risk factors are common among CKD patients, they can only in part explain the increased susceptibility to CVD (201). Non-traditional cardiovascular risk factors are important in the pathogenesis of CVD in CKD. These risk factors result in endothelial dysfunction which has a central role in the pathogenesis of CVD together with inflammation and atherosclerosis. Considering that CKD patients are more likely to die of CVD than to progress to End-Stage Renal Disease (ESRD), the search for novel CVD risk factors in this population may yield novel therapeutic targets. It is thought that perturbed arginine metabolism may potentially contribute to the high CVD rates in CKD.

Figure 1.9: The Arginine Metabolism Pathway

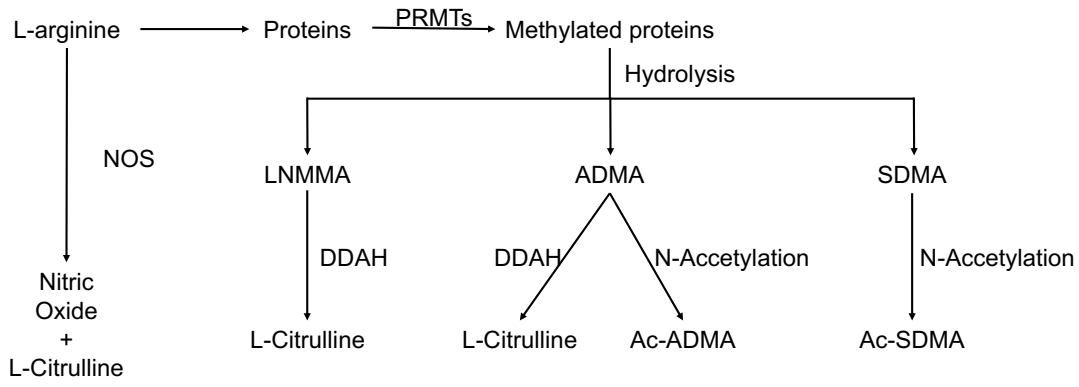

NOS: Nitric oxide synthetase
PRMTs: Protein methyltransferases
LNMMA: L-N-monomethylarginine
ADMA: Asymmetric dimethylarginine
SDMA: Symmetric dimethylarginine
DDAH: Dimethylarginine dimethylaminohydrolase
Ac-ADMA: Acetylated asymmetric dimethylarginine
Ac-SDMA: Acetylated symmetric dimethylarginine

Nitric oxide (NO) is a potent vasodilator and has important effects as a mediator of anti-thrombotic processes, growth inhibition and inflammation (202). In 1992 it was first reported that Asymmetric Dimethylarginine (ADMA) was a competitor to arginine,

the substrate used by nitric oxide synthetase (NOS) to produce NO (203). By comparing a group of six healthy individuals with a group of nine patients with end-stage renal disease on hemodialysis, the investigators found that the levels of dimethylarginines were substantially elevated in individuals with chronic kidney disease (CKD), and suggested that the accumulation of ADMA and concomitant inhibition of nitric oxide synthesis might contribute to hypertension, immune dysfunction, and cardiovascular disease in these patients. Therefore, ADMA impairs endothelial function and promotes atherosclerosis.

Symmetric dimethylarginine (SDMA) is more abundant than ADMA in patients with chronic kidney disease. Even though SDMA does not inhibit NOS directly, it may indirectly reduce NO production causing reduction in the intracellular arginine availability, since SDMA competes with the cationic amino acid transporter in the endothelial cell membrane (204). Therefore, SDMA also impairs endothelial function and promotes atherosclerosis. Furthermore, as a consequence of reduced NO availability, renovascular resistance increases and renal perfusion decreases (205). Thus, SDMA has emerged as an endogenous marker of renal function, as its levels are closely related to glomerular filtration rate. L-N-monomethylarginine (LNMMA) is another methyl derivative of the amino acid arginine. It is a potent NOS inhibitor and may accumulate in CKD. This molecule has been least studied in CKD.

Homoarginine (HMA) is an amino acid derivative found in trace amounts in the mammalian species. The exact pathways of HMA synthesis and its association with renal functions is not completely understood. It has been suggested that HMA is synthesized in the kidney by the transamidation of lysine. HMA may increase NO availability in 2 ways and enhance endothelial function. First, HMA may serve as a

precursor of NO. Second, it potentially increases the intracellular concentration of L-arginine, the main substrate for NO synthesis, by inhibiting the enzyme arginase (206-209).

HMA molecule has attracted significant attention because of its potential interactions with insulin secretion, platelet aggregation, blood pressure regulation and endothelial function (208, 210-212). There seems to be a strong association between low HMA levels and higher mortality risk in CAD and hemodialysis patients (213). Furthermore, low HMA levels are also associated with myocardial dysfunction and stroke (214, 215). In pre-dialysis patients, low HMA levels is a strong predictor of progression to dialysis and incident mortality (216). In hemodialysis patients, low HMA levels are associated with sudden cardiac death (SCD) and death due to heart failure (217).

Dimethylarginine dimethylaminohydrolase (DDAH) is strongly expressed in the kidneys (218) and converts ADMA into citrulline and methylamines. This ADMA conversion is important during renal homeostasis as <15% of total ADMA is excreted by kidneys in a non-metabolized form (218). In contrast to ADMA, the majority of SDMA is excreted in a non-metabolized form (204). LNMMA is partly degraded by DDAH and partly renally excreted (219, 220). Additionally, in a study with mice, it was shown that both ADMA and SDMA undergo N-acetylation forming asymmetric N∝-acetyldimethylarginine (AcADMA) and symmetric N∝-acetyldimethylarginine (AcSDMA) (221, 222).

Patients with mild-moderate CKD have elevated plasma levels of ADMA and SDMA compared to normal controls (223-226). This increase is more pronounced in ESRF (227, 228). Furthermore, some studies suggest that patients with elevated plasma ADMA and SDMA levels are at higher risk of CKD progression and incident

atherosclerotic cardiovascular events (229, 230). However, this finding is not well established and contradictory data exists (231). Circulating levels of ADMA are regulated by its release from methylated proteins, glomerular filtration and enzymatic degradation by DDAH. In patients with renal disease, the loss of DDAH activity contributes more to elevated ADMA than does reduced glomerular filtration. Genetic polymorphisms in DDAH-1 have been described that modify the activity of DDAH-1, and DDAH-2 activity is affected by redox balance. Upregulation of ADMA levels results in reduced nitric oxide generation, which underlies many of the clinical symptoms related to renal diseases and their vascular complications.

Figure 1.10: ADMA regulation in Chronic Kidney Disease

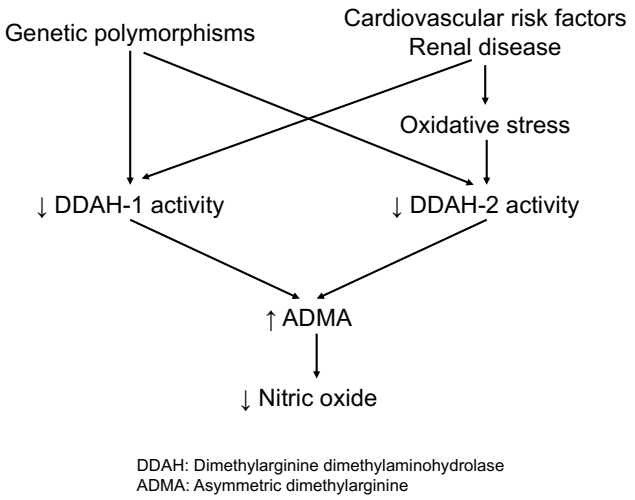

DDAH: Dimethylarginine dimethylaminohydrolase
ADMA: Asymmetric dimethylarginine

Patients with CKD treated by dialysis exhibit the highest SDMA concentrations before a dialysis session. Investigators who studied 20 individuals undergoing chronic hemodialysis reported that SDMA was efficiently removed during hemodialysis or hemodiafiltration **(232)**. In the same study, ADMA was removed less efficiently than SDMA by both methods (by a mean of 35% and 40%, respectively) **(232)**. Of note, the mean level of L-arginine was not substantially decreased by hemodialysis (5%),

although it was reduced by hemodiafiltration (26%). One study showed that hemodialysis was barely able to eliminate ADMA when a closed hemodialysis system was used **(233)**.

1.2.5.2 Markers of Inflammation

1.2.5.2.1 C-Reactive Protein (CRP)

As traditional risk factors cannot alone explain the unacceptable high prevalence and incidence of CVD in CKD, inflammation has been suggested to be a significant contributor. CKD is a hyperinflammatory disease characterized by an irreversible deterioration of renal function that gradually progresses to end-stage renal disease. The causes of the highly prevalent state of inflammation in ESRD are multiple, including decreased renal function, volume overload, comorbidity and intercurrent clinical events, factors associated with the dialysis procedure and genetic factors. Recent evidence suggests that several cytokine DNA polymorphisms may affect the inflammatory state as well as outcome in ESRD patients. Dysfunction of the immune system induced by the uremic milieu is considered to be the primary cause of hyperinflammation in patients with CKD **(234)**. Accumulation of uremic toxins can have detrimental effects on health and lead to uremic syndrome, cardiovascular disease, inflammation, and increased mortality **(235, 236)**. Alterations in the immune system in CKD by uraemia are associated with a state of immune dysfunction characterized by immune-depression that contributes to the high prevalence of infections among these patients, as well as by immune-activation resulting in inflammation that may contribute to cardiovascular disease **(234)**. Hypercytokinemia is a typical feature of uremia. Accumulation of proinflammatory cytokines as a

consequence of decreased renal elimination as well as oxidative stress, volume overload, and comorbidities contributed to hypercytokinemia in patients with CKD.

Figure 1.11: CRP Mediated Effects on Atherosclerosis

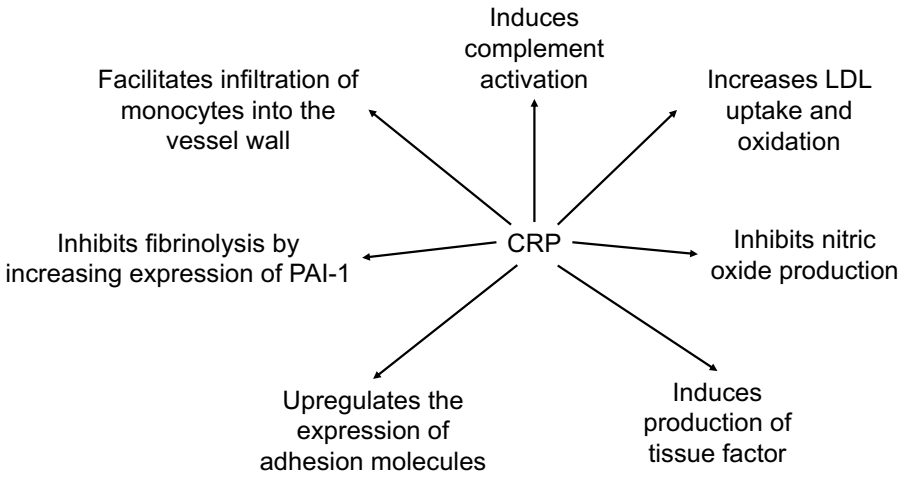

CRP: C-reactive protein
LDL: Low density lipoprotein
PAI: Plasminogen activator inhibitor

C-reactive protein (CRP) is the forerunner in the hunt for inflammatory markers and is subject to intensive research in numerous studies worldwide. Unlike other markers of inflammation, CRP levels are stable over long periods, have no diurnal variation, can be measured inexpensively with available high-sensitivity assays (hs-CRP), and have shown specificity in terms of predicting the risk of CAD **(237)**. CRP belongs to the pentraxin family of calcium dependent ligand-binding plasma proteins. The human CRP molecule is composed of five identical non-glycosylated polypeptide sub- units each containing 206 amino acid residues. The major part of the CRP present in the plasma comes from the liver, where the synthesis of CRP is mainly regulated by interleukin-6 (IL-6), which in turn is up-regulated by other inflammatory cytokines such as IL-1 and tumor necrosis factor (TNF)- ∝. CRP is also produced locally in atherosclerotic lesions by smooth muscle cells, lymphocytes and monocytic cells

(238). Upon dissociation of its pentameric structure, CRP subunits undergo a spontaneous and irreversible conformational change. The loss of the pentameric structure of CRP results in modified or monomeric CRP (mCRP), which is a naturally occurring form of CRP and it is a tissue-based rather than a serum-based molecule. mCRP is less soluble than CRP and tends to aggregate, and it has been described to induce mRNA of chemokines and the expression of adhesion molecules in human cultured coronary artery endothelial cells (EC) **(238)**. CRP may have a role in the genesis of atherosclerotic lesion, since it reduces the expression of nitric oxide (NO) synthetase and prostacyclin synthetase and binds LDL-C and promotes its uptake by macrophages, a key step in atherogenesis. CRP also up-regulates the expression of adhesion molecules on EC. All these phenomena are associated with atherogenesis **(239)**.

It has been shown that high-sensitivity C-reactive protein (hs-CRP) is elevated in patients with CKD **(240)**. CRP is associated with increased cardiovascular disease in healthy middle-aged men and women **(241-243)**. It is the same for people older than 65 years without renal insufficiency **(244-246)**. CRP is an independent risk factor for the development of atherosclerosis in patients on hemodialysis and peritoneal dialysis **(247-253)**. Furthermore, several studies indicate that CRP may be a predictor of adverse clinical outcomes (cardiovascular mortality, all-cause mortality, hospitalization) in CKD **(254-260)**.

As interventions directed towards traditional risk factors have, so far, not proven to be very effective, controlled studies are needed to evaluate if various pharmacological as well as non-pharmacological anti-inflammatory treatment strategies, alone or in

combination, may be an option to affect the unacceptable high cardiovascular mortality rate in this patient group.

1.2.5.2.2 Myeloperoxidase (MPO)

The phagocytic enzyme myeloperoxidase (MPO) acts as a frontline defender against microorganisms. However, increased MPO levels have been found to be associated with complex and calcified atherosclerotic lesions and incident cardiovascular disease.

MPO uses hydrogen peroxide to oxidize chloride to the strong-oxidizing agent hypochlorous acid, a toxic agent to various biomolecules such as lipoproteins and the eNOS substrate L-arginine **(261)**. Thus, MPO promotes LDL modifications through various pathways such as the reaction between HOCl generated by MPO and tyrosine residues of ApoB100, generation of reactive nitrogen species (RNS) resulting in proatherogenic nitrosilated LDL, and MPO-catalyzed addition of thiocyanate to the LDL leading to the formation of carbamylated LDL (cLDL) **(262)**. Additionally, MPO can oxidize NO to nitrite thus abolishing its protective properties on the vascular wall **(261)**.

Increased MPO levels have been found to be associated with complex and calcified atherosclerotic lesions and incident cardiovascular disease. MPO levels correlate with angiographic evidence of coronary atherosclerosis and cardiovascular events in subjects with chest pain within the general population **(263-265)**. Oxidised lipids are important players in the initiation and progression of atherosclerotic changes. The oxidation of LDL by HOCl generated in MPO-catalyzed reaction is thought to be a proatherogenic event which precedes the formation of foam cells, a hallmark of atherosclerotic plaque development.

In a prospective case–control study in apparently healthy individuals, MPO predicted future risk of CAD independent of other cardiovascular risk factors **(266)**. MPO concentrations were found to be elevated in patients with stable CAD **(267)**, ACS **(268, 269)**, and acute MI **(270, 271)**. MPO concentrations were further associated with the severity of CAD **(272)** and with complex lesion morphology on angiography **(273)**. Furthermore, MPO–DNA complexes were positively associated with thrombin generation and significantly elevated in patients with severe coronary atherosclerosis or extremely calcified coronary arteries **(274)**.

Myeloperoxidase can also participate in the destabilization of atherosclerotic plaques. It has been shown that the products of the reaction catalyzed by MPO can induce endothelial cell death, including apoptosis, leading to their subsequent desquamation and erosion. They can also affect the expression of tissue factor **(275)**.

In patients with end-stage CKD undergoing haemodialysis, serum MPO levels have been found to correlate with ox-LDL, with levels of markers of inflammation and prospective mortality risk **(276-278)**. Interestingly, in haemodialysis patients, MPO activity has been associated with aortic stenosis as well **(279)**.

1.3 Aims and Hypotheses of this Thesis

CKD is associated with increased risk of CVD and CVD remains the most common cause of morbidity and mortality in this group of patients. However, current invasive and non-invasive diagnostic approaches are poorly predictive of future cardiovascular events in patients with CKD. In this regard, some non-invasive tests that are both safe and relatively accurate and which can risk stratify this population would be valuable.

1.3.1 Aims of this Thesis:

Chapter 3: To investigate the prognostic utility of OS-CMR imaging and FT-CMR derived myocardial deformation properties in asymptomatic CKD patients with and without DM.

Chapter 4: To evaluate the potential of T1 mapping at rest and during adenosine stress as a novel method for ischaemia detection without the use of Gadolinium contrast in patients with CKD.

Chapter 5: To compare the utility of OS-CMR imaging and Stress CMR T1 mapping in the diagnosis of CAD in patients with CKD.

Chapter 6: The aim of this study is to compare CMR assessed PVAT volumes in participants with and without CKD. Furthermore, the prognostic value (and the possible paradox) of PVAT in predicting major adverse events in patients with CKD was investigated.

Chapter 7: To investigate the relationship between biochemical markers of endothelial dysfunction and myocardial oxygenation and perfusion response to stress, using oxygen-sensitive cardiovascular magnetic resonance (OS-CMR) and stress T1 mapping respectively in patients with CKD.

1.3.2 Hypotheses of this Thesis:

Chapter 3: The blunted myocardial oxygenation response to stress and abnormal myocardial deformation in patients with CKD without known coronary artery disease is an independent predictor of adverse events.

Chapter 4: In patients with CKD, stress T1 response is impaired and can differentiate between remote, ischaemic and infarcted segments.

Chapter 5: In patients with CKD, stress T1 response is a more accurate method of diagnosing myocardial ischaemia than stress OS-CMR response.

Chapter 6: When compared to normal individuals, patients with CKD will have higher epicardial fat volumes. Furthermore, lower PVAT would be a predictor of adverse events in patients with CKD.

Chapter 7: In CKD patients, higher levels of ADMA and lower levels of HMA are associated with worsening myocardial oxygenation and perfusion as assessed by OS-CMR and stress T1 responses to stress.

CHAPTER 2: METHODS

This chapter elaborates the general methodologies used in all the research studies.

2.1 Study Protocol

2.1.1 Ethics

The study protocol was approved by the Southern Adelaide Health Service/Flinders University Human Research Ethics Committee (Ethics Number 380.10). All study participants gave written informed consent.

2.1.2 Study Population

This has been described in the relevant chapters.

2.1.3 Preparation

All participants were screened for ensuring their MRI safety using a standard Flinders Medical Centre MRI safety form (Figure 2.1A) or Cardiac Research and Imaging Centre (CRIC) Safety Form (Fig 2.1B).

All metals and metallic objects were removed prior MRI scan. Intravenous cannulation was established beforehand. An explanation of breath-holding commands was given at the start of the examination. Participants who were claustrophobic or had implantable metals, pacemakers, defibrillators, cerebral aneurysm clips were excluded. All participants were explained the effects of stress adenosine. All participants had 12 Lead electrocardiogram (ECG) performed prior to the CMR. This was done to rule out second and third-degree heart blocks.

Figure 2.1: MRI Safety Forms. A, Flinders Medical Centre. B, CRIC

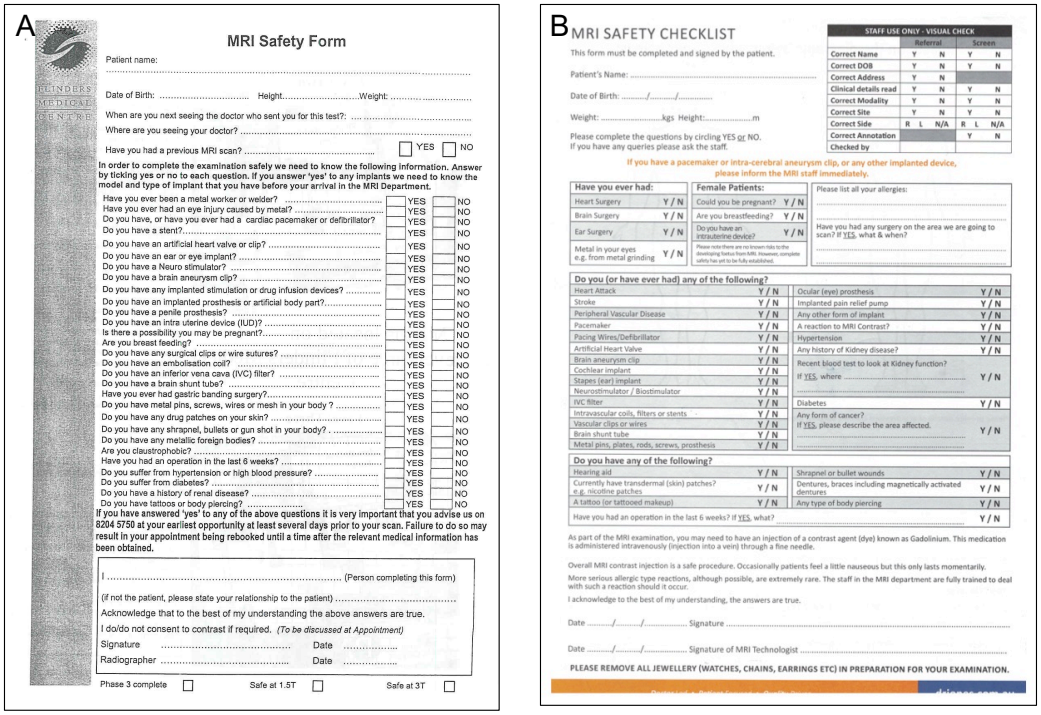

Four ECG electrodes for 1.5T machine (or three for the 3.0T machine) were placed on the anterior chest wall. Coil configuration included a spine array coil embedded in the scan table and a flex array coil placed over the patient's anterior chest wall. A foam wedge was placed under the patient's knees for comfort. A baseline ECG, heart rate and blood pressure were performed before the stress imaging.

2.2 CMR Image Acquisition 2.2.1 Multi Plane Localisers

The localisers and cine methods were employed as previously described (280). Firstly, a set of multi-slices, multi-planar images were acquired. These comprised axial, coronal and sagittal images acquired in a single breath-hold, on every heartbeat, captured cycle for diastolic gating. The field of view (FOV) was adjusted in the antero-posterior direction.

Single shot Half-Fourier Single Shot Turbo Spin Echo (HASTE) with T2-weighted black-blood technique was acquired with free breathing. Fast Imaging with Steady Precession (TrueFISP or TRUFI) with white blood technique was acquired with free breathing.

Figure 2.2: Sequence of images demonstrating the acquisition of the long axis and short axis planes for cine imaging. Initially, multi-planar transverse localiser (A), in the plane indicated by the solid line in (A), scout images are then performed in the vertical long axis (VLA) plane (B). The resultant VLA scout is used to prescribe (as indicated by the solid line in B) the horizontal long axis (HLA) scout (C). Using the HLA and VLA scouts, three short axis (SA) slices (D-F) are next acquired with the basal slice parallel to the atrio-ventricular (AV) groove (indicated by 3 solid lines in C). Adapted from Selvanayagam et al Cardiovascular Magnetic Resonance—Basic Principles, Methods and Techniques in Hybrid cardiovascular Imaging Dilazian and Pohost (Eds) 2005 Blackwells Scientific Publications.

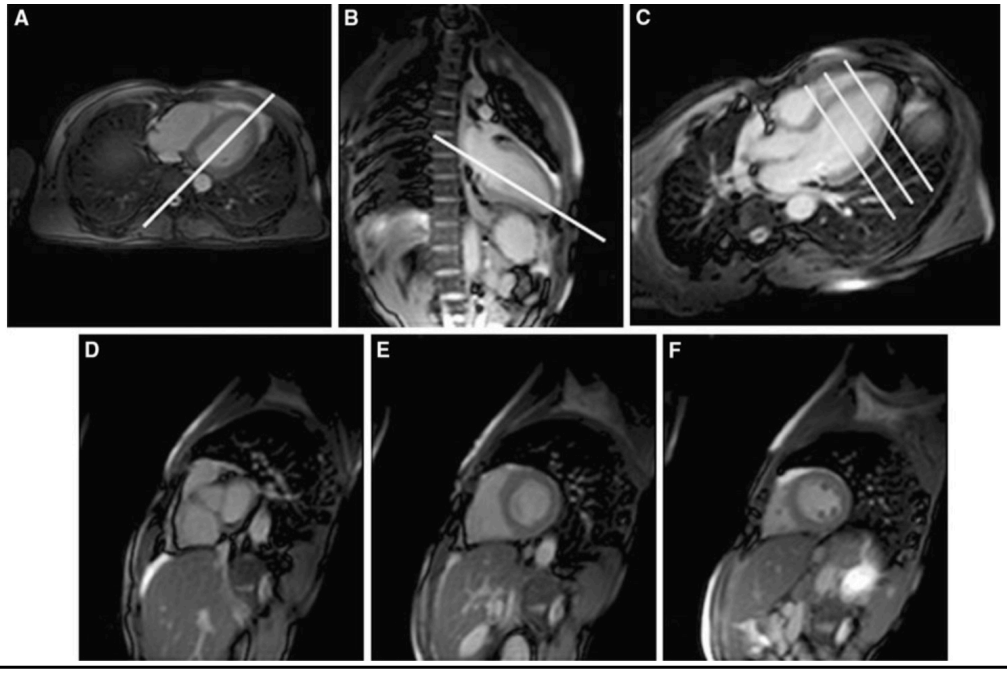

2.2.1.1 Two Chamber (Vertical Long Axis or VLA) Localiser

One slice was planned from the axial view parallel to the interventricular septum, bisecting the left ventricle through the mitral valve and the apex (Figure 2.2B). It was acquired with a single breath hold and captured cycle for diastolic gating. An example of image acquisitions from a research participant was shown below.

2.2.1.2 Four Chamber (Horizontal Long Axis or HLA) Localiser

One slice was planned from the VLA view, bisecting the left ventricle through the mitral valve and the apex on a single breath hold, captured cycle for diastolic gating (Figure 2.2C).

2.2.1.3 Short Axis (SA) Localiser

Three short axis slices were acquired using the VLA and HLA views with the most basal slice parallel to the atrio-ventricular groove in both planes, perpendicular to the long axis of the left ventricle, single breath hold with captured cycle (Figures 2.2D, 2.2E and 2.2 F).

2.2.2 Cine Imaging

Figure 2.3: To acquire HLA cine (C) the mid ventricular SA scout (A) is used to position the slice through the maximum lateral dimensions of both ventricles and avoid the LVOT as illustrated by panels (A) and (B). To acquire the VLA cine (E), the mid ventricular SA scout is again used and placed in the plane as indicated in panel (D). Adapted from Selvanayagam et al Cardiovascular Magnetic Resonance—Basic Principles, Methods and Techniques in Hybrid cardiovascular Imaging Dilazian and Pohost (Eds) 2005 Blackwells Scientific Publications.

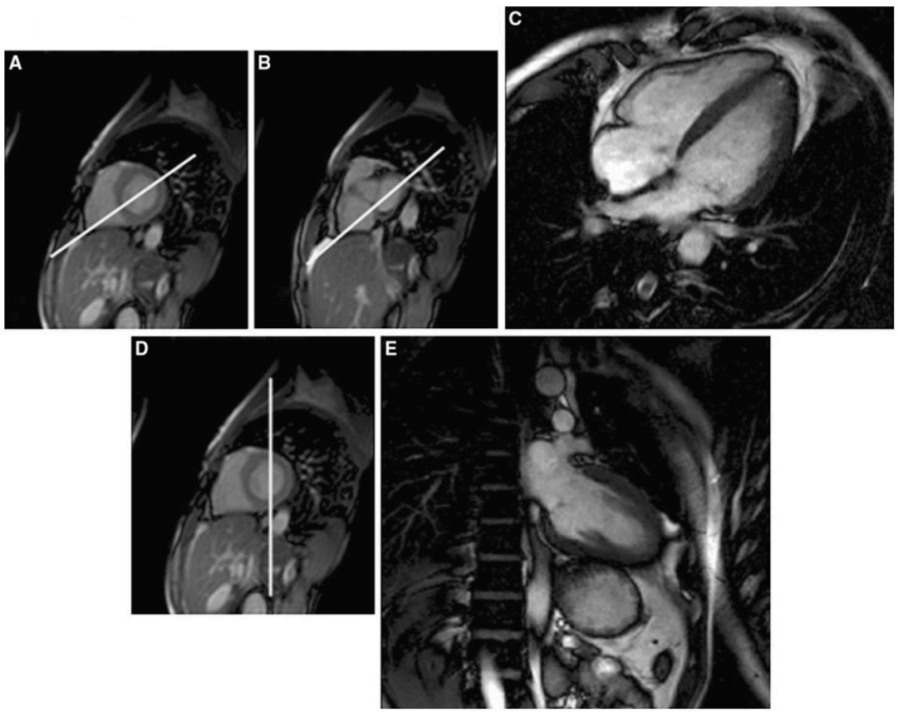

Cine images were acquired in VLA, HLA and ten SA images covering the entire left ventricle, using a retrospective ECG gating steady-state free precession (SSFP) sequence (repetition time (TR) 3 ms, echo time (TE) 1.5 ms, flip angle (FA) 55˚, 18 phases). All research participants underwent ventricular function imaging.

2.2.2.1 Two Chamber (Vertical Long Axis or VLA) Cine

One slice was planned parallel to the ventricular septum on a short axis view, bisecting the left ventricle through the mitral valve and the apex on the HLA view (Figure 2.3E).

2.2.2.2 Four Chamber (Horizontal Long Axis or HLA) Cine

Figure 2.4: To acquire LVOT cine (C) the most basal SA scout (B) is used to position the slice bisecting the LVOT and posterolateral left ventricular wall and rotating the slice on the VLA cine (A) through the apex of the heart. To acquire the LVOT cross-cut cine (E), the LVOT cine is used and placed in the plane perpendicular to it through the aortic valve and into the proximal aorta as indicated in panel (D).

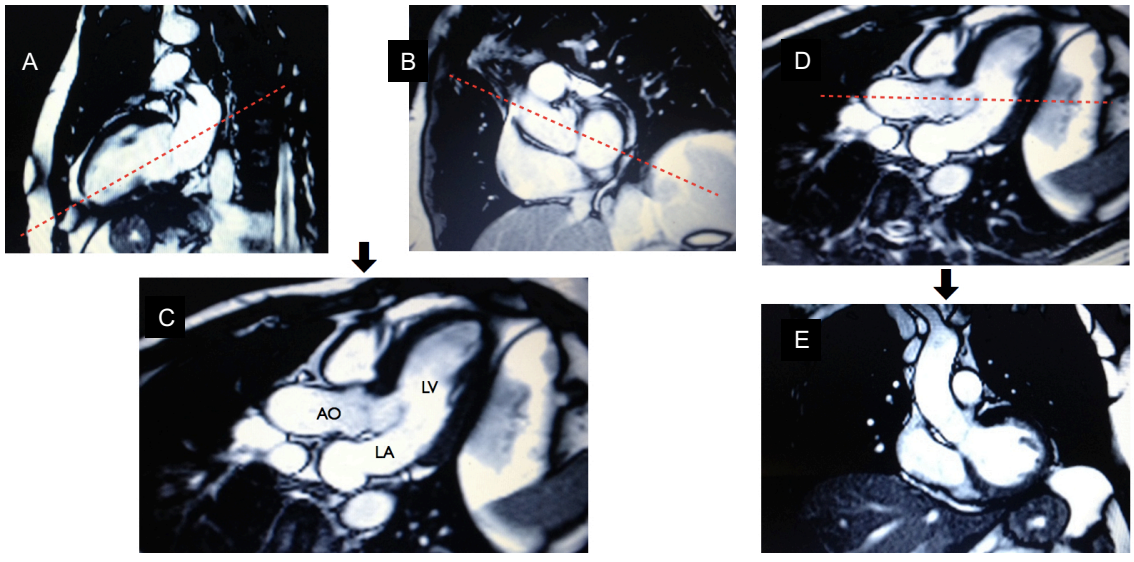

One slice was planned to bisect the left ventricle through the mitral valve and the apex on a VLA, bisecting the left and right ventricles on a SA view and rotated through the apex (Figure 2.3C). It was acquired on a single breath hold with retrospective gating.

2.2.2.3 Left Ventricular Outflow Tract (LVOT) Cine

One slice was planned to bisect the LVOT and posterolateral left ventricular wall on the most basal short axis view, rotating the slice on the VLA view through the apex of the heart (Figure 2.4C). It was acquired on a single breath hold with retrospective gating.

2.2.2.4 Left Ventricular Outflow Tract (LVOT) Cross Cut Cine

The slice was positioned perpendicular to the LVOT cine through the aortic valve and into the proximal ascending aorta (Figure 2.4E).

2.2.2.5 Short Axis (SA) Cine

Ten slices were planned from the VLA and HLA cines in end diastole perpendicular to the long axis of the left ventricle in line with the atrioventricular groove, covering from the mitral valve to the apex (Figure 2.5). Slice thickness was 8 mm with 2 mm inter-slice gap.

Figure 2.5: This demonstrates the resultant HLA (A), VLA (B) and short axis cine stack from base to apex (bottom panel). Adapted from Selvanayagam et al Cardiovascular Magnetic Resonance— Basic Principles, Methods and Techniques in Hybrid cardiovascular Imaging Dilazian and Pohost (Eds) 2005 Blackwells Scientific Publications.

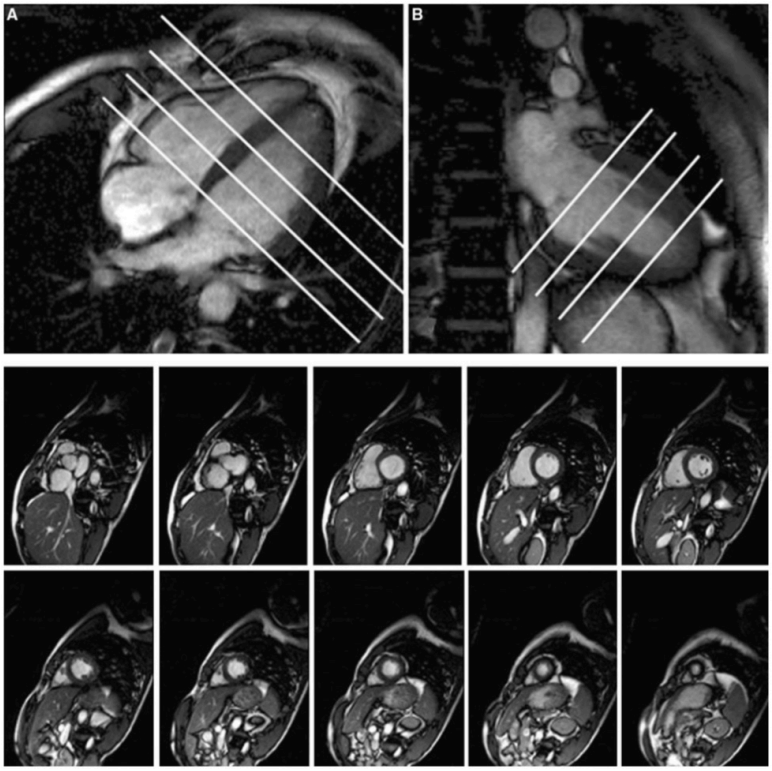

2.2.3 Oxygen-Sensitive CMR (OS-CMR) Imaging

OS-CMR, also known as Blood Oxygen Level Dependent (BOLD) imaging was acquired in a 3 Tesla MRI scanner (Siemens, 3T Trio, 4 channel Body Flex coil). The participants were instructed to refrain from caffeine 24 hours prior to the scan. A single midventricular slice was acquired at mid-diastole using a T2-prepared ECG-gated SSFP sequence (TR 2.86 ms, TE 1.43 ms, T2 preparation time 40 ms, matrix 168 x 192, FoV 340 x 340 mm, slice thickness 8 mm, FA 44°) [92]. If required, frequency scout and shim adjustments were performed to minimise off-resonance artefacts. A set of 4-6 OS-CMR images were acquired at rest during a single breath-hold over six heart beats. Six stress OS-CMR images identical to the ones acquired at rest were acquired at peak adenosine stress (140 µg/kg per minute) 90 seconds

after initiation for at least 3 minutes. Stress heart rate and blood pressure were obtained every minute of adenosine infusion. Each participant was questioned about the occurrence of adenosine effects: chest pain or tightness, shortness of breath, flushing, headache, and nausea. Figure 2.6 shows an example of a resting and stress OS-CMR imaging in a CKD participant.

Figure 2.6: Example of OS-CMR imaging at rest (A) and after Adenosine Stress (B).

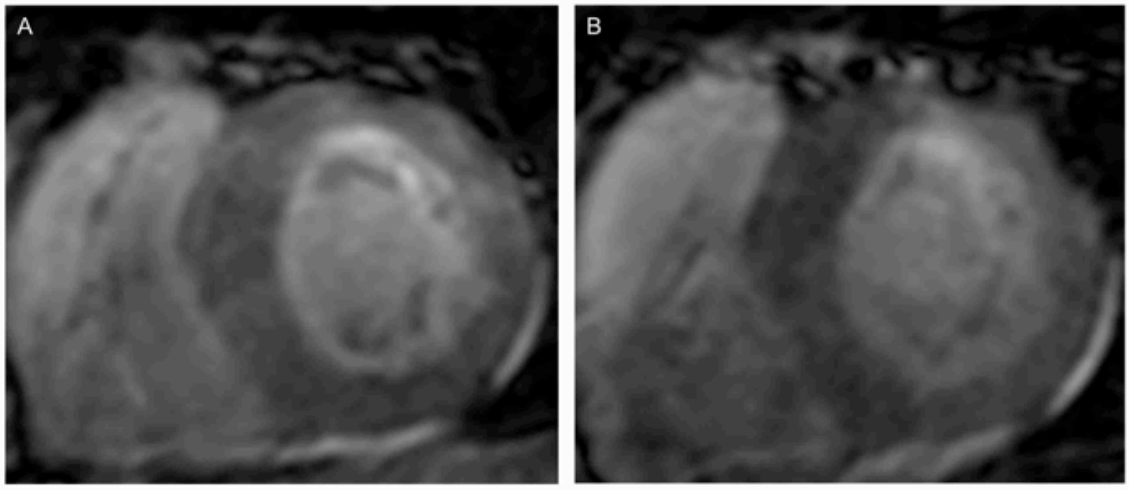

2.2.4 T1 mapping – ShMOLLI sequence

T1 mapping were performed on a 3-T clinical MR scanner (Siemens, Skyra), utilizing the Shortened Modified Look-Locker Inversion recovery (ShMOLLI) sequence (129). ShMOLLI T1-maps were based on 5-7 images with specific TI~100-5000 ms, collected using SSFP readouts in a single breath-hold, typically: TR/TE~201.32/1.07 ms, flip angle=35°, matrix=192x144, 107 phase encoding steps, interpolated voxel size=0.9x0.9x8 mm, cardiac delay time TD=500 ms; 206 ms acquisition time for single image. Native T1 mapping were performed on 3 slices (basal, mid-ventricular and apical) at mid-diastole with a complete rim of myocardium (basal slice) and LV cavity visible (apical slice).

During adenosine stress (140 μg/kg per minute), another set of 3 T1 maps were acquired on slices corresponding to the rest images using the same protocol. The images were acquired, while continuing adenosine stress, every 40 seconds starting at 250 seconds after initiation. Stress heart rate and blood pressures were obtained every minute of adenosine infusion. Each participant was questioned about the occurrence of adenosine effects: chest pain or tightness, shortness of breath, flushing, headache, and nausea.

2.3 CMR Image Analysis

2.3.1 Ventricular Volumes, Function and Mass

Ventricular volumes and function were analysed using CMR^{42} software on a cine SA stack. The most basal slice was defined as the one with at least 50% of myocardium. The end-diastolic phase was first identified which is the phase with largest left ventricular cavity size. Using a mid-ventricular slice, the phases were advanced until the end-systolic phase when the smallest cavity was reached. Endocardial and epicardial contours were manually drawn on all slices in both the diastolic and systolic phases (Figure 2.7).

The CVI^{42} software automatically calculated the volumes and mass (Figure 2.8). The ventricular volumes and mass were indexed to body surface area (BSA). The septal and lateral wall diameters were measured in end-diastole at mid- ventricular level from short-axis view.

Figure 2.7: End diastolic (A) and end-systolic (B) views with the left and right ventricular contours.

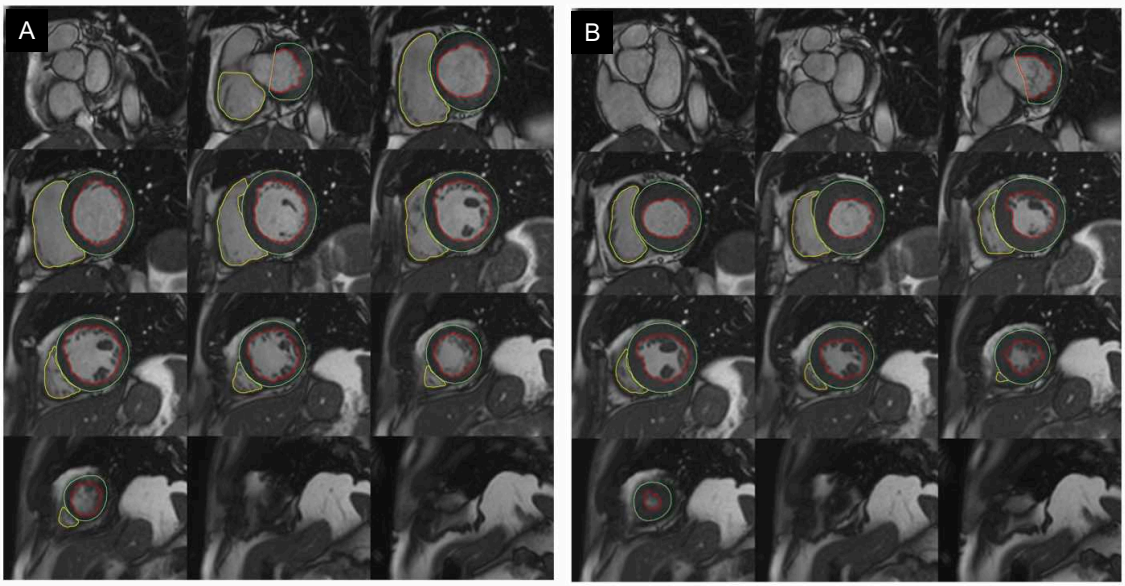

Figure 2.8: Example of volumetric and mass analysis by CVI[42] software.

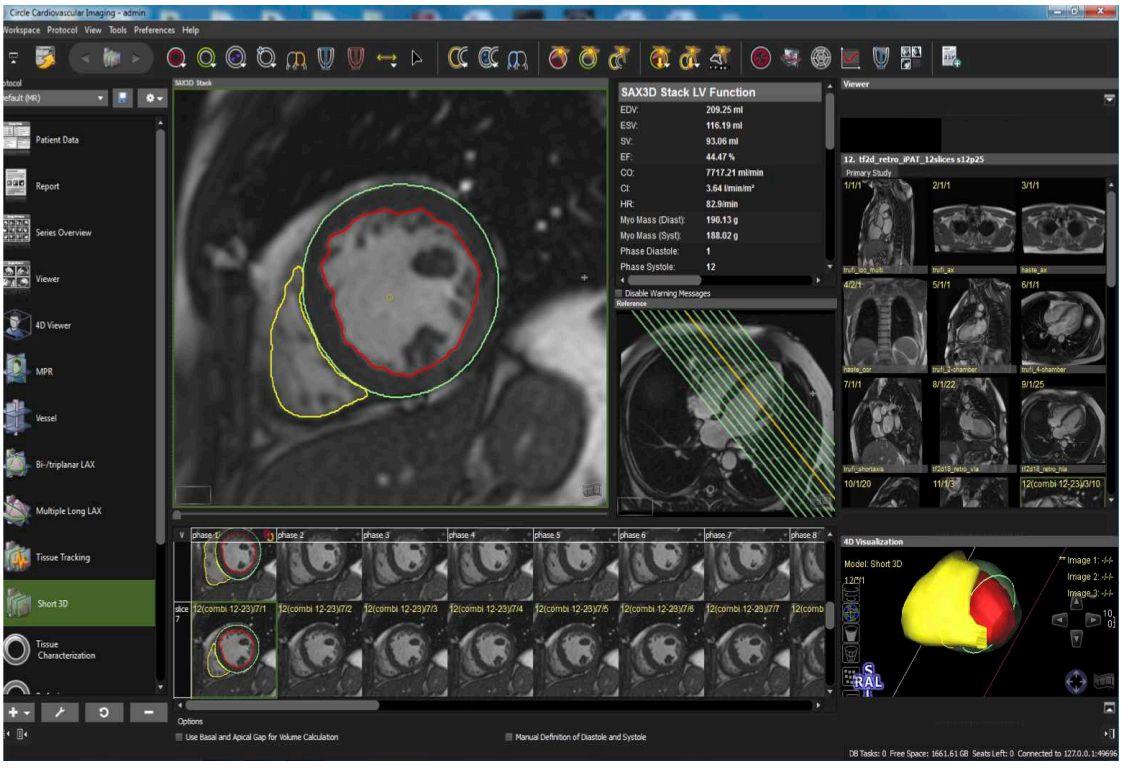

2.3.2 OS-CMR Analysis

OS-CMR images were analysed after manually tracing the endocardial and epicardial contours using CMR^{42} software, Version 4.1 - 5.9, Circle Cardiovascular Imaging Inc. (Calgary, Canada). Analysis of OS-CMR SI were performed as previously described (119). Each midventricular short-axis OS-CMR image was divided into 6 segments (anterior, anterolateral, inferolateral, inferior, inferoseptal, and anteroseptal) according to the American Heart Association 17-segment model. The CMR software measured Myocardial SI after manually tracing the endocardial and epicardial contours.

Figure 2.9: OS-CMR Analysis using CVI^{42}.

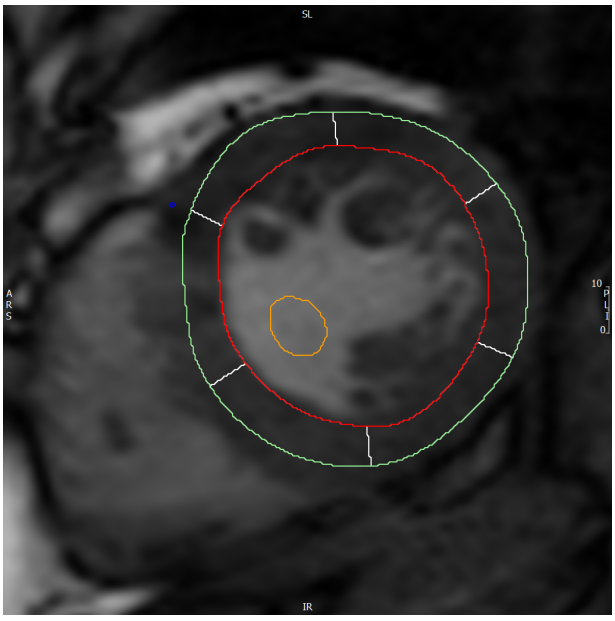

$SI = SI_0/(1-\beta e^{-TR/T1})$

$\Delta SI = (SI_{STRESS} - SI_{REST})/SI_{REST} \times 100\%$

SI = Corrected signal intensity
SI_0 = Mean SI (for each segment)
β = 0.59
T1 = 1220 msec
} Determined empirically for this sequence
TR = Image-dependent time between acquisition of sections of k-space, governed by the heart rate (replaced by the RR interval)
ΔSI = Percentage change in corrected SI

The mean myocardial SI within each segment was obtained, both at rest and stress, and corrected to variations in heart rate with the following equation as follows:

$$SI = SI_0 / (1 - \beta e^{-TR/T1})$$

where, T1= 1220 ms and β=0.59 (determined empirically for this sequence), SI_0= the measured signal intensity, SI= signal intensity corrected to heart rate, and TR is the image-dependent time between acquisition of sections of k-space, governed by the heart rate (replaced by the RR interval). The SI change was calculated as:

$$\Delta SI = (SI_{Stress} - SI_{Rest})/SI_{Rest} \text{ X } 100\%$$

where, SI_{Rest} = OS-CMR SI at rest, and SI_{Stress} = OS-CMR after adenosine stress.

2.3.3 CMR- Feature Tracking (FT-CMR) Analysis

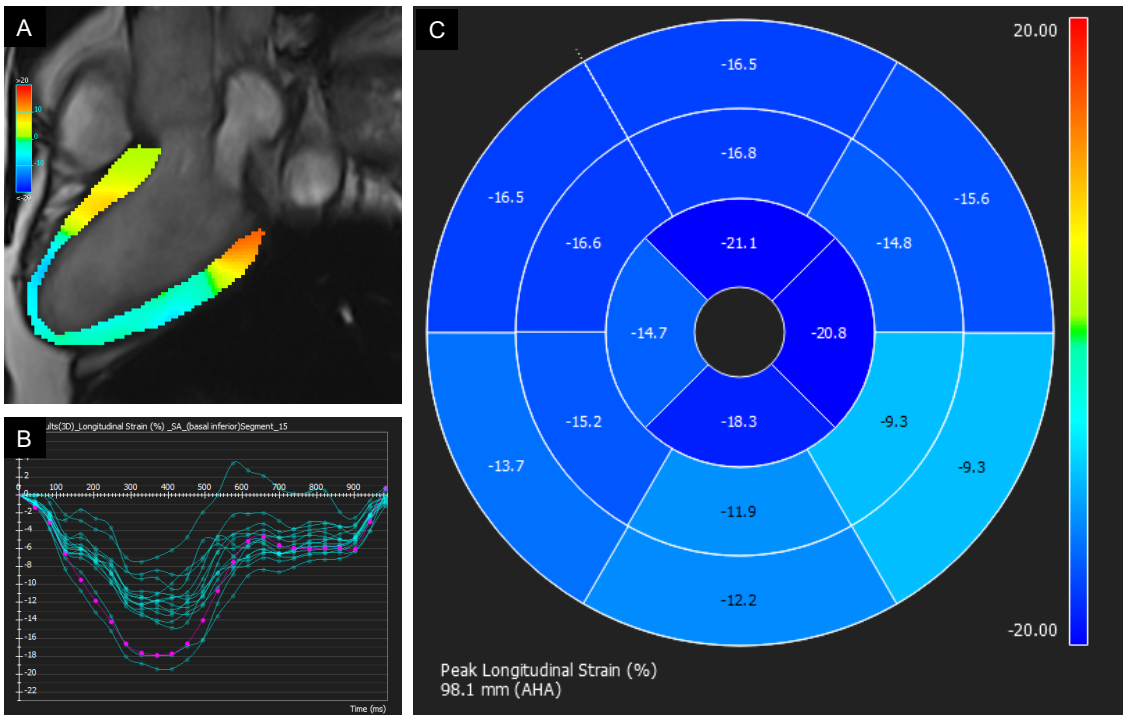

Figure 2.10: Analysis of longitudinal strain by FT-CMR. A, LVOT view with segmental strain overlay. B, Plot of segmental longitudinal strain against time. C, Peak regional longitudinal strain (AHA 16 segment model).

This was performed with CMR[42] Version 5.9.1 (Circle Cardiovascular Imaging Inc, Calgary, Canada). Using the Feature Tracking module, endocardial and epicardial contours were traced in end-diastole using the 3-dimensional short-axis stack.

Similarly, contours were traced in the 3 long axes cine images in end-diastole after defining the extent of the left ventricular cavity. The anterior right ventricular insertion point was marked on the short-axis slices. The software then calculated GLS semi-automatically. MD was then calculated as the standard deviation of the times to peak segmental (AHA 17 segment model) longitudinal strain.

2.3.4 T1 map analysis

Figure 2.11: Analysis of T1 maps. A, Automatic segmentation of the short axis T1 map after manually drawing the endocardial and epicardial contours. B, Regional T1 values (AHA 16 segment model).

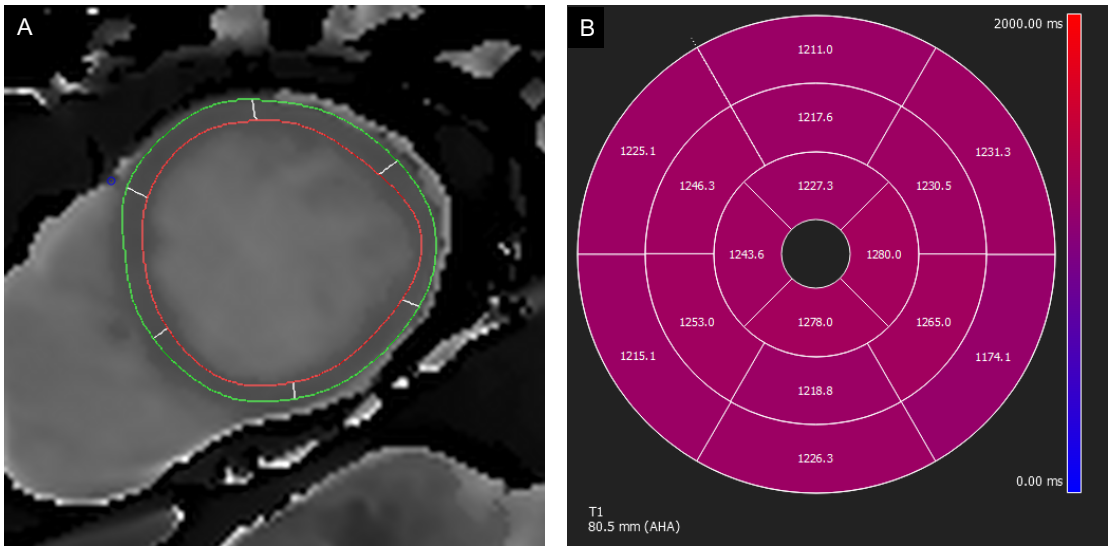

CMR analysis was performed with CMR[42] Version 5.9.1 (Circle Cardiovascular Imaging Inc, Calgary, Canada). Myocardial T1 analysis was performed on the T1 maps acquired during rest and stress. The CMR software measured Myocardial T1 after manually tracing the endocardial and epicardial contours. The 3 short-axis T1 map images (basal, mid-ventricular and apical) were divided into 16 segments according to the American Heart Association 17-segment model. The mean myocardial T1 within each segment was obtained, both at rest and stress. The T1 change was then calculated as:

$$\Delta T1 = (T1_{Stress} - T1_{Rest})/T1_{Rest} \times 100\%$$

2.3.5 Epicardial Fat Analysis

Epicardial fat is the adipose tissue that directly surrounds the heart (between the myocardium and visceral layer of pericardium). Pericardial fat is located on the external surface of the parietal pericardium. Paracardial fat refers to the combination of epicardial and pericardial fat and denotes the total amount of fat surrounding the heart. In this chapter, Periventricular Adipose Tissue (PVAT) is defined as the paraventricular fat that surrounds the ventricles.

Figure 2.12: Analysis of periventricular fat on the diastolic phase of short axis cine views.

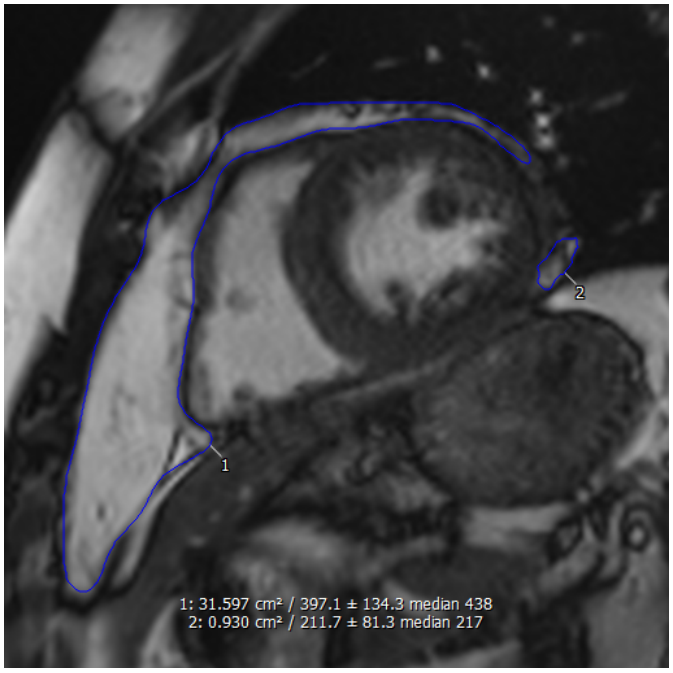

Image analysis was carried out using CMR[42] Version 5.9.1 (Circle Cardiovascular Imaging Inc, Calgary, Canada). Areas of PVAT were traced on consecutive end diastolic short-axis images beginning with the most basal slice at the level of the mitral valve and moving apically through the stack until the most inferior margin of

adipose tissue was traced. PVAT fat areas were calculated, and volumes were derived using a modified Simpson's rule.

2.4 Serum Biochemistry

All participants had blood samples collected for routine biochemistry, cell counts, haemoglobin, troponin T, CRP, thyroid stimulating hormone (TSH), Parathormone levels (PTH), iron studies and lipid studies. eGFR was calculated from serum creatinine using the CKD-Epidemiological Collaboration Formula.

A further sample of blood was spun at 4000 rpm for 10 minutes at 4°C and the serum collected and stored in a -80°C freezer for analysis of biochemical markers of endothelial dysfunction. These samples were later thawed and analysed as follows. 20 µL of sample plasma, calibrator or QC was mixed with 20 µL internal standard solution (containing 1 µM d6-ADMA, 1 µM d6-SDMA, 25 µM d7-citrulline, 2 µM d4-homoarginine, and 100 µM d6-ornithine). Following the addition of 150 µL 0.1% formic acid in methanol the sample was vortex mixed for 3 min at 2000 rpm to extract the analytes. Centrifugation at 18,000g for 5 min precipitated the proteins. An aliquot (5 µL) of the supernatant layer was injected onto an Atlantis HILIC column (2.1 x 150 mm, 3 µm, Waters, Sydney, Australia) for analysis. A gradient mobile phase consisting of (A) 0.1% v/v formic acid in acetonitrile and (B) 10% v/v acetonitrile, 0.1% v/v formic acid and 10 mM ammonium formate in water was used at a flow rate of 0.4 mL/min. The starting mobile phase was 95% A, 5% B which was varied linearly over 16 min to 50 % A, 50% B then returned to the initial conditions and equilibrated for 4 min prior to injection of the next sample. The mass spectrometer was run in positive ionization mode with data collected using a Waters proprietary MSE data acquisition method at low collision (3 V) and a high collision energy ramp (8-14 V).

Parent or selected fragment ions were used for detection and quantification based on their monoisotopic mass. The qToF Premier (Waters, Sydney, Australia) mass spectrometer was run in positive ionisation mode with data collected using Waters proprietary MS^E data acquisition method. Mass spectrometer settings were as follow: capillary voltage 3.0 kV, sampling cone voltage 24.0 eV, extraction cone voltage 5.0 eV, source temperature 100 °C, desolvation temperature 300 °C, cone gas flow 30 L/Hr, desolvation gas flow 400.0 L/Hr, MS^E function 1 collision energy 3.0 V, MS^E function 2 collision energy ramp 8.0 – 14.0 V, collision Cell Entrance 2.0, collision Exit -10.0, collision Gas Flow 0.60 mL/min. Parent or selected fragment ions were used for detection and quantitation based on their monoisotopic mass. Retention times, corresponding parent or fragment mass, MS^E acquisition channel and QC performance data (five independent determinations at each of two concentrations) for each analyte are shown in Table 2.1.

Table 2.1: Analysis of Arginine metabolites.

Analyte	RT (min)	MS^E channel	Ion	m/z[1]	Int Std	QC_{low}[2] %CV	QC_{high}[2] %CV
ADMA	11.93	1	parent	203.16	d6-ADMA	6.4	7.1
L-ARG	11.06	1	parent	175.13	d4-HMA	9.0	10.0
CIT	9.34	1	fragment	159.09	d7-CIT	6.1	4.0
HMA	11.15	1	parent	189.15	d4-HMA	1.6	1.4
L-NMMA	11.38	1	parent	189.15	d4-HMA	8.6	14.4
ORN	11.38	1	parent	133.11	d6-ORN	5.1	3.5
SDMA	11.75	1	parent	203.16	d6-SDMA	4.2	4.3

Legend: ADMA, asymmetric dimethylarginine; L-ARG, L-arginine; CIT, L-citrulline; HMA, L-homoarginine; L-NMMA,N^G –monomethyl-L-arginine; ORN, L-ornithine; SDMA, symmetric dimethylarginine

[1]m/z for the positively charged analyte ion, that is $[M+H]^+$, data was extracted with a mass window of 0.05 Da

[2]QC_{low} and QC_{high} were prepared by spiking pooled human plasma (n=5) with a known amount of analyte.

CHAPTER 3: PROGNOSTIC UTILITY OF OXYGEN-SENSITIVE CARDIOVASCULAR MAGNETIC RESONANCE (OS-CMR) IMAGING IN DIABETIC AND NON-DIABETIC CHRONIC KIDNEY DISEASE (CKD) PATIENTS WITHOUT KNOWN CORONARY ARTERY DISEASE.

3.1 Introduction

Patients with chronic kidney disease (CKD) exhibit an increased incidence of cardiovascular disease (CVD), and cardiovascular mortality is about 10 – 30 times higher when compared to the non-CKD population, despite stratification for diabetes (9). Although renal transplantation significantly improves survival, CVD is still one of the most frequent causes of death post-transplant and accounts for 35-50% of all-cause mortality (40). The majority of the CKD patients with coronary artery disease (CAD) are asymptomatic and have multi-vessel coronary disease(5). Assessment of left ventricular function and CAD (both epicardial and microvascular dysfunction) is essential to define cardiovascular risk in these patients.

Reduction in LVEF generally occurs late in heart failure (281). Changes in myocardial deformation properties, such as Global Longitudinal Strain (GLS) and Myocardial Dispersion (MD), can precede reduction in LVEF and therefore provide insights into subclinical cardiac function in a variety of cardiac diseases (282, 283). Feature Tracking CMR (FT-CMR) allows quantification of strain, analogous to speckle tracking echo strain, using the standard steady-state free-precession (SSFP) sequence for ventricular volume assessment. It is a feasible and highly reproducible technique (284), and has been validated against CMR myocardial tagging (285, 286). Furthermore, although identifying subclinical cardiac dysfunction, FT-CMR derived

global strain and MD have been shown to predict adverse heart failure, and arrhythmic outcomes in ischaemic (287-290) and non-ischaemic diseases of the heart (290-292).

As outlined in chapter 1, current functional cardiac investigations are neither sensitive nor specific for assessment of myocardial ischaemia in CKD patients. Blood Oxygen Level Dependent CMR (BOLD-CMR), or Oxygen Sensitive CMR (OS-CMR), uses the paramagnetic properties of deoxygenated haemoglobin as an intrinsic contrast so that the transverse magnetisation or T2 time is increased when there is a drop in the proportion of deoxyhaemoglobin and decreased when there is a rise in the proportion of deoxyhaemoglobin. Myocardial deoxygenation or ischemia is characterized by a net relative increase of deoxygenated haemoglobin in the capillary blood and thus leads to T2 shortening, i.e. a drop in the OS-CMR Signal Intensity (ΔSI). OS-CMR has moderate accuracy in detecting significant epicardial coronary artery disease (125).

A recent study by our group utilising OS-CMR demonstrated significantly blunted myocardial oxygenation response to stress in CKD patients with no known cardiac disease when compared to healthy and hypertensive controls (127). In the current study we examine the prognostic utility of OS-CMR imaging and FT-CMR derived myocardial deformation properties in asymptomatic CKD patients with and without DM. We hypothesized that blunted myocardial oxygenation response to stress and abnormal myocardial deformation could be independent predictors of adverse events in asymptomatic CKD patients.

3.2 Methods

3.2.1 Study Population

79 participants with CKD were invited to participate at Flinders Medical Centre, a tertiary teaching hospital in South Australia, in 2012 – 2017. 36 of these 79 participants had already been recruited and their CMR scans performed and analysed as part of another study. The other 43 participants were recruited prospectively. Patients were included if they had severe renal failure as defined by an eGFR< 30 mL/min/1.73 m^2, or were requiring dialysis, or had a previous renal transplant with reasonable renal function (eGFR> 45 mL/min/1.73 m^2). Patients were excluded if they had standard MRI contraindications, asthma, second or third-degree heart block, left ventricular ejection fraction (LVEF) < 45%, or clinical heart failure. All participants gave written informed consent, and the study was approved by Southern Adelaide Clinical Human Research Committee (HREC/17/SAC/86). All 79 participants were prospectively followed for major adverse events (MAE), defined as all cause death, myocardial infarction, ventricular arrhythmia and hospitalization for pulmonary oedema.

3.2.2 Serum Biochemistry

All participants had blood samples collected for routine biochemistry, cell counts, haemoglobin, troponin T, CRP, thyroid stimulating hormone (TSH), Parathormone levels (PTH), iron studies and lipid studies. eGFR was calculated from serum creatinine using the CKD-Epidemiological Collaboration Formula.

3.2.3 CMR Protocol

All participants underwent scanning in a 3-T clinical MR scanner (Siemens, 3 T) and were instructed to refrain from caffeine 24 hours prior to the scan. The scans were performed with adenosine stress as previously described (127). Stress heart rate and blood pressures were obtained every minute of adenosine infusion. Each participant was questioned about the occurrence of adenosine effects: chest pain or tightness, shortness of breath, flushing, headache, and nausea.

3.2.4 CMR Analysis

CMR analysis was performed with CMR^{42} Version 4.1 and later versions (Circle Cardiovascular Imaging Inc, Calgary, Canada). Analysis of ventricular volumes, left ventricular mass and OS-CMR SI were performed as previously described **(119)**. The OS-CMR ΔSI was calculated as:

$$\Delta SI = (SI_{Stress} - SI_{Rest})/SI_{Rest} \text{ X } 100\%$$

where, SI_{Rest} = OS-CMR SI at rest, and SI_{Stress} = OS-CMR after adenosine stress.

Using the Feature Tracking module, endocardial and epicardial contours were traced in end-diastole using the 3-dimensional short-axis stack. Similarly, contours were traced in the 3 long axes cine images in end-diastole after defining the extent of the left ventricular cavity. The anterior right ventricular insertion point was marked on the short-axis slices. The software then calculated GLS semi-automatically. MD was then calculated as the standard deviation of the times to peak segmental (AHA 17 segment model) longitudinal strain.

3.3 Statistical analysis

All analysis was performed using Stata 15.0 (StataCorp, college Station, Texas, USA). Descriptive statistics are presented as mean +/- standard deviation for normally distributed continuous variables, median (inter-quartile range) for skewed continuous variables and as frequency (%) for categorical variables. Differences in patient characteristics between those that experienced a MAE and those that did were compared using independent t-tests and either chi-squared test of association or Fishers Exact as appropriate.

Each subject follow-up time was from the date of enrolment into the study until April 2018 or the date of death. For patients that experienced one or more MAE, their follow-up time was split according to the dates of the MAEs. We used Cox regression to perform univariate and multivariate analysis and obtain hazard ratios for OS-CMR, GLS and MD on MAE. Each subject was permitted to have multiple MAE events in the analysis. Standard errors were adjusted for within-subject correlation using the cluster(id) vce(robust) option in Stata. We tested the final multivariate model for the assumption of proportional odds both overall and for each variable separately using the proportional hazards test based on the Schoenfeld residuals. We also showed the estimated survival rates by GLS and MD status using unadjusted Kaplan-Meier curves that were categorised into binary variables with cut-points of -14% and 70 milliseconds respectively.

3.4 Results

Of the total of 79 patients, 32 patients had diabetes mellitus, 19 were receiving dialysis and 10 patients had a previous renal transplant at study entry. The mean follow-up was 2.7 years (range 0.3 to 7.2 years). A total of 15 (19%) patients had

events. There was a total of 29 events, of which 21 events were observed in 12 diabetic patients. There were 9 deaths, 6 non-fatal myocardial infarcts, 1 ventricular arrhythmia and 13 heart failure admissions.

Table 3.1 compares the baseline characteristics of patients who did and did not have events. There was no significant difference between the two groups with regards to age, sex or eGFR. There was a higher likelihood of patients experiencing events of being diabetic (80% versus 31%; p= <0.01), being on dialysis (40% versus 20%; p= 0.17or having increased indexed left ventricular mass (88.2 ± 24.1 gm versus 62.2 ± 14.9 gm, p= <0.01). Furthermore, patients who had events had significantly impaired GLS compared to those that did not (-14.6 ± 4.0 % versus -17.4 ± 3.6 %; p= <0.01).

Table 3.1 Comparison Between CKD Patients With and Without Major Adverse Events (MAE)

	CKD patients without MAE (n=64)	CKD patients with MAE (n=15)	*p*-value
Age (years)	62.3 ± 12.6	66.2 ± 12.3	0.28
Male sex	41 (64)	10 (67)	1.00
BMI (kg/m^2)	29.2 ± 6.8	25.9 ± 4.7	0.08
eGFR (mL/min/1.73 m^2)	23 ± 20.8	21.1 ± 18.6	0.73
Dialysis	13 (20)	6 (40)	0.17
Diabetes Mellitus	20 (31)	12 (80)	<0.01
LVEF (%)	68.9 ± 9.9	61.9 ± 13.7	0.03
LVMi (g/m^2)	62.2 ± 14.9	88.2 ± 24.1	<0.01
GLS (%)	-17.4 ± 3.6	-14.6 ± 4.0	<0.01
MD (milliseconds)	113.2 ± 51.6	96.3 ± 28.9	0.23
Dyslipidemia	28 (44)	6 (40)	1.00
Smoking History	21 (33)	6 (40)	0.76
Anti-platelet Agent	11 (17)	0 (0)	0.11
Beta blocker	23 (36)	5 (33)	1.00
ACE inhibitor	18 (28)	1 (7)	0.10
Angiotensin Receptor Blocker	12 (19)	3 (20)	1.00
Calcium channel blocker	30 (47)	3 (20)	0.08
Statin	26 (41)	6 (40)	1.00

Data are presented as n (%) or mean ± SD.

3.4.1 Age, Co-morbidities and Serum Biochemistry

On univariate Cox regression analysis (Table 3.2), age and diabetes mellitus were significant predictors of future adverse events while only a trend was noted for eGFR.

Table 3.2: Results of univariate Cox regression for adverse events in the CKD Patients

	Hazard Ratio	95% CI	*p*-value
Age (years)	1.07	1.00 – 1.13	0.04
eGFR (mL/min/1.73 m^2)	0.98	0.95 – 1.01	0.16
Diabetes Mellitus	5.63	1.60 – 19.87	0.01
LVMi (g/m^2)	1.04	1.01 – 1.06	<0.01
LVEF (%)	0.92	0.87 – 0.97	<0.01
RVEF (%)	0.97	0.92 – 1.02	0.18
MD (milliseconds)	0.99	0.98 – 1.00	0.16
GLS (%)	1.27	1.10 – 1.45	<0.01
Negative OS-CMR ΔSI (%)	4.29	1.09 – 16.88	0.04
OS-CMR ΔSI (continuous variable) (%)	0.94	0.91 – 0.98	<0.01

Table 3.3 Results of multivariate Cox regression for adverse events in the CKD Patients

	Hazard Ratio	95% CI	*p*-value
Age (years)	1.05	1.01 – 1.09	0.01
LVMi (g/m^2)	1.03	1.01 – 1.05	0.01
LVEF (%)	0.94	0.87 – 1.01	0.06
eGFR (mL/min/1.73 m^2)	1.01	0.98 – 1.04	0.48
GLS (%)	1.16	0.96 – 1.40	0.14
Negative OS-CMR ΔSI (%)	3.09	0.98 – 9.74	0.05
OS-CMR ΔSI (continuous variable) (%)[1] **All Subjects** **Subjects without Diabetes** **Subjects with Diabetes**	0.95 0.84 1.01	0.90 – 1.01 0.77 - 0.91 0.95 – 1.07	0.08 <0.01 0.76

[1]There was a significant SI change X Diabetes interaction (HR=1.16, 95% CI=1.05-1.27; p=<0.01).

On multivariate Cox regression analysis (Table 3.3), age and diabetes were significant predictors whereas eGFR was not. There was a significant interaction

between diabetes and OS-CMR ΔSI and this is described in more detail later. Higher values of serum urea, creatinine, C-reactive protein, or being on dialysis did not significantly increase risk.

3.4.2 CMR Ventricular volumes and mass

Indexed LV mass and LVEF were significant predictors of adverse events on univariate analysis, while RVEF was not. On multivariate analysis, indexed LV mass was an independent predictor of adverse events, while only a trend was noted for LVEF.

3.4.3 Change in OS-CMR SI with Stress

Figure 3.1: Kaplan-Meier survival graph showing CKD patients with negative OS-CMR SI change values had significantly higher major adverse events (MAE) rate compared to those with positive OS-CMR SI change values (p=<0.01).

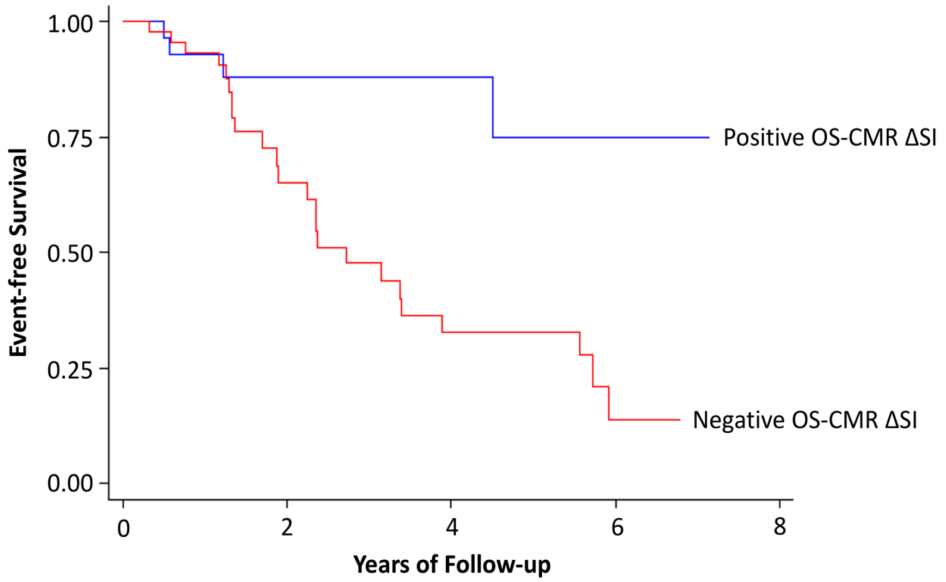

26% (12/47) of participants with negative OS-CMR ΔSI had adverse events versus only 9% (3/32) of those with positive ΔSI (p=0.001). On univariate analysis, negative

OS-CMR ΔSI was associated with adverse outcome (HR=4.29, 95% CI= 1.09-16.88, p=0.04).

Figure 3.1 shows the estimated survival according to a positive ΔSI versus negative ΔSI. Furthermore, SI as a continuous variable was also significantly associated with adverse outcomes (HR=0.94, 95% CI= 0.91-0.98, p= <0.01).

During multivariate Cox regression analysis, an interaction term was introduced between the OS-CMR ΔSI (as a continuous variable) and diabetes mellitus since this was significant (HR=1.16, 95% CI=1.05-1.27; p=<0.01) (Table 3.3). Amongst subjects without DM there was a significant protective effect of the OS-CMR ΔSI (HR=0.84, 95% CI=0.77 – 0.91; p= <0.01) (Figure 3.2). However, amongst subjects with DM, the effect OS-CMR ΔSI did not predict risk (HR=1.01, 95%CI=0.95-1.07; p=0.76). Therefore, those with DM have a poor outcome and those without DM and an impaired OS-CMR ΔSI also have poor outcome.

Figure 3.2: Estimated survival according to SI change (OS-CMR ΔSI) and presence or absence of DM from multivariate Cox regression analysis after adjustment for age, GLS, LVEF, indexed LV mass and eGFR (p=<0.01). OS-CMR ΔSI values used here are +10% and -10% which represent approximately 1 SD above and 1 SD below the mean Δ OS-CMR respectively.

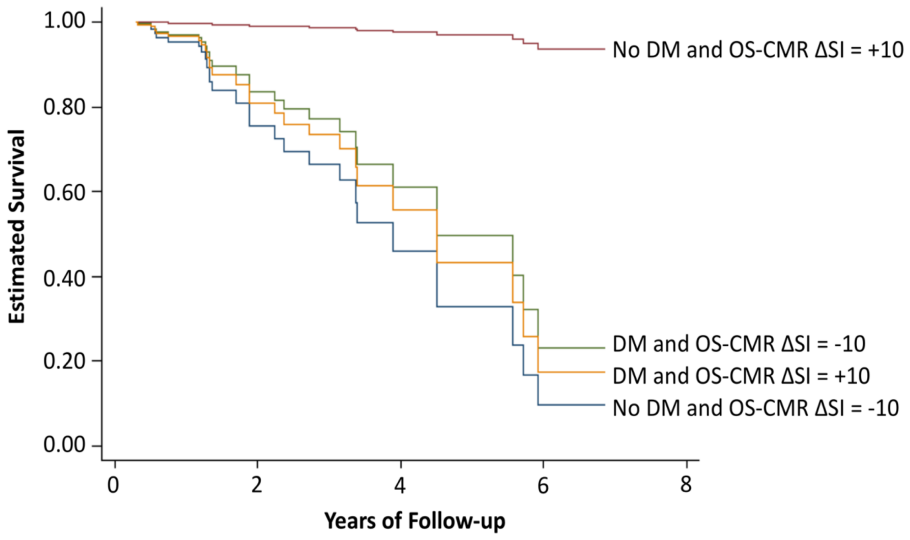

On multivariate analysis, negative OS-CMR ΔSI was an independent predictor of future adverse events (HR=3.09, 95% CI= 0.98 – 9.78, p=0.05).

Table 3.4 compares the characteristics of the CKD patients with and without DM. There was no significant difference between the age of the patients or the need for dialysis in the two groups. Patients with diabetes had poorer renal function, increased indexed LV mass and reduced LV systolic function as denoted by lower LVEF and impaired GLS. Myocardial oxygenation response to stress, as measured by OS-CMR ΔSI, was impaired in both groups. This impairment was worse in patients with DM when compared to those without (OS-CMR ΔSI -1.8 ± 14.3 vs 4.1 ± 10.2, p= 0.04), with the impairment being seen in all three coronary artery territories.

Table 3.4: Clinical Characteristics and CMR findings in CKD Patients With and Without DM

	CKD patients without DM (n=47)	CKD patients with DM (n=32)	p value
Age (years)	63.1 ± 12.8	63.5 ± 12.3	0.89
eGFR	25.2 ± 23.6	18.5 ± 13.4	0.15
Hypertension	36 (77)	28 (88)	0.26
LVMi	60.8 ± 14.6	75.7 ± 22.3	<0.01
LV Ejection Fraction, %	69.3 ± 9.7	65.3 ± 12.3	0.11
Dialysis	12 (26)	7 (22)	0.79
GLS	-17.7 ± 3.7	-15.6 ± 3.7	0.02
MD	118 ± 58.5	102.2 ± 31.0	0.17
OS-CMR ΔSI (all territories)	4.1 ± 10.2	-1.8 ± 14.3	0.04
OS-CMR ΔSI (LAD territory)	5.1 ± 12.5	-1.2 ± 16.0	0.05
OS-CMR ΔSI (LCx territory)	4.9 ± 11.7	-2.8 ± 16.0	0.02
OS-CMR ΔSI (RCA territory)	2.2 ± 12.6	-1.4 ± 14.9	0.25
Adverse Events	3 (6)	12 (38)	<0.01

Data are presented as n (%) or mean ± SD.

3.4.4 Feature Tracking CMR (FT-CMR) derived Global Longitudinal Strain (GLS) and Mechanical Dispersion (MD)

FT-CMR derived GLS was significantly associated with adverse events (HR=1.27, 95% CI= 1.10-1.45, P=<0.01) on univariate analysis (Figure 3.3). Even though there was a significant correlation between GLS and log MD (r=0.29, p=0.01), MD failed to predict adverse events (HR=0.99, 95% CI= 0.98 – 1.00, p= 0.16). On multivariate analysis, there was a trend noted for GLS to predict MAE (HR=1.16, 95% CI= 0.96-1.4, p=0.14).

Figure 3.3: Kaplan-Meier survival graph showing CKD patients with GLS > -14 had significantly higher major adverse events (MAE) rate compared to those with GLS < -14 (p=<0.01).

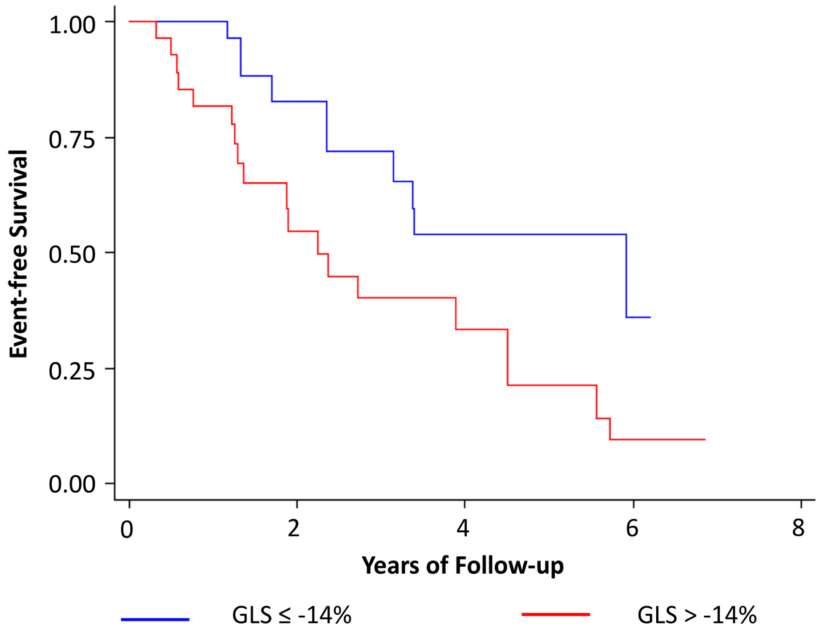

3.5 Discussion

This is the first study to assess the ability of OS-CMR CMR to predict cardiac prognosis in any population. Here it has been shown that in CKD patients, the blunted myocardial oxygenation response to stress as assessed by the OS-CMR

CMR technique is associated with adverse prognosis, driven by the predictive capacity in the non-diabetic population. Specifically, in the non-diabetic population, an impaired OS-CMR signal to stress was associated with a risk of a major adverse event rate equivalent to the diabetic population. Our findings may have implications for the future risk stratification of CKD patients.

Painless myocardial ischaemia occurs more commonly in the CKD patients compared to individuals with normal renal function, and is associated with a higher mortality rate in CKD patients (19). Epicardial and/or microvascular coronary disease is often present in this population (20, 21) and can cause silent or asymptomatic myocardial ischaemia (5, 6). Both microvascular and epicardial coronary diseases are associated with a higher major adverse cardiac event rate (6, 22). Therefore, there is a strong case for the investigation of this very high-risk group of patients even before development of symptoms that suggest CAD. In this regard, a non-invasive test that can risk stratify this population would be valuable. Despite the need, a non-invasive test for the accurate diagnosis of coronary artery disease in this high-risk CKD group, which is both sensitive and safe, is lacking. Current diagnostic investigations of myocardial ischaemia have lower sensitivity and specificity in CKD patients.

OS-CMR CMR technique using adenosine has the capability of detecting ischaemia from both epicardial and microvascular coronary artery disease without the use of gadolinium contrast and without issues of blunted chronotropic response. It exploits the paramagnetic properties of deoxyhaemoglobin as an endogenous contrast agent, with increased deoxyhaemoglobin content leading to signal reduction on T2-weighted images (120). A previous prospective study assessing the diagnostic

accuracy of OS-CMR in suspected CAD yielded an accuracy of 84%, a sensitivity of 92%, and a specificity of 72% for detecting myocardial ischemia and 86%, 92%, and 72%, respectively, for identifying significant coronary stenosis (125). We have previously demonstrated impaired myocardial oxygenation response to stress in CKD population without previously known epicardial CAD, irrespective of the degree of left ventricular hypertrophy and the presence of diabetes mellitus (127). Patients with both negative and positive OS-CMR SI Change values had similar degree of epicardial CAD (as defined by stenosis of >50%), implying the involvement of microvascular disease contributing to blunted myocardial oxygenation response and poorer cardiac prognosis.

Myocardial ischaemia has been attributed to coronary steal in patients with multi-vessel CAD associated with significant reductions in blood flow to microvascular collateral-dependent myocardium (293). Our current study suggests that blunted myocardial oxygenation to stress is predictive of future adverse cardiac events and is consistent with previous studies that have demonstrated that abnormal myocardial perfusion scintigraphy in CKD patients was associated with higher incidence of cardiac events and mortality (30-36). Furthermore, myocardial perfusion PET derived coronary flow reserve (CFR, defined as the ratio of peak to resting flow) has been shown to be strongly associated with cardiovascular risk regardless of CKD severity (29). The changes in CFR were detectable in stages 1-4 CKD without further changes in stage 5 or dialysis dependant CKD. This may suggest that the cause of microvascular dysfunction in CKD patients is associated with CKD rather than associated with the effects of dialysis.

Our findings in diabetic patients are similar to a recent study where it was shown that patients with Type 2 DM had worse OS-CMR ΔSI when compared to non-diabetic controls (BOLD ΔSI 7.3±7.8 vs 17.1 ±7.2). (294) In our study, the impairment is seen to be worse in both the diabetic and non-diabetic groups and the likely cause for this is the inclusion of patients with eGFR <30 mL/min/1.73m² in our cohort whereas this was an exclusion criterion in the other study. The difference in the OS-CMR oxygenation response between the diabetic and non-diabetic patients in our study is not regional but involves all three coronary artery territories (see Table 4). Coronary microvascular dysfunction and endothelial dysfunction in DM and CKD can lead to both impaired resting global myocardial perfusion and a failure to increase coronary blood flow during stress. This can explain the presence of multi-territory involvement of oxygenation impairment in our study. It may be worthwhile to mention here that not all the impairment in myocardial oxygenation in our diabetic group would be due to the presence of diabetes per se, as associated conditions like worse renal function and LVH can also result in myocardial oxygenation impairment independent of the presence of diabetes.

Despite more deoxygenation to stress being seen in our diabetic cohort, OS-CMR SI change was not a significant independent predictor of adverse events in these patients. There can be several reasons to explain this finding. Diabetes itself is a very strong risk factor for CAD and perhaps, when present, statistically overshadows the importance of other physiological mechanisms contributing to CAD risk. Furthermore, presence of diabetes was associated with worse renal function, increased indexed LV mass, reduced LVEF and more impaired GLS. All of these can result in poor clinical outcomes and therefore reduce the predictive capability of OS-CMR ΔSI as an independent predictor of adverse events in this very complex group of patients.

Due to the risk of nephrogenic systemic fibrosis with gadolinium contrast in patients with severe renal dysfunction, gadolinium studies were not undertaken in the CKD cohort who instead underwent FT-CMR strain evaluation as a measure of myocardial fibrosis. Abnormal left ventricular (LV) geometry and functions are correlated with a poor cardiovascular prognosis and detected frequently in CKD patients (295, 296). Left ventricular ejection fraction is preserved in early-stage CKD, but systolic deformation is abnormal, consistent with an adverse cardiovascular prognosis (297). Worsening of renal function has been associated with a sub-clinical reduction of systolic function as quantified by 2D strain analysis (298). Pathophysiologically, GLS is a parameter that is measured at rest and is thought to mainly relate to replacement fibrosis (scar) and/or interstitial fibrosis. MD is predominantly related to interstitial fibrosis. OS-CMR SI change, on the other hand, is a parameter that is measured both at rest and at stress and is thought to mainly relate to myocardial ischemia. Egred *et al* have shown that scarred myocardium has lower stress OS-CMR response (299). Therefore, scarred myocardium may result in both impaired GLS and reduced OS-CMR SI change. In our study there was a weak correlation between OS-CMR and GLS (r=-0.04, p= 0.72) and both were significant predictors of adverse events on univariate analysis. However, our study also indicates that GLS was not an independent predictor of adverse events on multivariate analysis whereas OS-CMR ΔSI was (in the non-diabetic population) suggesting mechanisms independent of myocardial scarring affecting the prognosis in these patients. As microvascular dysfunction can affect the OS-CMR response but not GLS in these patients, this would be the likely cause for the poor prognosis in these patients.

3.5.1 Limitations

Due to the small sample size, these results are hypothesis-generating and therefore need to be confirmed with larger studies. Secondly, CTCA or invasive coronary angiogram was not performed (due to advanced renal failure) in our patient cohort and therefore it may be possible that some patients might have had significant undiagnosed CAD. However, care was taken during recruitment to exclude patients with known CAD, positive other stress investigations and/or even symptoms suggestive of CAD. Thirdly, the CKD patients were unable to have gadolinium contrast due to the risk of nephrogenic systemic fibrosis, therefore late gadolinium enhancement could not be performed. Non-contrast T1 mapping would have been useful for assessing diffuse fibrosis, but unfortunately, this was not available at the study centre at the time of commencement of study. Lastly, although image quality was generally good, artefacts could not always be resolved with frequency and shim adjustments and this could lead to reduced specificity.

3.6 Conclusion

This study confirms the hypothesis that blunted myocardial oxygenation response to stress is an independent predictor of adverse events in non-diabetic patients with CKD. This may lead to better detection of asymptomatic ischaemia in this high-risk population, especially in the non-diabetic population, and perhaps improve overall cardiac prognosis and survival in these patients. However, the question of whether medical management or intervention is indicated in such CKD patients with asymptomatic ischaemia, and whether it improves prognosis, needs to be answered by prospective randomised controlled studies.

3.7 Future Directions

This pilot study needs to be confirmed with larger, multi-centre studies, which may allow inclusion of patients with less severe kidney disease into the study. Multi-centre randomized control trials are needed to examine the short-term and long-term outcome of medical versus revascularisation therapy in the renal failure population with silent myocardial iscahemia.

CHAPTER 4: GADOLINIUM FREE CARDIAC MAGNETIC RESONANCE (CMR) STRESS T1 MAPPING IN PATIENTS WITH CHRONIC KIDNEY DISEASE (CKD).

4.1 Introduction

Cardiovascular disease is the leading cause of mortality in patients with chronic kidney disease (CKD). Currently available functional tests to assess for myocardial ischaemia are neither sensitive nor specific in CKD. Therefore, there is an unmet need for a non-invasive test that is sensitive, specific and safe in this very high-risk group of patients with CKD. In the previous chapter it was shown that in CKD patients, the blunted myocardial oxygenation response to stress as assessed by the OS-CMR technique is associated with adverse prognosis. This could be one such method novel to investigate for possible CAD in this group of patients.

Recent studies have shown that T1 mapping, when used with a vasodilator stress, can distinguish between normal, ischaemic, infarcted and remote (i.e. segments without ischaemia or infarct in the heart of patients with diagnosed CAD) myocardium without the need for gadolinium contrast agents (144). This method has subsequently been validated against invasive coronary measures for the accurate detection and differentiation between epicardial coronary artery disease and microvascular dysfunction (145). This technique may also be of specific use in the chronic kidney disease population where both epicardial coronary artery disease and microvascular dysfunction are common and use of gadolinium-based contrast agents is not preferred. T1 mapping technique may have a few advantages over OS-CMR. Firstly, the method of stress T1 mapping described in the studies above used measurements in three myocardial slices whereas OS-CMR measurements (described in chapter 3)

were performed on one slice only. Secondly, T1 mapping can be performed on both 1.5T and 3T magnets and therefore can be widely available to all centres whereas OS-CMR measurements require a 3T magnet which has limited availability.

In this chapter we aimed to evaluate the potential of T1 mapping at rest and during adenosine stress as a novel method for ischaemia detection without the use of Gadolinium contrast in patients with CKD. We hypothesized that in patients with CKD, stress T1 response is impaired and can differentiate between remote, ischaemic and infarcted segments.

4.2 Methods

4.2.1 Study Population

34 patients with CKD and 7 healthy age-matched controls underwent scanning in a 3-T MR scanner (Siemens, Skyra) between 2017 – 2019. Of the 34 patients, 14 patients had known CAD, as defined by presence of symptoms consistent with IHD and either previous myocardial infarction or demonstrated myocardial ischaemia on functional testing (exercise stress testing, stress echocardiography or nuclear myocardial perfusion scan). The remainder 20 patients did not have diagnosed CAD or symptoms to suggest CAD. Patients were included if they had severe renal failure as defined by an eGFR< 30 mL/min/1.73 m^2, or were requiring dialysis, or had a previous renal transplant with reasonable renal function (eGFR> 45 mL/min/1.73 m^2). 7 of the 20 patients without CAD were receiving dialysis and 1 patient was a previous renal transplant recipient. 8 of the 14 patients without CAD were receiving dialysis and none had received a renal transplant prior to the study. Standard MRI contraindications, asthma, second or third-degree heart block, left ventricular ejection fraction (LVEF) < 45%, and clinical heart failure were exclusion criteria.

All participants gave written informed consent, and the study was approved by the regional ethics committee (HREC/17/SAC/86).

4.2.3 CMR Protocol

All participants underwent scanning in a 3-T clinical MR scanner (Siemens, 3 T Skyra) and were instructed to refrain from caffeine 24 hours prior to the scan. All scans started with Half-Fourier single-shot turbo spin echo and Fast imaging with steady precession localizers. Cine images were acquired in vertical and horizontal long-axis, and 10 short-axis images covering the entire left ventricle, using a retrospective ECG gating steady-state free precession (SSFP) sequence (repetition time [TR] 3 ms, echo time [TE] 1.5 ms, flip angle 55°, 18 phases).

For T1 map imaging, the same method as that published by Liu et al (144, 145) was used. In brief, 3 slices (basal, mid-ventricular and apical) were acquired at mid-diastole. Resting T1-maps (ShMOLLI) were acquired using 5-7 images with specific TI = 100-5000 ms, collected using SSFP readouts in a single breath-hold, typically: TR/TE= 201.32/1.07 ms, flip angle = 35°, matrix = 192x144, 107 phase encoding steps, interpolated voxel size = 0.9 x0.9x8mm, cardiac delay time TD = 500 ms; 206 ms acquisition time for single image.

During adenosine stress (140 µg/kg per minute), T1 maps were acquired in the 3 slices corresponding to the rest images. The images were acquired, while continuing adenosine stress, every 40 seconds starting at 250 seconds after initiation. Stress heart rate and blood pressures were obtained every minute of adenosine infusion. Each participant was questioned about the occurrence of adenosine effects: chest pain or tightness, shortness of breath, flushing, headache, and nausea.

4.2.4 CMR Analysis

CMR analysis was performed with CMR[42] Version 5.9.1 (Circle Cardiovascular Imaging Inc, Calgary, Canada). Left ventricular mass and left and right ventricular volumes and functions were calculated using the 3-dimensional short-axis stack by tracing the endocardial and epicardial contours in end-diastole and end-systole. Left ventricular mass, left and right ventricular end-diastolic volumes, and end-systolic volumes were indexed to body surface area.

Myocardial T1 analysis was performed on the T1 maps acquired during rest and stress. The operator did not have the information regarding patient characteristics at the time of analysis and therefore was blinded to this information. The CMR software measured Myocardial T1 after manually tracing the endocardial and epicardial contours. The 3 short-axis T1 map images (basal, mid-ventricular and apical) were divided into 16 segments according to the American Heart Association 17-segment model, with omission of the segment 17 which is the true apex of the heart and cannot be assessed on the short axis. The mean myocardial T1 (measured in milliseconds, msec) within each segment was obtained, both at rest and stress. The T1 change was then calculated as:

$$\Delta T1 = (T1_{Stress} - T1_{Rest})/T1_{Rest} \times 100\%$$

Using the Feature Tracking module, endocardial and epicardial contours were traced in end-diastole using the 3-dimensional short-axis stack. Similarly, contours were traced in the 3 long axes cine images in end-diastole after defining the extent of the left ventricular cavity. The anterior right ventricular insertion point was marked on the short-axis slices. The software then calculated GLS semi-automatically. MD was then

calculated as the standard deviation of the times to peak segmental (AHA 17 segment model) longitudinal strain.

4.2.5 Defining Segments

When using CMR, ischaemic segments should ideally be described as those with perfusion abnormalities seen post gadolinium injection and infarcted segments should be described as those with delayed gadolinium enhancement. However, due to severe CKD, Gadolinium contrast was not administered. Hence, LGE was not to be performed, and irreversibly injured myocardial segments were defined as regions of myocardial thinning (end-diastolic wall thickness <6mm on cine CMR) with associated wall motion abnormalities and/or ECG Q waves. This provides an alternate, but clinically acceptable criteria for describing infarcted segments. CAD patients were defined as those with previously known history of myocardial infarction, known occlusive coronary artery disease on prior angiography and/or evidence of significant myocardial ischemia. For the latter case, significant myocardial ischemia was defined as those individuals with least moderate reversible myocardial ischaemia on imaging functional stress testing (exercise stress echocardiography or cardiac nuclear imaging) and/or those supplied by a major epicardial coronary artery with ≥ 70% stenosis on a prior coronary angiogram. Remote myocardial segments were defined as those with no demonstrable ischaemia or infarction.

4.3 Statistical Analysis

All analysis was performed using Stata 15.0 (StataCorp, college Station, Texas, USA). Descriptive statistics are presented as mean +/- standard deviation for normally distributed continuous variables, median (inter-quartile range) for skewed continuous variables and as frequency (%) for categorical variables. Comparisons

between groups were performed using 2-sided independent t-tests or Fishers Exact test as appropriate. All p values <0.05 were considered significant. The between-observer variance and the within-subject variance were estimated using a random intercept mixed-effects model. The between-observer CV was calculated using (between-observer variance/mean) x 100 and the within-subject CV was calculated using the (within-subject variance/mean) x 100.

4.4 Results

4.4.1 Baseline Characteristics

Table 4.1: Comparison Between CKD Patients With and Without CAD

	All CKD patients (n=34)	CKD patients without CAD (n=20)	CKD patients with CAD (n=14)	*p*-value[1]
Age (years)	61.4 ± 13.7	56.7 ± 14.7	68.2 ± 8.6	0.013
Male sex	20 (59)	11 (55)	9 (64)	0.728
BMI (kg/m^2)	31.6 ± 7.4	31.4 ± 8.1	31.9 ± 7.5	0.856
eGFR (mL/min/1.73 m^2)	15.4 ± 8.9	14.3 ± 9.0	17.0 ± 8.5	0.385
Dialysis	15 (44)	7 (35)	8 (57)	0.296
Diabetes Mellitus	20 (59)	7 (35)	13 (93)	0.001
LVEF (%)	60.2 ± 11.6	62.4 ± 8.7	57.2 ± 14.6	0.202
LVMi (g/m^2)	61.7 ± 19.0	61.4 ± 17.8	62.1 ± 21.2	0.918
Δ T1 (%)	5.2 ± 4.3	7.1 ± 4.1	2.6 ± 3.0	0.001
Dyslipidemia	10 (29)	5 (25)	5 (36)	0.704
Smoking History	6 (18)	4 (20)	2 (14)	1.00
Anti-platelet Agent	15 (44)	2 (10)	13 (93)	<0.001
Beta blocker	15 (44)	4 (20)	11 (79)	0.001
ACE inhibitor	8 (24)	5 (25)	3 (21)	1.00
Angiotensin Receptor Blocker	9 (26)	4 (20)	5 (36)	0.435
Calcium channel blocker	15 (44)	11 (55)	4 (29)	0.171
Statin	22 (65)	10 (50)	12 (86)	0.066

[1]For the comparison between CKD patients with and without CAD.

Of the 34 patients, 14 patients had known coronary artery disease, 20 patients had diabetes mellitus, 15 were receiving dialysis, 29 patients were hypertensive, and 10 patients had dyslipidemia. Of the 14 patients with CAD, 7 patients had incomplete revascularisation in the past (6 had coronary artery bypass grafting and 1 had percutaneous coronary intervention with stent insertion).

Table 4.1 compares the baseline characteristics of CKD patients with and without CAD. Patients with CAD were older, had worse GLS and higher eGFR. Importantly, all patients with CAD had diabetes mellitus and were on treatment with anti-platelet agents, beta blockers and statins. Very few patients without CAD were on such treatment.

4.4.2 Myocardial T1 Reactivity

When compared to normal controls, patients with CKD had higher resting T1 values (1202 ± 65 msec vs 1151 ± 50 msec, *p*= <0.001) and impaired ΔT1 (5.3 ± 5.8% vs 7.1 ± 3.8%, p= <0.001). Table 4.2 compares the T1 reactivity between the different segment types in the normal and CKD population. Figure 4.1 and Figure 4.2 are the graphical representation of the same data.

Table 4.2: T1 Reactivity in normal and CKD myocardial tissue

	Normal Controls	All CKD	CKD (No CAD)	CKD (with CAD)	Remote Segments	Ischaemic Segments	Infarcted Segments
Rest T1 (msec)	1151 ± 50	1202 ± 65	1203 ± 69	1199 ± 59	1185 ± 50	1207 ± 57	1265 ± 88
Stress T1 (msec)	1233 ± 54	1266 ± 86	1292 ± 89	1230 ± 65	1221 ± 58	1237 ± 71	1260 ± 67
T1 Reactivity (%)	7.1 ± 3.8	5.3 ± 5.8	7.2 ± 6.0	2.6 ± 4.2	3.0 ± 3.5	2.5 ± 4.6	-0.2 ± 5.8

Figure 4.1: Myocardial T1 at Rest and During Adenosine Stress. T1 values at rest in normal and remote tissue were similar and significantly lower than in ischemic regions. Infarct T1 was the highest of all myocardial tissue. During adenosine stress, normal and remote myocardial T1 increased significantly from baseline, while T1 in ischemic and infarcted regions remained relatively unchanged.

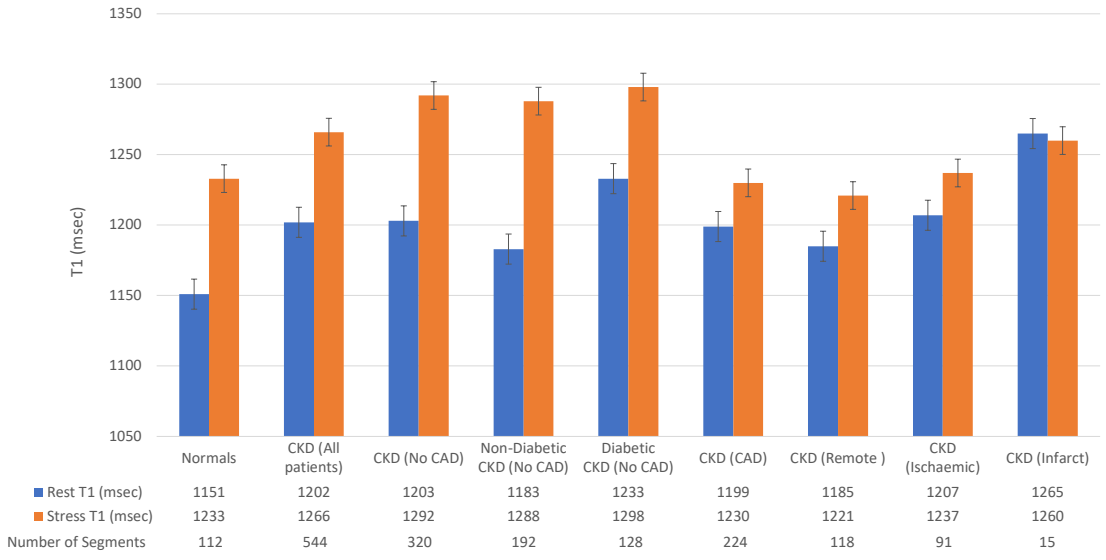

	Normals	CKD (All patients)	CKD (No CAD)	Non-Diabetic CKD (No CAD)	Diabetic CKD (No CAD)	CKD (CAD)	CKD (Remote)	CKD (Ischaemic)	CKD (Infarct)
Rest T1 (msec)	1151	1202	1203	1183	1233	1199	1185	1207	1265
Stress T1 (msec)	1233	1266	1292	1288	1298	1230	1221	1237	1260
Number of Segments	112	544	320	192	128	224	118	91	15

CKD patients with CAD had significantly lower ΔT1 when compared to CKD patients without CAD (2.6 ± 4.2% vs 7.2 ± 6.0%, p= <0.001). The resting T1 values for remote, ischaemic and infarcted myocardium were 1185 ± 50 msec, 1207 ± 57 msec, and 1265 ± 88 msec and ΔT1 values were 3.0 ± 3.5%, 2.5 ± 4.6%, and -0.2 ± 5.8% respectively.

Figure 4.2: Relative T1 reactivity (ΔT1) in the remote and ischaemic myocardium were significantly blunted compared to normal, and completely abolished in infarcted regions.

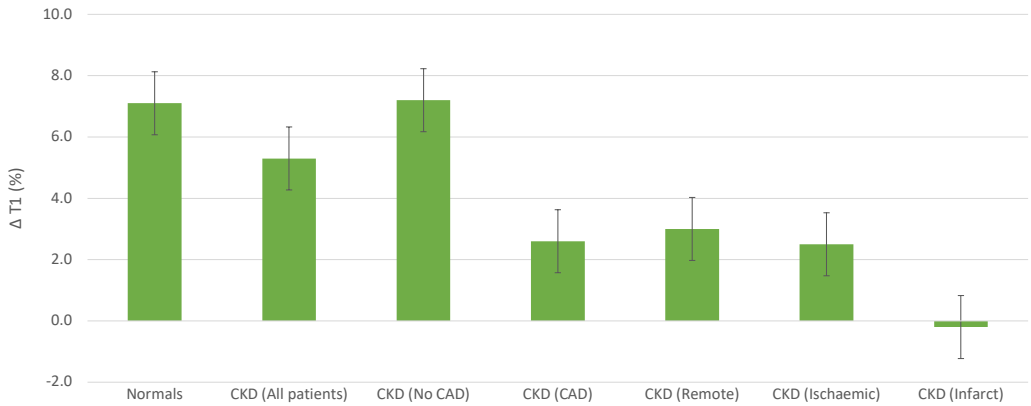

	Normals	CKD (All patients)	CKD (No CAD)	CKD (CAD)	CKD (Remote)	CKD (Ischaemic)	CKD (Infarct)
Δ T1 (%)	7.1	5.3	7.2	2.6	3.0	2.5	-0.2
Number of Segments	112	544	320	224	118	91	15

Compared to the non-diabetic CKD patients without CAD, the diabetic CKD patients without CAD had significantly higher resting T1 (1233 ± 60 msec vs 1189 ± 68 msec, $p<0.001$) values and blunted stress T1 reactivity (5.3 ± 4.3 % vs 7.9 ±6.7, $p<0.001$).

4.4.3 Reproducibility

To assess the inter-observer variability of stress myocardial responses, 80 myocardial segments (from 5 participants) were analysed by two experienced observers. To assess intra-observer variability, one of these observers reanalysed the 80 segments (at least 6 weeks after the initial analysis). Stress T1 mapping was highly reproducible with low intra-observer and inter-observer variabilities (co-efficient of variation 6.8% and 3.4%, respectively).

4.5 Discussion

This is the first study to assess Stress CMR T1 mapping in the diagnosis of myocardial ischaemia in the CKD population. Here it has been shown that stress T1 reactivity is impaired in the CKD population. Furthermore, stress T1 was able to distinguish between normal, ischaemic, infarcted and remote myocardium in the CKD population without the need for gadolinium contrast agents. These findings are similar, in all subgroups to that seen in a previous study (144) using the same methodology in non-CKD patients. However, the ΔT1 values are lower in our study likely due to significant microvascular disease in our advanced CKD patients. Significantly higher resting T1 in ischemic myocardium compared to normal controls and remote regions may help detection of ischemia without vasodilatory stress, in the absence of other causes of T1 elevations at rest (136, 137, 139, 141, 300, 301).

The oxygen demand-supply mismatch which results in myocardial ischaemia is governed by Myocardial Blood Flow (MBF) and Myocardial Blood Volume (MBV) (302, 303). Increase in oxygen demand causes coronary arteriole vasodilatation and capillary recruitment resulting in an increase in MBF (302). Higher MBF causes increase in MBV. Approximately 10% of the myocardial voxel content is occupied by blood volume, which therefore contributes to the myocardial T1 (134). Increased myocardial T1 values act as a surrogate for increased myocardial water; hence coronary vasodilatation, which increases MBV, is expected to prolong T1.

There are a few very important findings from this study that needs to be highlighted (Table 4.3):

1. Patients with CKD had significantly higher resting T1 values compared to normal volunteers (1202 ± 65 msec vs 1151 ± 50 msec, $p<0.001$) and lower stress T1 reactivity (5.3 ± 5.8 % vs 7.1 ± 3.8 %, $p<0.001$). The likely reason for the elevated baseline T1 findings in the CKD patients is interstitial myocardial fibrosis or increased resting MBV due to CAD (microvascular or epicardial) or a combination of the two processes. The lower stress T1 reactivity could be due to CAD (microvascular or epicardial).

2. Even though the non-CAD patients with CKD had significantly higher resting T1 values compared to normal volunteers (1203 ± 69 msec vs 1151 ± 50 msec, $p<0.001$), the stress T1 reactivity was similar (7.2 ± 6.0 % vs 7.1 ± 3.8 %, $p=0.839$). The reason for the elevated resting T1 is similar to above. However, the finding of similar stress T1 reactivity in the 2 groups is difficult to explain.

3. Even though the CAD patients with CKD had similar resting T1 values compared to non-CAD patients with CKD (1199 ± 59 msec vs 1203 ± 69 msec, p=0.469), the stress T1 reactivity was significantly impaired in the CAD patients with CKD (2.6 ±4.2 % vs 7.2 ± 6.0 %, p<0.001) and the likely explanation for this would be significant epicardial occlusive CAD in these patients.

4. Non-diabetic CKD patients without CAD had significantly lower resting T1 values when compared to diabetic CKD patients without CAD (1183 ± 68 msec vs 1233 ± 60 msec, p<0.001) and higher stress T1 reactivity (8.5 ± 6.6 % vs 5.3 ± 4.3 %, p<0.001). CKD itself is associated with microvascular dysfunction, but it seems these processes are more pronounced if the patient additionally has diabetes.

5. When compared to ischaemic segments, remote segments had lower resting T1 values (1185 ± 50 msec vs 1207 ± 57 msec, p=0.004) and only slightly higher stress T1 reactivity (3.0 ± 3.5 % vs 2.5 ± 4.6 %, p=0.390). This indicates the presence of significant interstitial myocardial fibrosis and microvascular CAD in the remote segments of CKD patients with CAD.

6. Infarcted segments have the highest resting T1 values and no stress T1 reactivity. The obvious reason for this is replacement fibrosis after myocardial infarction. When compared to ischaemic segments, infarcted segments had significantly higher resting T1 values (1265 ± 88 msec vs 1207 ± 57 msec, p=0.015) and lower stress T1 reactivity (-0.2 ± 5.8 % vs 2.5 ± 4.6 %, p=0.089).

Table 4.3: T1 profiles of myocardial tissue based on rest and stress native T1 mapping.

	Normal Controls	All CKD	CKD (No CAD)	CKD (with CAD)	Remote Segments	Ischaemic Segments	Infarcted Segments
Rest T1 (msec)	Normal	↑	↑	↑	↑	↑	↑↑
T1 Reactivity (%)	↑↑↑	↑↑	↑↑↑	↑	↑	↑	↔

In the previous chapter it was shown that the absolute change in the OS-CMR value was a significant predictor of adverse outcomes in the non-diabetic CKD population. It may be possible that this may hold true for stress T1 response too. Prognostic importance of stress T1 mapping in CKD and other disease conditions such as diabetes, hypertension, pulmonary hypertension, non-ischaemic cardiomyopathy, ischaemic heart disease and other inflammatory/immune-mediated diseases would be a very interesting area for future research.

4.5.1 Limitations

Our study has several limitations. Firstly, due to the small sample size, these results are hypothesis-generating and need to be confirmed with larger studies. Secondly, CTCA or invasive coronary angiogram was not performed (due to advanced renal failure) in our cohort without diagnosed CAD and therefore possible that some patients had significant undiagnosed CAD.

4.6 Conclusions

Adenosine stress and rest T1 mapping can differentiate between normal, infarcted, ischemic, and remote myocardial tissue classes with distinctive T1 profiles. Stress/rest T1 mapping with CMR holds promise for ischemia detection without the

need for gadolinium contrast. This technique may be of specific use in CKD population where coronary artery disease is common and is associated with poor clinical outcomes, but the use of gadolinium-based contrast agents is not possible or preferred.

4.7 Future Directions

This study paves the way for larger multi-centre studies to determine the wider diagnostic, and perhaps prognostic, value of stress T1 mapping in the CKD population to guide clinical decision-making and predict long-term prognosis. Larger clinical and population-based studies would be useful to produce standardized ranges for ΔT1, confirm our findings.

CHAPTER 5: COMPARISON OF THE DIAGNOSTIC UTILITY OF NOVEL GADOLINIUM-FREE CARDIOVASCULAR MAGNETIC RESONANCE STRESS IMAGING METHODS IN PATIENTS WITH CHRONIC KIDNEY DISEASE

5.1 Introduction

Chronic kidney disease is associated with a higher incidence and prevalence of coronary artery disease (both epicardial and microvascular) when compared to the normal population. CVD is the most frequent cause of death in patients with advanced CKD. Current functional tests for assessment of CAD has reduced sensitivity and specificity in the CKD population. The presence of asymptomatic myocardial ischaemia in CKD patients further complicates this problem.

Therefore, there is a need to develop novel methods of testing for CAD which is feasible in the CKD population. The previous 2 chapters look at two such novel techniques. In chapter 3 it has been shown that stress OS-CMR is impaired in CKD patients without symptoms or diagnosis of CAD and can offer prognostic information. In chapter 4 it has been shown that stress T1 reactivity is impaired in the CKD population. There is a gradient of T1 reactivity impairment from normal when compared to CKD patients without CAD and CKD patients with CAD, such that rest/stress T1 mapping may help distinguish between remote, ischaemic and infarcted myocardial segments in CKD patients without the use of Gadolinium based contrast agents. Although both methods avoid Gadolinium chelate contrast, and use IV adenosine vasodilatory stress, T1 mapping stress imaging uses 3 slices of the LV, as opposed to stress BOLD CMR method which only uses one slice. Hence, T1 methods give better coverage of the LV and, at least theoretically, may be a superior

diagnostic test in this population. No study has yet compared these 2 Gadolinium free methods of stress CMR assessment in CKD. The aim of this study is to compare the accuracy of these 2 methods in the diagnosis of coronary artery disease.

5.2 Methods

5.2.1 Study Population

19 patients with CKD and 7 healthy age-matched controls underwent scanning in a 3-T MR scanner (Siemens, Skyra) between 2017 – 2019. These were patients from the cohort in chapter 4 who had some form of functional testing (exercise stress test, stress echocardiography or nuclear myocardial perfusion scan) and/or invasive coronary angiography reports available for comparison. Of the 19 patients, 14 patients had known CAD. The remainder 5 patients did not have diagnosed CAD or symptoms to suggest CAD. Patients were included if they had severe renal failure as defined by an eGFR< 30 mL/min/1.73 m^2, or were requiring dialysis, or had a previous renal transplant with reasonable renal function (eGFR> 45 mL/min/1.73 m^2). Standard MRI contraindications, asthma, second or third-degree heart block, left ventricular ejection fraction (LVEF) < 45%, and clinical heart failure were exclusion criteria.

All participants gave written informed consent, and the study was approved by the regional ethics committee (HREC/17/SAC/86).

5.2.2 CMR Protocol

Cine imaging and stress OS-CMR and T1 imaging were performed as outlined in Chapter 2.

5.2.3 CMR Analysis

CMR analysis was performed with CMR[42] Version 5.9.1 (Circle Cardiovascular Imaging Inc, Calgary, Canada) as outlined in Chapter 2.

5.3 Statistical Analysis

All analysis was performed using Stata 15.0 (StataCorp, college Station, Texas, USA). Descriptive statistics are presented as mean +/- standard deviation for normally distributed continuous variables, median (inter-quartile range) for skewed continuous variables and as frequency (%) for categorical variables. Comparisons between groups were performed using 2-sided independent t-tests or Fishers Exact test as appropriate. Logistic regression was used to assess the association between each of the 2 tests (OS-CMR and T1) and the presence of CAD. The C-statistic was used to assess the diagnostic accuracy of the test, and a comparison of the C-statistics was used to determine whether OS-CMR or T1 change had greater diagnostic accuracy than the other. Sensitivity and Specificity were reported using the area-under the receiver operating curve. We also plotted the sensitivity and specificity against the recorded change in each test from rest to ischaemia. Reproducibility was assessed using the coefficient of variation (CV). The between-observer variance and the within-subject variance were estimated using a random intercept mixed-effects model. The between-observer CV was calculated using (between-observer variance/mean) x 100 and the within-subject CV was calculated using the (within-subject variance/mean) x 100.

5.4 Results

5.4.1 Baseline Characteristics

Of the total of 19 patients, 14 patients had CAD. Of the 14 patients with CAD,13 had Type 2 diabetes mellitus, 8 were receiving dialysis, 7 patients had incomplete revascularisation in the past (6 had coronary artery bypass grafting and 1 had percutaneous coronary intervention with stent insertion). Of the 5 patients without CAD, 2 had diabetes mellitus and 2 were receiving dialysis.

Table 5.1: Comparison Between CKD Patients With and Without CAD

	All CKD patients (n=19)	CKD patients without CAD (n=5)	CKD patients with CAD (n=14)	*p*-value[1]
Age (years)	63.2 ± 12.3	49.2 ± 10.5	68.2 ± 8.6	0.002
Male sex	12 (63)	3 (60)	9 (64)	0.877
BMI (kg/m^2)	31.9 ± 6.8	31.7 ± 4.8	31.9 ± 7.5	0.947
eGFR (mL/min/1.73 m^2)	16.7 ± 9.3	15.8 ± 11.3	17.0 ± 8.5	0.831
Dialysis	10 (53)	2 (40)	8 (57)	0.052
Diabetes Mellitus	15 (79)	2 (40)	13 (93)	0.015
LVEF (%)	57.9 ± 12.9	58.4 ± 7.6	57.2 ± 14.6	0.819
LVMi (g/m^2)	62.9 ± 18.4	65.2 ± 8.0	62.1 ± 21.2	0.650
Δ OS-CMR SI (%)	8.8 ± 6.8	11.2 ± 5.4	7.9 ± 7.2	0.300
Δ T1 (%)	3.7 ± 3.6	6.9 ± 3.5	2.6 ± 3.0	0.026
Dyslipidemia	7 (37)	2 (40)	5 (36)	0.877
Smoking History	3 (16)	1 (20)	2 (14)	0.757
Anti-platelet Agent	15 (79)	2 (40)	13 (93)	0.015
Beta blocker	11 (58)	0 (0)	11 (79)	0.003
ACE inhibitor	4 (21)	1 (20)	3 (21)	0.963
Angiotensin Receptor Blocker	7 (37)	2 (40)	5 (36)	0.877
Calcium channel blocker	7 (37)	3 (60)	4 (29)	0.231
Statin	16 (84)	4 (80)	12 (86)	0.757

[1]For the comparison between CKD patients with and without CAD.

Table 5.1 compares the baseline characteristics of CKD patients with and without CAD. Patients with CAD were more likely to be older, diabetic and be on treatment with anti-platelet agents, beta blockers and statins.

5.4.2 Correlation between Δ OS-CMR SI and Δ T1

There was a total of 114 segments analysed in the 19 CKD patients with 30 segments from the 5 patients in the 'CKD without CAD group' and 84 segments from the 14 patients in the 'CKD with CAD' group. We performed both patient-type analysis (using average OS-CMR SI and T1 values) and segment-type analysis (using individual OS-CMR SI and T1 values).

There was no correlation found between resting OS-CMR SI and T1 values (Figure 5.1) on segment-type analysis (r=-0.03, p=0.66) or patient-type analysis (r=0.20, p=0.25).

Figure 5.1: Correlation between Resting OS-CMR SI and Resting T1. A, Segment-type analysis and B, Patient-type analysis. There was no correlation seen between resting OS-CMR and resting T1 on either type of analysis.

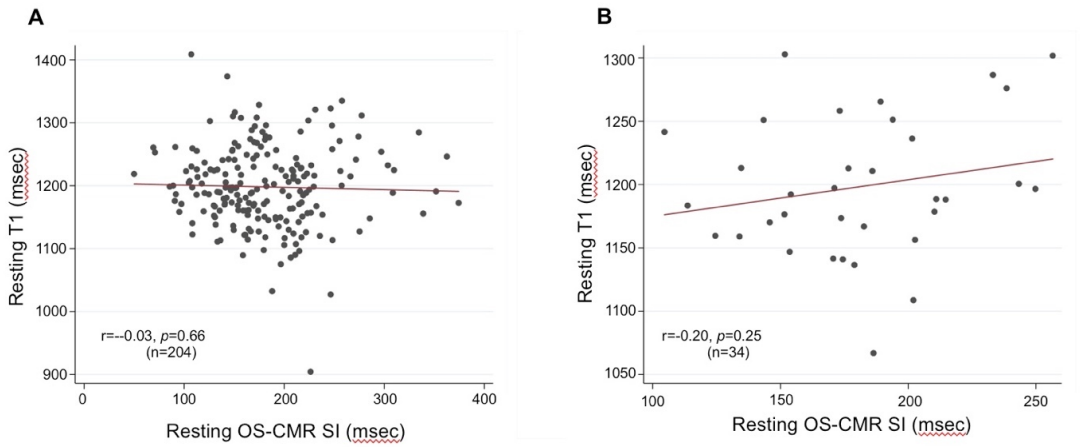

Again, no correlation was found between Δ OS-CMR SI and Δ T1 (Figure 5.2) on segment-type analysis (r=0.07, p=0.31) or patient-type analysis (r=0.12, p=0.48).

Figure 5.2: Correlation between Δ OS-CMR SI and Δ T1. A, Segment-type analysis and B, Patient-type analysis. There was no correlation seen between Δ OS-CMR and Δ T1 on either type of analysis.

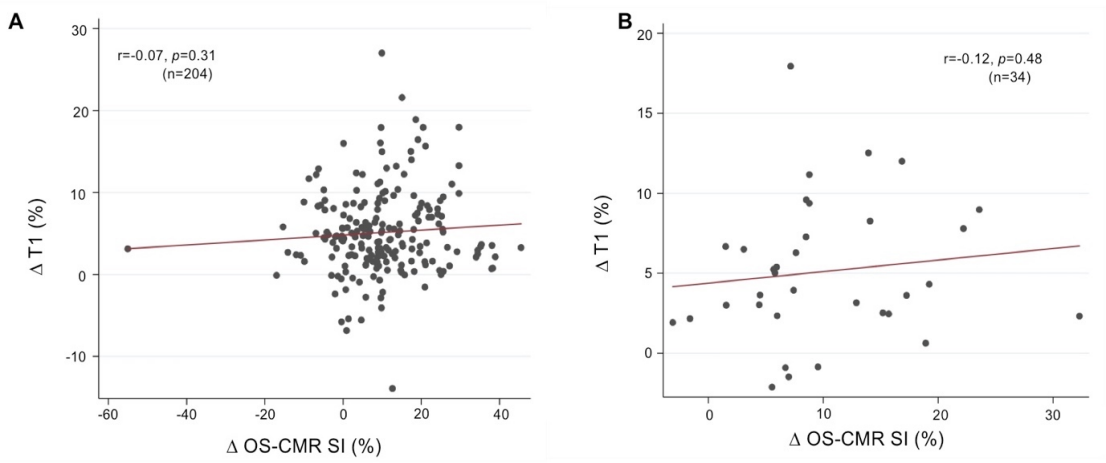

5.4.3 Predictive capacity of Δ OS-CMR SI and Δ T1 in diagnosing CAD in CKD patients

Figures 5.3A and 5.3B show the Receiver Operating Curves (ROC) for Δ OS-CMR SI and Δ T1 respectively. The area under the ROC curve (AUC), which is a measure of

Figure 5.3: ROC curves for Δ OS-CMR SI (A) and Δ T1 (B) in predicting CAD in CKD patients using segment-type analysis. Δ T1 was a more accurate test than Δ OS-CMR SI (area under curve of 0.84 versus 0.65, *p* = 0.057) for diagnosis of coronary artery disease in CKD patients.

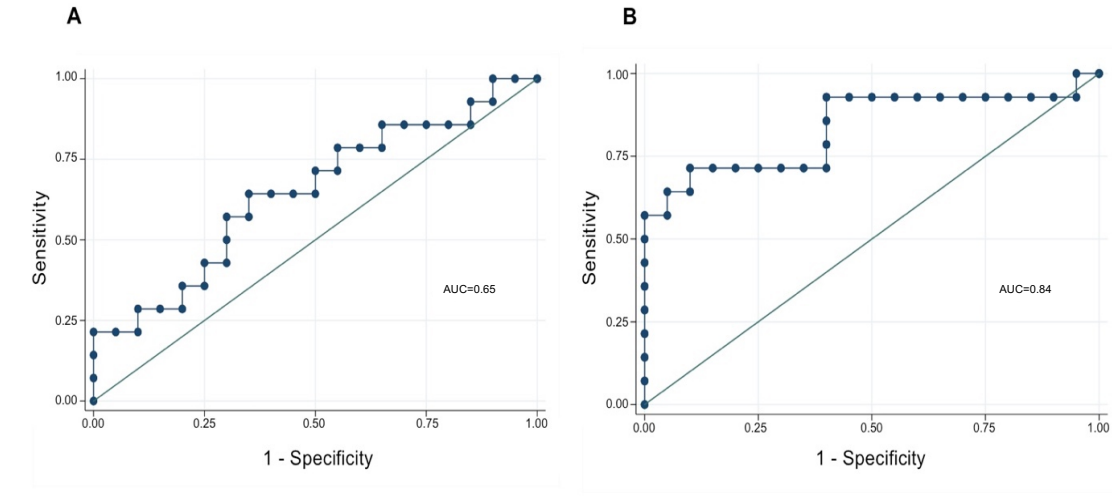

how well the test distinguished between the two groups of patients (CKD without CAD and CKD with CAD) was higher for Δ T1 compared to Δ OS-CMR SI (0.84 versus 0.65, p = 0.057).

Δ T1 was a better predictor of CAD in CKD patients (Odds ratio 0.63, 95%CI 0.46-0.88, p= 0.006) when compared to Δ OS-CMR (Odds ratio 0.93, 95%CI 0.84-1.03, p= 0.162) (Table 5.2). Therefore, for every unit fall in Δ T1, the likelihood of CAD increased by 59%, while for every unit fall in Δ OS-CMR, the likelihood of CAD increased by 7.5%.

Table 5.2: Predictive capacity of Δ OS-CMR SI and Δ T1 in predicting CAD in CKD patients using segment-type analysis.

	Odds Ratio	95% CI	*p*-value
Δ OS-CMR SI	0.93	0.84 – 1.03	0.162
Δ T1	0.63	0.46 – 0.88	0.006

5.4.4 Comparison of Δ OS-CMR SI and Δ T1 with other conventional tests for myocardial ischaemia in CKD patients

We compared the ability of Δ OS-CMR SI and Δ T1 to detect CAD in CKD patients with other conventional methods of assessment of coronary artery disease such as Exercise Stress Echocardiogram (ESE), Dobutamine Stress Echocardiogram (DSE), Nuclear stress test and Invasive Coronary Angiogram (Table 5.3 & Figure 5.4) using region-type analysis (based on coronary artery territories).

When interpreting the results of ESE/DSE and nuclear stress tests, the test result was called negative if there was no evidence for reversible myocardial ischaemia in the myocardial segment, and positive if there was reversible myocardial ischaemia in

Table 5.3: Comparison of Δ OS-CMR SI and Δ T1 with other conventional tests for myocardial ischaemia in CKD patients. Coronary artery territories with combined test negative had significantly higher Δ T1 values when compared to those with combined test positive. There was no significant difference seen in the Δ OS-CMR SI values.

			OS-CMR		T1 Mapping	
Test	Result	n	Δ OS-CMR SI (%)	*p*-value	Δ T1 (%)	*p*-value
ESE/DSE	Negative	16	7.9 ± 12.8	0.561	6.2 ± 5.4	0.016
	Positive	8	5.0 ± 7.7		0.9 ± 2.3	
Nuclear Scan	Negative	17	9.7 ± 7.4	0.279	5.2 ± 4.0	0.237
	Positive	4	5.4 ± 2.2		2.4 ± 4.6	
Coronary Angiogram	Negative	6	5.6 ± 17.4	0.778	2.0 ± 0.8	0.630
	Positive	21	7.0 ± 7.9		2.6 ± 2.7	
Combined Test	Negative	24	9.5 ± 10.5	0.285	5.6 ± 4.9	0.009
	Positive	24	6.7 ± 7.4		2.4 ± 2.9	

that myocardial segment. When interpreting the results of invasive coronary angiogram, the test result was called negative if the major epicardial coronary artery supplying that myocardial segment had < 70% stenosis and positive if the major epicardial coronary artery supplying that myocardial segment had ≥ 70% stenosis on a prior invasive coronary angiogram. We also assessed the ability of Δ OS-CMR SI and Δ T1 in differentiating between myocardial segments belonging to different coronary artery territories with any one of the above tests positive versus those with all tests negative.

Coronary artery territories with a negative DSE/ESE test had significantly higher Δ T1 values (Table 5.3) when compared to those with a positive DSE/ESE test (6.2 ± 5.4 vs 0.9 ± 2.3, p=0.016). However, Δ OS-CMR SI was not able to differentiate between those two groups. Neither Δ OS-CMR SI nor Δ T1 was significantly different in coronary artery territories with positive or negative results on nuclear stress test or

invasive coronary angiography. Coronary artery territories with all test negative had significantly higher Δ T1 values when compared to those with any test positive (5.6 ± 4.9 vs 2.4 ± 2.9, p=0.009). Again, Δ OS-CMR SI was not able to differentiate between these two groups.

5.4.5 Sensitivity and specificity of Δ OS-CMR SI and Δ T1 in predicting CAD in CKD patients

Figure 5.4A shows a plot of varying sensitivities and specificities of Δ OS-CMR SI in the diagnosis of CAD in CKD patients versus varying Δ OS-CMR SI values. At a cut-off Δ OS-CMR SI value of about 8% the test was approximately 65% sensitive and specific in distinguishing patients with and without CAD.

Figure 5.4: Plot of sensitivity/specificity versus test cut-off point for Δ OS-CMR SI (A) and Δ T1 (B) in predicting CAD in CKD patients using patient-type analysis. Overall Δ T1 was approximately about 75% sensitive and specific in diagnosing CAD at a cut-off value of about 4%, while Δ OS-CMR SI was only about 65% sensitive and specific in diagnosing CAD at a cut-off value of about 8%.

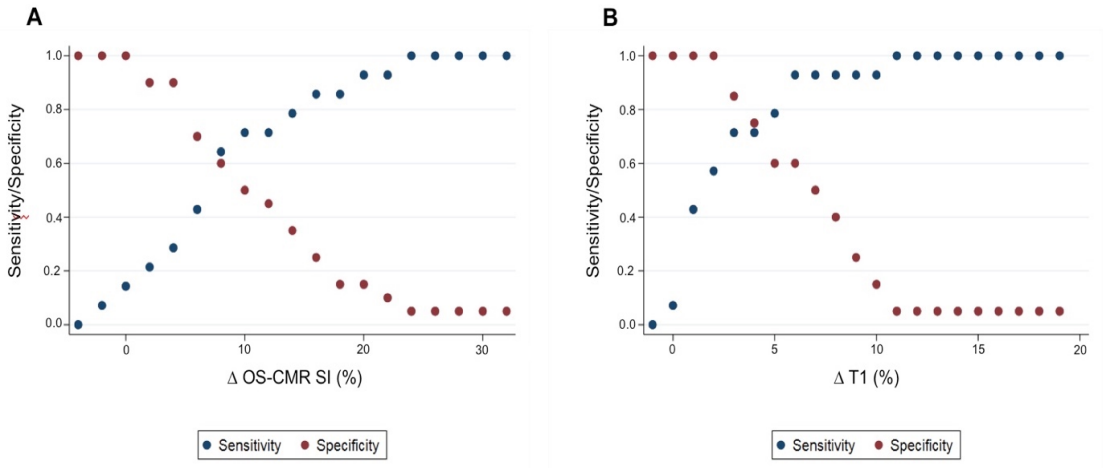

Figure 5.4B shows a similar plot using Δ T1 values. The test was approximately 75% sensitive and specific in distinguishing patients with and without CAD at a cut-off Δ T1 value of about 4%.

5.4.6 Test Reproducibility

Two experienced observers analysed ΔT1 in 5 subjects (80 myocardial segments). Stress T1 mapping was highly reproducible with low intra-observer and inter-observer variabilities (co-efficient of variation 6.8% and 3.4%, respectively).

The same observers analysed Δ OS-CMR SI in 8 subjects (48 myocardial segments) who were scanned twice at two different time points. There was good interobserver variability (co-efficient of variation 5.5%), but poor inter-scan variability (co-efficient of variation 26.6%).

5.5 Discussion

The pathophysiology of CAD and myocardial ischaemia is complex and therefore, before we discuss the results, it is important to understand what is measured by Δ OS-CMR SI and Δ T1 in comparison to other conventional tests for detection of myocardial ischaemia.

Progressive myocardial oxygen demand-supply mismatch during myocardial ischaemia leads to a sequence of events, starting with myocardial perfusion abnormalities and followed sequentially by metabolic alterations, wall motion abnormalities, ECG changes, and angina. This is known as the ischaemic cascade. The relative timings of the events assessed by the different diagnostic tests and the underlying pathophysiological processes involved are shown in Figure 5.5 and Table 5.4.

Figure 5.5: Progressive myocardial oxygen supply–demand mismatch leads to a sequence of events which eventually results in the symptom of angina. Shown here are the relative timings of the events assessed by the different tests for the assessment of myocardial ischaemia.

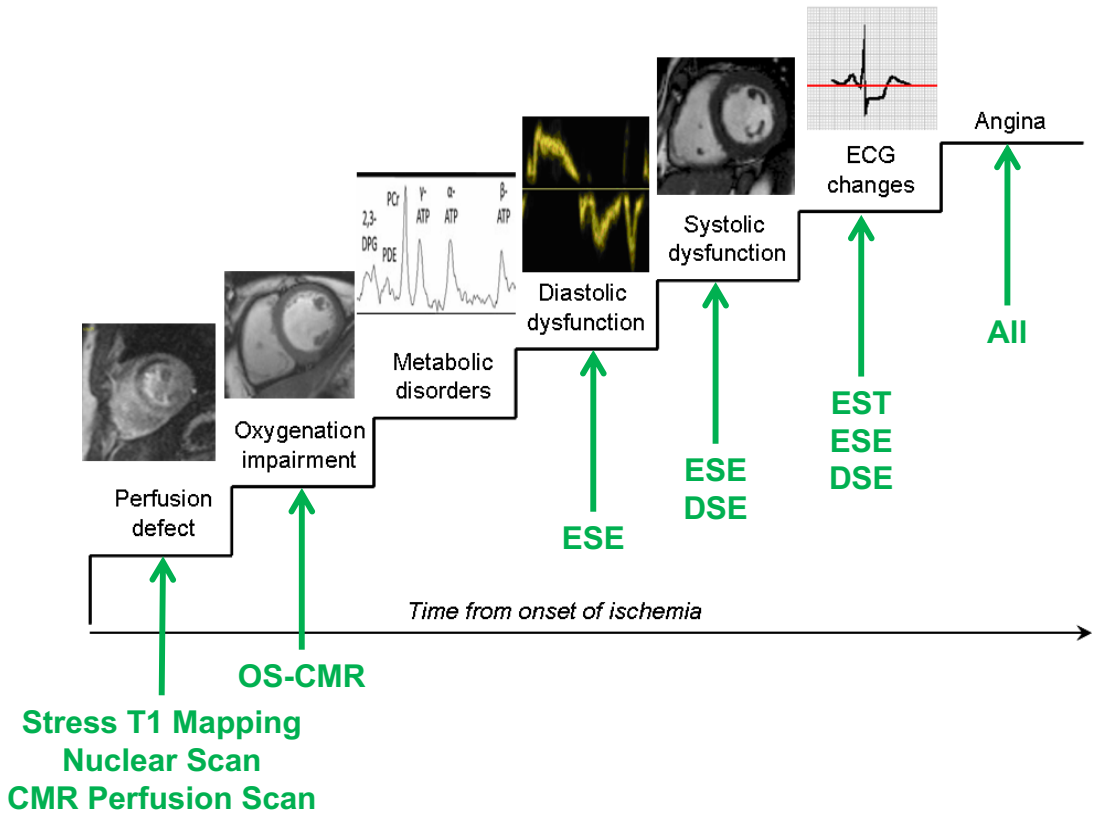

Exercise stress testing (EST) assessment depends on patient symptoms, ECG changes and hemodynamic response, all of which occur late in the ischaemic cascade. ESE and DSE findings are dependent on patient symptoms, ECG changes, hemodynamic response and systolic wall-motion abnormalities, which too occur relatively late in the ischaemic cascade. Nuclear perfusion scan and CMR based stress perfusion scan measure the relative change in myocardial blood flow (MBF) between rest and stress. Invasive coronary angiogram measures the narrowing in the lumen of epicardial coronary arteries (either due to fixed plaque disease or reversible coronary artery spasm). OS-CMR technique exploits the paramagnetic properties of the body's intrinsic contrast agent, haemoglobin. The transition from diamagnetic

oxyhemoglobin to paramagnetic deoxyhemoglobin results in a change in magnetic resonance signal intensity and thereby generates oxygen-dependent contrast. Therefore, OS-CMR could be a more sensitive technique for detecting CAD as ischemia is the initiator of the ischemic cascade. Myocardial blood volume (MBV) constitutes ~10% of the total myocardial volume at rest (142) and may increase two-fold during coronary vasodilatory stress (111, 143). Increased myocardial T1 values act as a surrogate for increased myocardial water; hence coronary vasodilatation, which increases MBV, is expected to prolong T1 and allow detection of microvascular and myocardial blood volume changes during ischemia. MBV may relate better to cardiomyocyte metabolism by reflecting changes in myocardial oxygen consumption, which is a more reliable marker of cellular ischemia.

Table 5.4: Comparison of the pathophysiological mechanisms involved in the various tests for the assessment of myocardial ischaemia in the CKD population.

	EST	DSE	ESE	Nuclear MPS	CT Coronary Angiogram	Invasive Coronary Angiography	CMR Perfusion Scan	ΔOS-CMR SI	Δ T1
MBV									✓
MBF				✓			✓		
Tissue Oxygenation								✓	
Tissue Perfusion				✓			✓		✓
Diastolic Dysfunction		✓	✓						
Systolic Dysfunction		✓	✓						
ECG Changes	✓	✓	✓	✓					
Angina	✓	✓	✓	✓			✓	✓	✓
Coronary Stenosis					✓	✓			
FFR					✓	✓			

It is recognised that the interplay between myocardial ischaemia, perfusion, and oxygenation in the setting of CAD is complex and that myocardial oxygenation and perfusion may become dissociated. Karamitsos et al. found that 40% of myocardial segments with stress myocardial blood flow below the cut-off of 2.45 mL/min/g did

not show deoxygenation (119). It is tempting to speculate that the normal oxygenation measurements seen in these segments with impaired perfusion indicate the absence of true ischaemia in these territories despite reduced regional blood flow. Arnold et al. studied the correlation between adenosine stress perfusion CMR and adenosine OS-CMR and also confirmed that oxygenation and perfusion were not strongly correlated (r= -0.26) (125).

The study described in this chapter extends these results further by showing that tissue oxygenation and MBV (as assessed by Δ OS-CMR SI and Δ T1) correlated poorly with myocardial blood flow (as assessed by nuclear perfusion scan). These results are more dissociated than that seen in the aforementioned studies that examined perfusion and oxygenation, and the likely cause for this is our patient group selection. In contrast to these prior studies, we studied patients with advanced kidney disease where microvascular disease is very prevalent. Nuclear perfusion scan or invasive coronary angiogram are less sensitive in detecting microvascular ischaemia and therefore did not correlate well with Δ OS-CMR SI and Δ T1 which are sensitive tests in this respect. There was better correlation seen between the novel tests and ESE/DSE which, although occurring later in the ischaemic cascade, are also sensitive to microvascular disease.

Both Δ OS-CMR SI and Δ T1 had moderate sensitivity and specificity (Table 5.5) and comparable to other conventional tests for the detection of myocardial ischaemia in CKD patients.

Table 5.5: Comparison of the sensitivities and specificities of Δ OS-CMR SI and Δ T1 with other conventional tests.

Test	EST	DSE	ESE	MPS	ΔOS-CMR SI	Δ T1
Sensitivity (%)	36	80	Possibly similar to DSE	69	65	75
Specificity (%)	91	89	Possibly similar to DSE	77	65	75

In this study Δ T1 seems to be a more accurate test than Δ OS-CMR SI in detecting CAD in the CKD population. However, one should exercise caution while interpreting the results of these tests, and it may even be possible that there is a degree of complimentary information to be derived from the two tests, as there may be other independent factors that influence the results from each of the two tests apart from the common pathology of stress induced myocardial ischaemia. The presence of diffuse interstitial fibrosis and resting myocardial ischaemia (i.e., higher MBV at rest and resultant lower perfusion reserve) in CKD patients may have resulted in higher resting T1 values and concomitant lower Δ T1 values. At the same time, CKD may be associated with metabolic changes to avert ischaemia in the face of hypoperfusion resulting in a down-regulation of energy requiring processes, such as that thought to occur in hibernating myocardium. This may result in a degree of physiological reserve that results in decreased tissue deoxygenation during hypoperfusion and therefore apparent higher Δ OS-CMR SI values in the patient group with advanced CKD than what would be expected. Furthermore, the high prevalence of balanced ischaemia in the CKD patients might have influenced the results of one test more than the other. Above discussed factors may also explain the poor correlation seen between resting OS-CMR versus resting T1 and also Δ OS-CMR SI versus Δ T1 in these patients. Furthermore, not only the accuracy but also the prognostic value of a test should be considered when deciding on the appropriate choice of investigation for detection of

CAD in CKD patients. It is important to note in this regard that in chapter 3 it was seen that even though the Δ OS-CMR SI was significantly lower in CKD patients (without CAD) with diabetes when compared to those without diabetes, Δ OS-CMR SI was an independent predictor of adverse outcomes in the non-diabetic patients but not in diabetic patients (304). At this time, prognostic data is lacking for Δ T1. Therefore, it seems, the interpretation of these two tests may be more complex and of more value in certain patient groups than in others.

As discussed in chapter 1, there is no consensus regarding the optimum choice of investigation (or the 'gold standard') for the diagnosis of myocardial ischaemia in the CKD population. Fractional flow reserve (FFR), which is a measure of ischaemia-related increase in blood flow and therefore indicates the likelihood of a coronary stenosis to cause myocardial ischaemia, was not performed as the use of contrast agents were avoided. In the absence of such a gold standard, Δ OS-CMR SI and Δ T1 have been compared to other tests like EST, ESE, DSE, nuclear scan and invasive coronary angiography which themselves have reduced sensitivity and specificity in the CKD population. Furthermore, the ability of these other tests and Δ T1 to predict outcomes in the CKD population is not known. This prognostic ability of a test should be considered more important than the correlation between the diagnostic abilities of the tests when deciding on the optimum choice of investigation. Larger studies assessing the diagnostic and prognostic ability of these tests are needed before we can confirm that one test is better than the other.

5.5.1 Limitations

This study has a few limitations. Firstly, due to the small sample size, these results are hypothesis-generating and therefore need to be confirmed with larger studies.

Secondly, CTCA or invasive coronary angiogram with FFR was not performed (due to advanced renal failure) in our cohort without diagnosed CAD and therefore it may be possible that some of them might have had significant undiagnosed CAD. However, care was taken while recruitment to exclude patients with known CAD or even symptoms suggestive of CAD. Thirdly, in the absence of a gold standard diagnostic test and prognostic information of the different tests in the CKD population it is difficult to conclude on a definite choice of investigation for the diagnosis or prediction of outcomes in this population.

5.6 Conclusions

Novel Gadolinium-free stress CMR techniques like T1 mapping and OS-CMR may be of specific use in CKD population where coronary artery disease is common and is associated with poor clinical outcomes but the use of gadolinium-based contrast agents is not preferred. In these patients with CKD, stress T1 response seems to be a more accurate method of diagnosing myocardial ischaemia than stress OS-CMR response. However, the interpretation of these tests may be complex. Furthermore, prognostic data is lacking for stress T1 mapping.

5.7 Future Directions

Our pilot study needs to be confirmed with larger, multi-centre studies, which may allow including the comparatively larger cohort of patients with less severe kidney disease into the study. Clinical outcome studies with stress T1 is lacking. Patients with abnormal Δ OS-CMR SI or Δ T1 response could be randomised to preventive treatment strategy versus current observation strategy with a view to follow-up the cardiovascular outcomes over time.

CHAPTER 6: VENTRICULAR PARACARDIAL FAT CONTENT IN CHRONIC KIDNEY DISEASE (CKD) PATIENTS

6.1 Introduction

Excess adiposity is associated with increased cardiovascular risk (146). More important than the total amount of adipose tissue is the location of adipose tissue. Previous studies have shown that central (trunk and abdomen) as opposed to peripheral (hips and thighs) adipose tissue confers the greatest cardio-metabolic risk and therefore waist-to-hip ratio is a better predictor of cardiovascular disease than Body Mass Index (BMI) (148-150). However, this measurement of general obesity is not always associated with increased cardiovascular risk (151) as some people with abnormal waist-to-hip ratio may have a low cardiovascular risk and vice versa. Therefore, a regional fat content with a more accurate risk prediction capability is warranted.

Epicardial fat is the adipose tissue that directly surrounds the heart (between the myocardium and visceral layer of pericardium) and is in direct contact with the coronary vasculature. Pericardial fat is located on the external surface of the parietal pericardium. Periventricular adipose tissue is defined as the pericardial tissue around the ventricles. Most of the pericardial fat in adults is located in the interventricular groove, atrio-ventricular groove and the ventricles. Therefore, periventricular epicardial adipose tissue accounts for almost all the pericardial adipose tissue.

Epicardial fat can be difficult to distinguish from pericardial fat on CMR cine images. Paracardial fat refers to the combination of epicardial and pericardial fat and denotes the total amount of fat surrounding the heart. This is much easier to measure. In this

thesis, Paraventricular Adipose Tissue (PVAT) is defined as the total amount of fat that surrounds the ventricles.

Increased epicardial fat volume has been implicated in coronary artery disease (148, 163-182), atrial fibrillation (183, 184) and adverse cardiovascular outcomes (185-187). In another study, coronary flow reserve was shown to significantly correlate with periventricular adipose tissue independent of cardiovascular risk factors, but not with the total epicardial adipose tissue volume.

Two in three (63%) of Australians are overweight or obese and the prevalence is expected to increase exponentially over the next decade (305). This growing national health crisis has implications for kidney disease as obesity is a potent risk factor for both the development and progression of kidney disease. One-third of chronic kidney disease cases in Australia could be related to excess weight (306). Being obese doubles the risk of developing CKD compared to someone who has a healthy body weight, while overweight people increase their risk of developing CKD by 1.5 times (306). Obesity also indirectly impacts on CKD via the mediating effect on increasing the risk of developing diabetes and high blood pressure, which are the two most common causes of end-stage kidney disease in Australia (1). In patients with ESKD an “obesity paradox” has been reported, i.e. a higher body mass index (BMI) is paradoxically associated with better outcomes (200, 307-309). It is not known if this paradox relationship seen with BMI extends to the paracardiac fat content in the CKD population.

The aim of this study is to compare CMR assessed PVAT volumes in participants with and without CKD. Furthermore, the prognostic value (and the possible paradox) of PVAT in predicting major adverse events in patients with CKD was investigated.

The hypothesis is that when compared to normal individuals, patients with CKD will have higher epicardial fat volumes. Furthermore, lower PVAT would be a predictor of adverse events in patients with CKD.

6.2 Methods

6.2.1 Study Population

84 patients with CKD and 13 healthy age-matched controls underwent scanning in a 3-T MR scanner (Siemens, Trio or Skyra) between 2012 – 2019. Patients were included if they had severe renal failure as defined by an eGFR< 30 mL/min/1.73 m^2, or were requiring dialysis, or had a previous renal transplant with reasonable renal function (eGFR> 45 mL/min/1.73 m^2). Standard MRI contraindications, asthma, second or third-degree heart block, left ventricular ejection fraction (LVEF) < 45%, and clinical heart failure were exclusion criteria.

All participants gave written informed consent, and the study was approved by Southern Adelaide Clinical Human Research Committee (HREC/17/SAC/86).

Figure 6.1 shows the distribution of recruited participants into different cohorts. Of the 13 normal controls (Non-CKD Cohort), none had diagnosed CAD. Of the 84 patients (CKD Cohort), 14 patients had known CAD. The remainder 70 patients did not have diagnosed CAD or symptoms to suggest CAD at the time of recruitment. Six of these 70 patients were diagnosed with myocardial infarction and significant CAD within 1 year of their recruitment into the study, thus increasing the total number of CKD patients with CAD to 20 (CKD with CAD Cohort). Therefore, there were total of 64 CKD patients remaining without CAD at the end of 1 year after recruitment (CKD without CAD Cohort). 61 patients, all without CAD at the time of recruitment (CKD

Follow-up Cohort) and recruited prior to March 2018, were prospectively followed for major adverse events (MAE), defined as all cause death, myocardial infarction, ventricular arrhythmia and hospitalization for pulmonary oedema.

Figure 6.1: Flowchart showing the distribution of 109 recruited participants into the different cohorts.

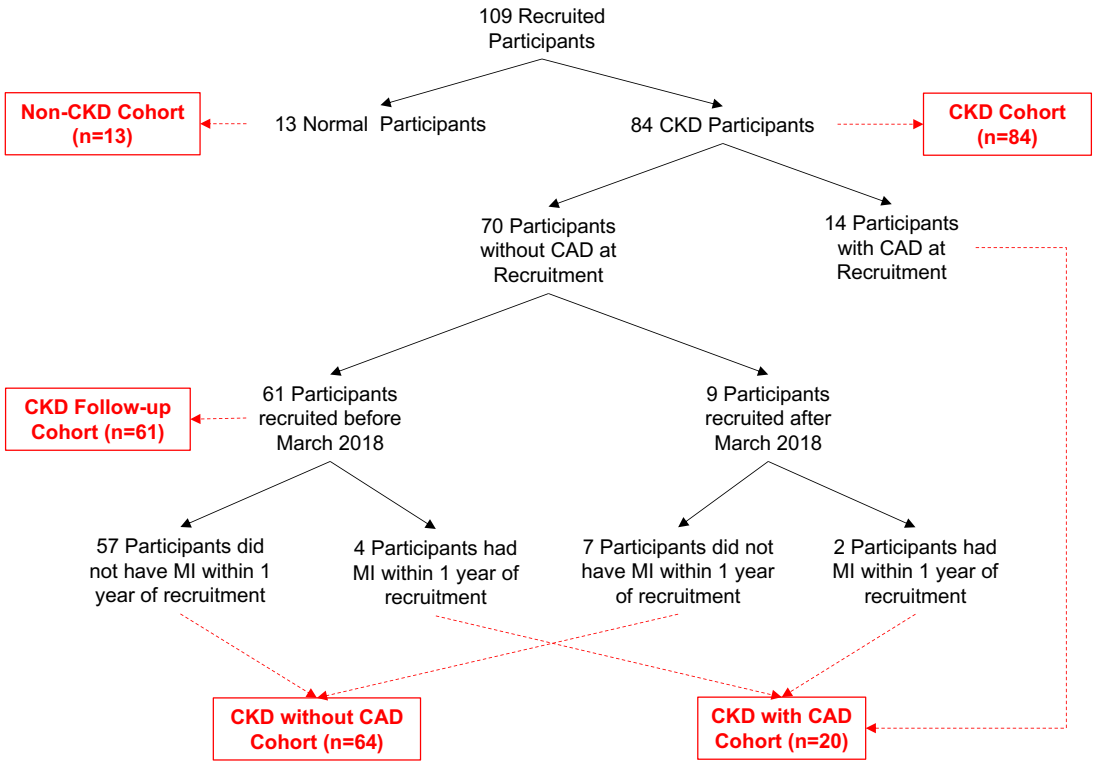

6.2.2 CMR Protocol

All participants underwent scanning in a 3 Tesla clinical MR scanner (Siemens, 3T Trio and Skyra). Cine imaging, rest/stress OS-CMR imaging and rest/stress T1 imaging were performed as described in chapter 2.

6.2.3 CMR Analysis

PVAT volumes, OS-CMR and T1 maps were analysed offline using proprietary software (CVI 42, version 5.9.1) as described in chapter 2.

6.3 Statistical analysis

All analysis was performed using Stata 15.0 (StataCorp, college Station, Texas, USA). Descriptive statistics are presented as mean +/- standard deviation for normally distributed continuous variables, median (inter-quartile range) for skewed continuous variables and as frequency (%) for categorical variables. Differences in patient characteristics between those that experienced a MAE and those that did were compared using independent t-tests and either chi-squared test of association or Fishers Exact as appropriate. Reproducibility was assessed using the coefficient of variation (CV). The between-observer variance and the within-subject variance were estimated using a random intercept mixed-effects model. The between-observer CV was calculated using (between-observer variance/mean) x 100 and the within-subject CV was calculated using the (within-subject variance/mean) x 100.

Each subject follow-up time was from the date of enrolment into the study until April 2018 or the date of death. For patients that experienced one or more MAE, their follow-up time was split according to the dates of the MAEs. Cox regression was used to perform univariate and multivariate analysis and obtain hazard ratios for OS-CMR, GLS and MD on MAE. Each subject was permitted to have multiple MAE events in the analysis. Standard errors were adjusted for within-subject correlation using the cluster(id) vce(robust) option in Stata. The final multivariate model was tested for the assumption of proportional odds both overall and for each variable separately using the proportional hazards test based on the Schoenfeld residuals.

6.4 Results

6.4.1 Baseline Characteristics

Table 6.1 compares the baseline characteristics of the CKD and non-CKD Cohorts. CKD patients had higher indexed left ventricular mass and lower eGFR. Age, gender, BMI, presence of hypertension and left ventricular ejection fraction were not significantly different between the 2 groups. Of the total of 84 CKD patients, 45 patients had diabetes mellitus, 71 were hypertensive, 24 were receiving dialysis and 11 patients had a previous renal transplant at study entry.

Table 6.1 Comparison Between CKD cohort and Non-CKD cohort

	Normal Cohort (n=13)	CKD cohort (n=84)	*p*-value
Age (years)	60.1 ± 11.2	64.1 ± 12.7	0.287
Male sex	8 (62)	55 (65.4)	0.765
BMI (kg/m^2)	25.6 ± 3.1	29.8 ± 6.9	0.034
Dialysis	0 (0)	24 (28.6)	0.034
Diabetes Mellitus	0 (0)	45 (53.6)	<0.001
LVEF (%)	67.9 ± 6.4	64.3 ± 11.9	0.29
LVMi (g/m^2)	50.5± 8.7	65.6 ± 18.8	0.006
PVAT	176.8 ± 83.0	225.2 ± 113.9	0.145
Dyslipidemia	0 (0)	33 (39.3)	0.004
Hypertension	0 (0)	71 (84.5)	<0.001
Anti-platelet Agent	0 (0)	24 (28.6)	0.034
Beta blocker	0 (0)	35 (41.7)	0.003
ACE inhibitor	0 (0)	19 (22.6)	0.067
Angiotensin Receptor Blocker	0 (0)	23 (27.4)	0.034
Calcium channel blocker	0 (0)	38 (45.2)	0.001
Statin	0 (0)	46 (54.8)	<0.001

Data are presented as n (%) or mean ± SD.

Table 6.2 compares the baseline characteristics of non-CKD cohort, CKD without CAD cohort and CKD with CAD cohort. There was a significant difference between the groups with regards to indexed left ventricular mass and a trend noted for

differences between the groups with regards to age and PVAT. Gender and BMI was not significantly different between the 3 groups.

Table 6.2 Comparison Between Non-CKD Participants and CKD Patients With and Without Coronary Artery Disease (CAD)

	Normal Cohort (n=13)	CKD without CAD Cohort (n=64)	CKD with CAD Cohort (n=20)	*p*-value
Age (years)	60.1 ± 11.2	62.8 ± 13.3	68.8 ± 9.9	0.096
Male sex	8 (62)	43 (67)	12 (60)	0.81
BMI (kg/m^2)	25.6 ± 3.1	29.8 ± 6.8	29.7 ± 7.4	0.109
Dialysis	0 (0)	13 (20)	11 (55)	0.001
Diabetes Mellitus	0 (0)	28 (44)	17 (85)	<0.001
LVEF (%)	67.9 ± 6.4	65.3 ± 10.7	60.6 ± 14.8	0.148
LVMi (g/m^2)	50.5± 8.7	64.8 ± 16.7	67.8 ± 24.7	0.018
PVAT (ml)	176.8 ± 83.0	218.4 ± 124.1	245.1 ± 61.2	0.22
Dyslipidemia	0 (0)	25 (39)	9 (45)	0.008
Hypertension	0 (0)	55 (86)	16 (80)	<0.001
Anti-platelet Agent	0 (0)	10 (16)	12 (60)	<0.001
Beta blocker	0 (0)	21 (31)	11 (55)	0.002
ACE inhibitor	0 (0)	15 (23)	2 (10)	0.091
Angiotensin Receptor Blocker	0 (0)	16 (25)	4 (20)	0.116
Calcium channel blocker	0 (0)	30 (47)	3 (15)	<0.001
Statin	0 (0)	30 (47)	13 (65)	<0.001

Data are presented as n (%) or mean ± SD.

61 CKD patients were followed up for a mean of 2.1 years. A total of 10 (16.4%) patients had events. There was a total of 15 events, of which 13 events were observed in 9 diabetic patients. There were 5 deaths, 4 non-fatal myocardial infarcts, 6 heart failure admissions and no ventricular arrhythmias. Table 6.3 compares the baseline characteristics of patients who did and did not have events. There was no significant difference between the two groups with regards to age, sex, eGFR or being on dialysis. There was a higher likelihood of patients experiencing events to be diabetic (90% versus 39.2%; p = 0.004) and have increased indexed left ventricular mass (84.5 ± 20.6 gm versus 63.4 ± 16.7 gm, p = 0.003).

Table 6.3 Comparison Between CKD Patients With and Without Major Adverse Events (MAE)

	CKD patients without MAE (n=51)	CKD patients with MAE (n=10)	*p*-value
Age (years)	62.6 ± 13.5	67.4 ± 10.5	0.214
Male sex	33 (65)	7 (70)	0.749
BMI (kg/m^2)	30.2 ± 7.1	24.9 ± 4.5	0.003
eGFR (mL/min/1.73 m^2)	15.6 ± 7.6	20.7 ± 15.6	0.316
Dialysis	10 (20)	4 (40)	0.164
Diabetes Mellitus	20 (39)	9 (90)	0.004
LVEF (%)	67.1 ± 10.4	62.8 ± 14.6	0.378
LVMi (g/m^2)	63.4 ± 16.7	84.5 ± 20.6	0.003
PVAT (ml)	221.6 ± 123.6	198.9 ± 55.3	0.360
Dyslipidemia	22 (43)	4 (40)	0.857
Hypertension	43 (84)	6 (60)	0.384
Anti-platelet Agent	11 (22)	0 (0)	0.107
Beta blocker	17 (33)	5 (50)	0.325
ACE inhibitor	14 (28)	1 (10)	0.244
Angiotensin Receptor Blocker	12 (24)	3 (30)	0.665
Calcium channel blocker	26 (51)	2 (20)	0.074
Statin	24 (47)	5 (50)	0.868

Data are presented as n (%) or mean ± SD.

6.4.2 Paraventricular Adipose Tissue volumes in participants with and without CKD

Although PVAT volume was higher in the CKD patients compared to the non-CKD volunteers (Figure 6.2), this difference did not reach statistical significance (225.2 ± 113.9 mls versus 176.8 ± 83 mls, p = 0.145) and there was only a trend noted. Furthermore, PVAT volume was elevated in the CKD patients with CAD when compared to the CKD patients without CAD (Figure 6.2) but this difference also did not reach statistical significance (245.1 ± 61.2 mls versus 218.4 ± 124.1 mls, p = 0.358).

Figure 6.2: Comparisons of Paraventricular Adipose Tissue (PVAT) volume between non-CKD and CKD cohorts (A) and CKD without and with CAD cohorts (B).

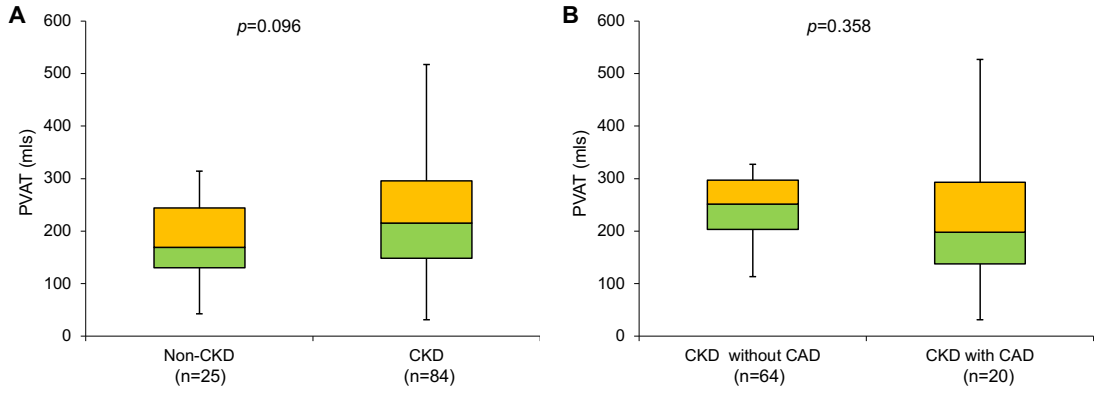

6.4.3 Paraventricular Adipose Tissue volumes in CKD patients with and without major adverse events (MAE)

PVAT volume was noted to be lower in the patients experiencing adverse events (Table 6.3) but this did not reach statistical significance (198.9 ± 55.3 mls versus 221.6 ± 123.6 mls, p = 0.360).

6.4.4 Association between Paraventricular Adipose Tissue (PVAT) volume in the CKD Cohort and patient baseline characteristics: Age, Gender, BMI, Renal Function (eGFR), Diabetes Mellitus, Hypertension, Dialysis and Troponin T (TnT).

In the CKD cohort, the PVAT volume was significantly higher in the males when compared to females (243.4 ± 113.5 mls versus 185.9 ± 104.1 mls, p = 0.026). PVAT was not significantly influenced by diabetes mellitus, hypertension or dialysis (Figure 6.3).

Figure 6.3: Influence of gender (A), diabetes mellitus (B), hypertension (C) and dialysis (D) on Paraventricular Adipose tissue (PVAT) volume in the CKD cohort (84 patients).

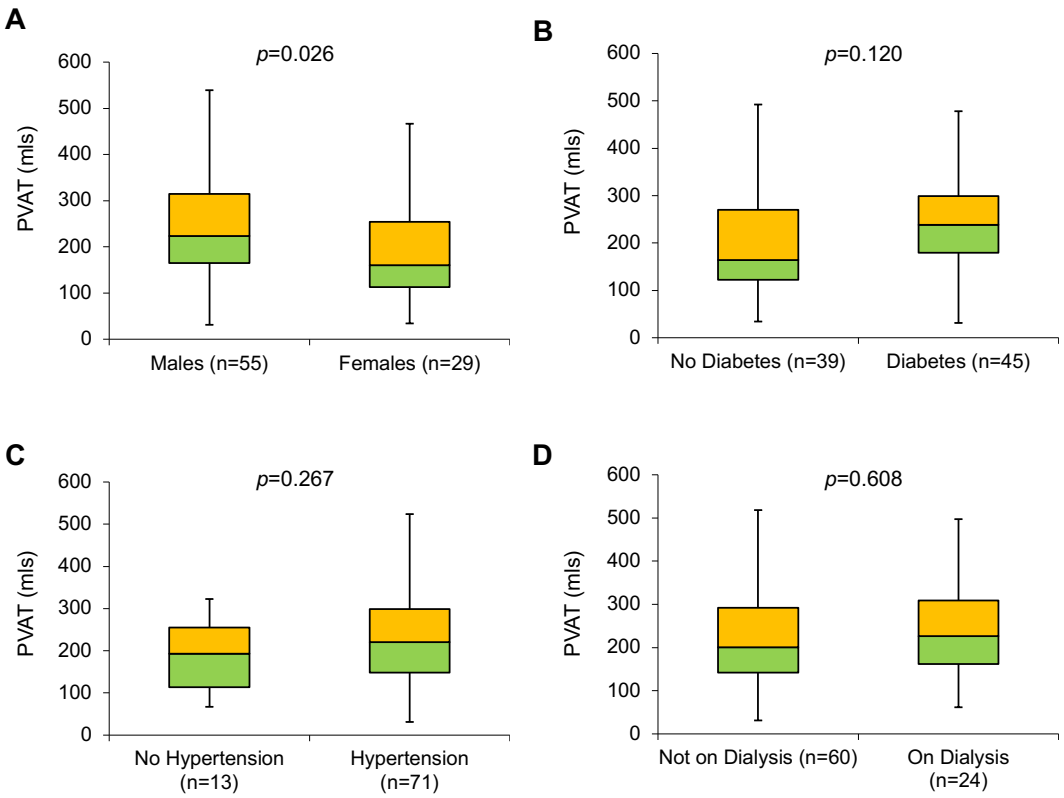

In the CKD cohort, there were good correlations seen between PVAT and BMI ($r=0.494$, $p<0.001$) and between PVAT and age ($r=0.322$, $p=0.003$). There were no significant correlations seen between PVAT and renal function (eGFR) or Troponin T (Figure 6.4).

Figure 6.4: Correlation between Peri-Ventricular Adipose Tissue (PVAT) and age (A), BMI(B), eGFR (C) and Troponin T (D).

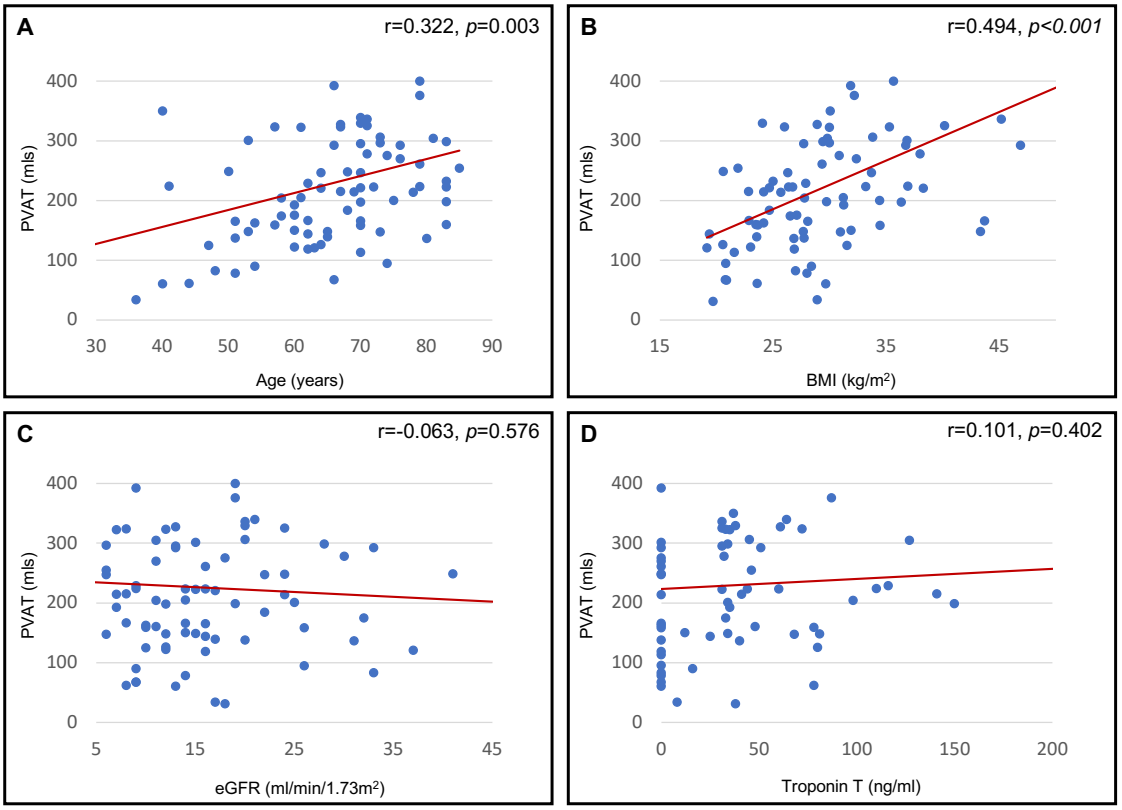

6.4.5 Association between Paraventricular Adipose Tissue (PVAT) volume in the CKD Cohort and CMR derived parameters: Left Ventricular Ejection Fraction (LVEF), Indexed Left Ventricular Mass (LVMi), Stress OS-CMR and Stress T1 Mapping.

In the CKD cohort, there were no significant correlations seen between PVAT and LVEF, LVMi, stress OS-CMR or stress T1 mapping (Figure 6.5).

Figure 6.5: Correlation between Peri-Ventricular Adipose Tissue (PVAT) and LVEF (A), LVMi(B), Δ OSCMR (C) and Δ T1 (D).

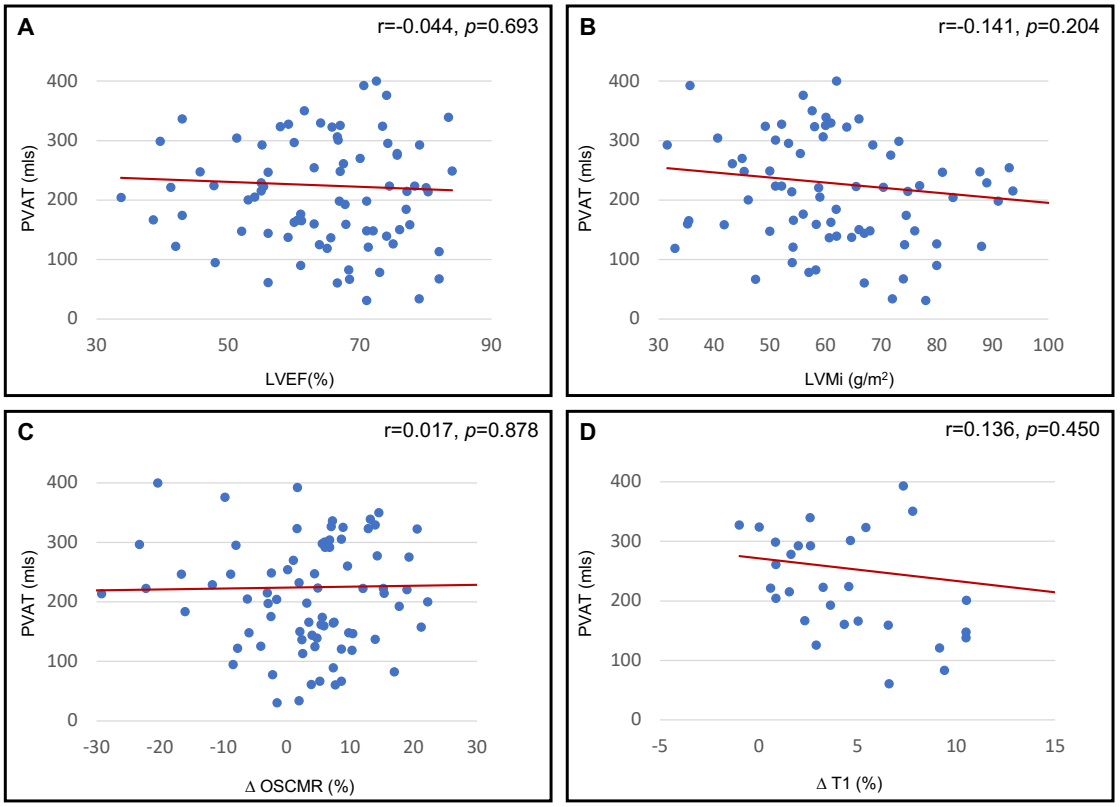

6.4.6 Paraventricular Adipose Tissue volume as a predictor of adverse events in CKD

Univariate Cox regression analysis (Table 6.4) was performed on the data from the 61 CKD patients (all without CAD) who were followed up for MAE. This showed that age, indexed left ventricular mass (LVMi), left ventricular ejection fraction (LVEF) and diabetes mellitus were significant predictors of future adverse events while renal function (eGFR) and PVAT were not.

Table 6.4: Results of univariate Cox regression for adverse events in the CKD Patients			
	Hazard Ratio	**95% CI**	***p*-value**
Age (years)	1.067	1.017 – 1.120	0.008
eGFR (mL/min/1.73 m^2)	0.999	0.961 – 1.037	0.939
Diabetes Mellitus	8.526	1.964 – 37.019	0.004
LVMi (g/m^2)	1.034	1.011 – 1.057	0.003
LVEF (%)	0.922	0.882 – 0.964	<0.001
PVAT	1.004	0.999 – 1.008	0.116

On multivariate Cox regression analysis (Table 6.5), age, indexed left ventricular mass (LVMi), left ventricular ejection fraction (LVEF) and diabetes mellitus were significant predictors of future adverse events while renal function (eGFR) and PVAT were not.

Table 6.5: Results of multivariate Cox regression for adverse events in the CKD Patients			
	Hazard Ratio	**95% CI**	***p*-value**
Age (years)	1.102	1.030 – 1.180	0.005
eGFR (mL/min/1.73 m^2)	1.018	0.980 – 1.057	0.363
Diabetes Mellitus	16.382	2.239 – 119.883	0.006
LVMi (g/m^2)	1.037	1.009 – 1.066	0.010
LVEF (%)	0.881	0.826 – 0.940	<0.001
PVAT	1.001	0.993 – 1.009	0.796

6.4.7 Test Reproducibility

Two observers analysed PVAT volumes in 20 subjects. PVAT volume was highly reproducible with low intra-observer and inter-observer variabilities (co-efficient of variation 5.1% and 6.4%, respectively).

6.5 Discussion

This is the first CMR study to assess the PVAT volumes in patients with CKD and to investigate the prognostic utility of PVAT in these patients. Here it was shown that

when compared to non-CKD participants, there was a trend for increased PVAT volumes in the CKD patients. This increased PVAT volume, however, did not seem to be a marker of adverse events. In fact, PVAT volumes were lower, although not significantly, in CKD patients who experienced adverse events compared to the CKD patients who did not experience adverse events.

Epicardial fat is brown fat and develops from splanchnopleuric mesoderm and gets its blood supply from the coronary arteries while pericardial fat develops from the primitive thoracic mesenchyme and gets its blood supply from the non-coronary arteries (152). Epicardial fat is biologically active and may play a central role in the association between obesity and cardiovascular disease. In obesity epicardial fat volume increases and it becomes hypoxic and dysfunctional (159), resulting in a shift in its metabolic profile. Adipokines can have both endocrine and paracrine functions that influence the development of cardiovascular disease, and in particular CAD. Increased epicardial fat leads to additional mass on both ventricles that can increase the work demands on the heart and result in left ventricular hypertrophy (161). Moreover, epicardial fat thickness is positively correlated with myocardial lipid content and may affect cardiomyocyte function (162). Epicardial fat has been implicated in coronary artery disease (148, 163-182), atrial fibrillation (183, 184) and adverse cardiovascular outcomes (185-187).

Increased epicardial fat is associated with the more traditional metabolic risk factors such as BMI, dyslipidemia, impaired fasting glucose, Type 2 Diabetes Mellitus (T2DM) and hypertension. CKD is often the result of one or more of the above risk factors (188). Furthermore, obesity is common amongst patients with moderate-severe CKD (189, 190). Epicardial fat has been shown to be increased in CKD

patients. Epicardial fat thickness is significantly greater in patients on hemodialysis compared with healthy controls and positively correlated with hemodialysis duration (191, 192). Echocardiographically assessed epicardial fat tissue thickness has been shown to correlate with oxidant biomarkers in CKD and CKD disease progression (193). In another study, it was seen that in stage 3-5 pre-dialysis CKD patients, coronary calcification and IL-6 were predictors of epicardial fat thickness (194). Thus, inflammation, as also seen with increased epicardial fat, could be a possible link between the pathogenesis of CAD and chronic kidney disease.

Cardiovascular magnetic resonance (CMR) imaging has been validated for the measurement of epicardial and pericardial fat volume (154, 155). In adults, epicardial fat commonly exists in the atrioventricular and interventricular grooves, whereas in juveniles it is found around the atrial free wall and two atrial appendages (152, 153). In this study the total fat volume around the ventricles is quantified from the level of the mitral valve down, and therefore this would include the fat in the atrioventricular groove and around the ventricles. Since the study was done in an adult population (average age 64.1 ± 12.7 years), the atrial free wall and atrial appendages were not expected to have significant volumes of adipose tissue adjacent to it and therefore were not assessed.

In the general population, obesity is associated with increased cardiovascular risk and decreased survival. In the CKD population, however, the relationship between excess adiposity and cardiovascular risk is complex. In the CKD population, observational studies have reported contradictory findings about the association between obesity and mortality. Previous studies of people on hemodialysis have suggested an ‘obesity paradox’, where being obese is protective against all-cause

and cardiovascular mortality (196, 197). Other studies have reported a U- or J-shaped association between obesity measured by BMI and mortality, with a higher risk of death in underweight and morbidly obese categories compared with normal weight (198, 199). In a recent metanalysis, it was shown that, in hemodialysis patients, for every 1 kg/m^2 increase in BMI, there was a 3% and 4% decrease in risk of all cause death and cardiovascular-related mortality, respectively (200). In CKD stages 3-5, the reduction in risk for all-cause mortality per kg/m^2 rise in BMI was 1% (200).

BMI may not necessarily be an accurate marker of adiposity in people with CKD. This measurement of general obesity is not always associated with increased cardiovascular risk (151) as some people with abnormal waist-to-hip ratio may have a low cardiovascular risk and vice versa. Therefore, a regional fat content with a more accurate risk prediction capability is warranted. PVAT is one such regional fat content and is studied here. In this study, PVAT volumes correlated strongly with BMI suggesting that CKD patients with higher BMI had significantly raised PVAT volumes. However, there was only a non-significant increase in the PVAT volume in CKD patients who did not experience adverse events compared to patients who experienced adverse events. It may be possible that in larger studies, and possibly with a longer follow-up duration, this difference may become significant. That finding will then be in line with the obesity paradox described above.

It is known that eGFR, Troponin T and OS-CMR can give valuable prognostic information in CKD patients. In the current study, there was no significant correlation seen between PVAT and eGFR (marker of renal function), Troponin T (marker of myocyte damage), ΔOS-CMR (myocardial oxygenation) or ΔT1 (myocardial blood

volume). It may be possible that the reason for this poor performance of PVAT in CKD was the small sample size of this study. Larger studies are required to assess the utility of CMR assessed PVAT in CKD patients.

6.5.1 Limitations

Due to the small sample size the results in this study are prone to type II error. These results are hypothesis-generating and therefore need to be confirmed with larger studies. Secondly, CTCA or invasive coronary angiogram was not performed (due to advanced renal failure) in our patient cohort and therefore it may be possible that some patients might have had significant undiagnosed CAD. Thirdly, the CKD patients were unable to have gadolinium contrast due to the risk of nephrogenic systemic fibrosis, therefore late gadolinium enhancement could not be performed. Fourth limitation would be the lack of atrial cine stack during the CMR assessment which meant that the adipose tissue around the atria could not be measured. A further limitation was that both epicardial and pericardial fat were ascertained and not just epicardial fat. Lastly, although image quality was generally good, artefacts could not always be resolved with frequency and shim adjustments and this could lead to reduced specificity.

6.6 Conclusion

In this study there was a trend seen for the Paraventricular Adipose Tissue (PVAT) volume to be increased in patients with CKD when compared to participants without CKD. However, this increased PVAT volume did not seem to be an independent predictor of adverse events in the small population that was studied.

6.7 Future Direction

This pilot study needs to be confirmed with larger, multi-centre studies, which may allow inclusion of patients with less severe kidney disease into the study. Larger and multi-centre studies are needed to examine the prognostic utility of PVAT in CKD patients and the use of PVAT in the short-term and long-term outcome of medical versus revascularisation therapy in the renal failure population with silent myocardial iscahemia.

CHAPTER 7: ARGININE METABOLITES AS BIOMARKERS OF MYOCARDIAL ISCHAEMIA, ASSESSED WITH CARDIAC MAGNETIC RESONANCE IMAGING IN CHRONIC KIDNEY DISEASE

7.1 Introduction

Cardiovascular disease (CVD) is common in CKD and it is estimated that 25-47% patients with severe CKD have significant coronary artery disease, heart failure or left ventricular hypertrophy (2-4). Although traditional cardiovascular risk factors are common among advanced CKD patients, they can only in part explain the increased susceptibility to CVD (201). Cardiovascular risk factors result in endothelial dysfunction which has a central role in the pathogenesis of CVD together with inflammation and atherosclerosis. Further studies are required to understand better the mechanisms underlying the increased cardiovascular risk in the CKD patients and whether assessment of endothelial dysfunction can help better quantitate the cardiovascular risk in CKD.

Reduced nitric oxide (NO) bioavailability is a major risk factor for cardiovascular disease and progression to kidney failure in patients with chronic kidney disease (CKD) (310-312). The endothelium is important to the maintenance of vascular tone (313). Endothelial nitric oxide synthase (eNOS) catalyzes the conversion of L-arginine (ARG) and L-homoarginine (HMA) to NO (314). eNOS has a much higher affinity for ARG than HMA. NO is released from the endothelium in response to shear stress and plays an important role in flow-mediated dilatation (FMD) (315). Furthermore, NO also inhibits oxidation of LDL (316), platelet aggregation (317), adhesion of monocytes and leukocytes to the endothelium (318), and smooth muscle

cell proliferation (319). NO therefore has important effects as a mediator of antithrombotic processes, growth inhibition and inflammation.

HMA is an amino acid derivative that may increase nitric oxide availability and enhance endothelial function. Involvement of HMA in the regulation of vascular function is supported by the direct association between the plasma levels of HMA with hemodynamic response to ischemia in the forearm (208). Various studies in the past have shown that low HMA levels are associated with adverse events in the CKD population (213, 216, 217).

Methylation of L-arginine (Arg) residues in certain proteins by protein methyltransferases (PMRTs) and subsequent proteolysis yields L-N-monomethylarginine (LNMMA), asymmetric dimethylarginine (ADMA) and symmetric dimethylarginine (SDMA). LNMMA, ADMA and SDMA are inhibitors (MMA > ADMA ≫ SDMA) of eNOS activity.

LNMMA is a methyl derivative of the amino acid arginine. It is a potent eNOS inhibitor and may accumulate in CKD. ADMA is a competitor to arginine and a potent inhibitor of eNOS (203), and thus may cause endothelial dysfunction (320, 321). Increased levels of ADMA are seen with increasing age, hypercholesterolemia, hypertension, hypertriglyceridemia, diabetes mellitus, insulin insensitivity, hyperhomocysteinemia and renal failure (320, 322-328), all of which are known risk factors for atherosclerosis. Furthermore, elevated plasma ADMA concentration has been identified as an independent risk factor for progression of atherosclerosis, cardiovascular death and all-cause mortality (329-331). Symmetric dimethylarginine (SDMA) does not inhibit eNOS directly, but it may indirectly reduce NO production

causing reduction in the intracellular arginine availability, since SDMA competes with the cationic amino acid transporter in the endothelial cell membrane (204).

L-citrulline is a by-product when NO is synthesized from L-arginine by NOS. Arginine can also be metabolized by arginase which hydrolyses it to ornithine (ORN) and urea. Therefore, arginase may reciprocally regulate the production of NO and an increased enzyme activity can induce endothelial dysfunction (332-334).

Myocardial oxygenation and perfusion response to stress, using oxygen-sensitive cardiovascular magnetic resonance (OS-CMR) and stress T1 mapping respectively, are impaired in CKD patients with and without known CAD. Furthermore, the impaired OS-CMR response is associated with major adverse events (death, myocardial infarction, ventricular arrhythmia and heart failure admissions).

Further studies are required to understand the relation between endothelial dysfunction (as indirectly assessed by measuring ADMA, SDMA and HMA) and myocardial ischaemia (as assessed with stress OS-CMR and stress T1 mapping) in CKD. This study aims to investigate this relationship. In particular, we hypothesized that in CKD patients, higher levels of ADMA and lower levels of HMA are associated with worsening myocardial oxygenation and perfusion as assessed by OS-CMR and stress T1 responses to stress.

7.2 Methods

7.2.1 Study Population

38 patients with CKD were invited to participate at Flinders Medical Centre (FMC) and the South Australian Health and Medical Research Institute (SAHMRI) between 2017 – 2019. Patients were included if they had severe renal failure as defined by an

eGFR< 30 mL/min/1.73 m^2, or were requiring dialysis, or had a previous renal transplant with reasonable renal function (eGFR> 45 mL/min/1.73 m^2). Patients were excluded if they had standard MRI contraindications, asthma, second or third-degree heart block, left ventricular ejection fraction (LVEF) < 45%, or clinical heart failure. All participants gave written informed consent, and the study was approved by Southern Adelaide Clinical Human Research Committee (HREC/17/SAC/86).

7.2.2 Serum Biochemistry

All participants had 10 ml of blood collected for routine biochemistry, cell counts, haemoglobin, troponin T, CRP, thyroid stimulating hormone (TSH), Parathormone levels (PTH), iron studies and lipid studies. eGFR was calculated from serum creatinine using the CKD-Epidemiological Collaboration Formula.

A further sample of blood was centrifuged at 4000 rpm for 10 minutes at 4°C and the serum collected and stored in a -80°C freezer for analysis of biochemical markers of endothelial dysfunction. These samples were later thawed for analysis. 20 µL of sample plasma, calibrator or QC was mixed with 20 µL internal standard solution (containing 1 µM d6-ADMA, 1 µM d6-SDMA, 25 µM d7-citrulline, 2 µM d4-homoarginine, and 100 µM d6-ornithine). Following the addition of 150 µL 0.1% formic acid in methanol the sample was vortex mixed for 3 min at 2000 rpm to extract the analytes. Centrifugation at 18,000g for 5 min precipitated the proteins. An aliquot (5 µL) of the supernatant layer was injected onto an Atlantis HILIC column (2.1 x 150 mm, 3 µm, Waters, Sydney, Australia) for analysis. A gradient mobile phase consisting of (A) 0.1% v/v formic acid in acetonitrile and (B) 10% v/v acetonitrile, 0.1% v/v formic acid and 10 mM ammonium formate in water was used at a flow rate of 0.4 mL/min. The starting mobile phase was 95% A, 5% B which was varied linearly

over 16 min to 50 % A, 50% B then returned to the initial conditions and equilibrated for 4 min prior to injection of the next sample. The mass spectrometer was run in positive ionization mode with data collected using a Waters proprietary MSE data acquisition method at low collision (3 V) and a high collision energy ramp (8-14 V). Parent or selected fragment ions were used for detection and quantification based on their monoisotopic mass. The qToF Premier (Waters, Sydney, Australia) mass spectrometer was run in positive ionisation mode with data collected using Waters proprietary MS^E data acquisition method. Mass spectrometer settings were as follow: capillary voltage 3.0 kV, sampling cone voltage 24.0 eV, extraction cone voltage 5.0 eV, source temperature 100 °C, desolvation temperature 300 °C, cone gas flow 30 L/Hr, desolvation gas flow 400.0 L/Hr, MS^E function 1 collision energy 3.0 V, MS^E function 2 collision energy ramp 8.0 – 14.0 V, collision Cell Entrance 2.0, collision Exit -10.0, collision Gas Flow 0.60 mL/min. Parent or selected fragment ions were used for detection and quantitation based on their monoisotopic mass.

Table 7.1: Analysis of Arginine metabolites.

Analyte	RT (min)	MS^E channel	Ion	m/z[1]	Int Std	QC_{low}[2] %CV	QC_{high}[2] %CV
ADMA	11.93	1	parent	203.16	d6-ADMA	6.4	7.1
L-ARG	11.06	1	parent	175.13	d4-HMA	9.0	10.0
CIT	9.34	1	fragment	159.09	d7-CIT	6.1	4.0
HMA	11.15	1	parent	189.15	d4-HMA	1.6	1.4
L-NMMA	11.38	1	parent	189.15	d4-HMA	8.6	14.4
ORN	11.38	1	parent	133.11	d6-ORN	5.1	3.5
SDMA	11.75	1	parent	203.16	d6-SDMA	4.2	4.3

Legend: ADMA, asymmetric dimethylarginine; L-ARG, L-arginine; CIT, L-citrulline; HMA, L-homoarginine; L-NMMA,N^G –monomethyl-L-arginine; ORN, L-ornithine; SDMA, symmetric dimethylarginine

[1]m/z for the positively charged analyte ion, that is $[M+H]^+$, data was extracted with a mass window of 0.05 Da

[2]QC_{low} and QC_{high} were prepared by spiking pooled human plasma (n=5) with a known amount of analyte.

Retention times, corresponding parent or fragment mass, MS^E acquisition channel and QC performance data (five independent determinations at each of two concentrations) for each analyte are shown in Table 7.1.

7.2.3 CMR Protocol

All participants underwent scanning in a 3 Tesla clinical MR scanner (Siemens, 3T Trio and Skyra). Cine imaging, rest/stress OS-CMR imaging and rest/stress T1 imaging were performed as described in chapter 2.

7.2.4 CMR Analysis

Left ventricular volumes, OS-CMR and T1 maps were analysed offline using proprietary software (CVI 42, version 5.9.1) as described in chapter 2.

7.3 Statistical analysis

All analysis was performed using SPSS software package (IBM Corporation, New York, U.S.A.). Descriptive statistics are presented as mean +/- standard deviation for normally distributed continuous variables, median (inter-quartile range) for skewed continuous variables and as frequency (%) for categorical variables. The analysed associations between clinical and demographic variables and individual arginine metabolites using either simple or partial correlation analysis.

7.4 Results

7.4.1 Baseline Characteristics

Table 7.2 details the baseline characteristics of the 38 CKD patients. The average age of the patients was 62.2 ± 13.5 years and 63% were male. 20 patients had Diabetes mellitus, 16 were on dialysis and 12 had dyslipidemia. 12 patients had

diagnosed coronary artery disease (CAD) of which 6 patients had undergone revascularization (5 had coronary artery bypass grafting and 1 had percutaneous intervention with a stent inserted).

Table 7.2 Baseline Characteristics

	CKD patients (n=38)
Age (years)	62.2 ± 13.5
Male sex	24 (63.2)
BMI (kg/m^2)	31.1 ± 7.4
eGFR (mL/min/1.73 m^2)	15.1 ± 8.5
Dialysis	16 (42.1)
Diabetes Mellitus	20 (52.6)
LVEF (%)	62.3 ± 11.7
LVMi (g/m^2)	61.7 ± 18.6
Dyslipidemia	12 (31.6)
Smoking History	8 (21.1)
Anti-platelet Agent	15 (39.5)
Beta blocker	16 (42.1)
ACE inhibitor	10 (26.3)
Angiotensin Receptor Blocker	10 (26.3)
Calcium channel blocker	19 (50.0)
Statin	23 (60.5)

Data are presented as n (%) or mean ± SD.

7.4.2 Arginine metabolite levels in normal volunteers and CKD patients

Pooled plasma from 5 healthy volunteers (2 males and 3 females) were analysed to determine the arginine metabolite values in normal individuals. For each analyte, 4 quality controls were included - unspiked pooled plasma and pooled plasma spiked with known concentrations of the analytes (low, medium and high) in order to cover all the possible ranges. Table 7.3 shows the comparison between the arginine metabolites levels in the normal volunteers and CKD patients.

Table 7.3: Arginine metabolites in CKD patients and in normal volunteers.		
Analyte	**Normal Volunteers (pooled plasma)**	**CKD Patients (n=38)**
ADMA (μM)	0.505 ± 0.019	0.780 ± 0.149
L-ARG (μM)	213.8 ± 23.6	182.7 ± 39.6
CIT (μM)	42.6 ± 1.7	96.7 ± 29.0
HMA (μM)	2.40 ± 0.14	1.28 ± 0.61
L-NMMA (μM)	0.115 ± 0.013	0.101 ± 0.041
ORN (μM)	71.1 ± 1.7	84.7 ± 22.5
SDMA (μM)	0.505 ± 0.037	1.784 ± 0.669
Legend: ADMA, asymmetric dimethylarginine; L-ARG, L-arginine; CIT, L-citrulline; HMA, L-homoarginine; L-NMMA,N^G –monomethyl-L-arginine; ORN, L-ornithine; SDMA, symmetric dimethylarginine		

As expected, CKD patients had much higher ADMA (0.780 ± 0.149 μM vs 0.505 ± 0.019 μM) and SDMA (1.784 ± 0.669 μM vs 0.505 ± 0.037 μM) and lower HMA (1.28 ± 0.61 μM vs 2.40 ± 0.14) values when compared to the normal controls.

7.4.3 Arginine metabolite levels in CKD patients with and without CAD.

Figure 7.1: Arginine metabolite levels in CKD patients with and without CAD.

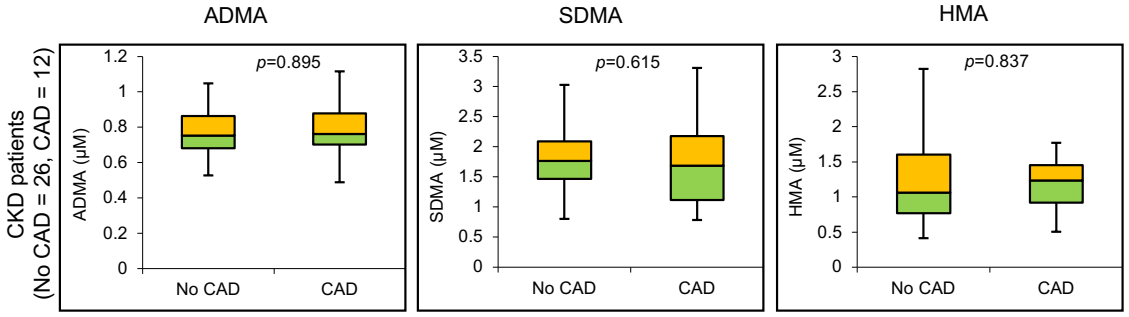

There were no significant differences in the levels of ADMA, SDMA or HMA in CKD patients with and without CAD (Figure 7.1).

7.4.4 Association between Arginine metabolites and patient baseline characteristics: Age, Gender, BMI, Renal Function (eGFR), Diabetes Mellitus, Hypertension, Dialysis, Troponin T (TnT) and hs-CRP.

HMA levels were significantly higher in male patients (n=24) compared to female patients (n=14) with CKD (1.376 μM ± 0.610 μM vs 0.962 μM ± 0.396 μM, $p = 0.029$). There was a trend for HMA to be higher in hypertensive patients (n=5) compared to non-hypertensive patients (n=33) with CKD (1.281 μM ± 0.566 μM vs 0.845 μM ± 0.507 μM, $p = 0.113$). Apart from these, gender, diabetes mellitus, hypertension or having dialysis did not significantly influence the levels of arginine metabolites (Figure 7.2).

SDMA levels significantly reduced with increasing BMI ($r = -0.432$, $p = 0.007$). Worsening renal function (as denoted by reducing eGFR) was associated with higher SDMA levels ($r = -0.472$, $p = 0.003$). Raised troponin T levels correlated significantly with higher ADMA levels ($r = 0.444$, $p = 0.006$) and lower HMA levels ($r = -0.329$, $p = 0.047$). There was a trend for HMA levels to fall with increasing age ($r = -0.265$, $p = 0.108$). Apart from these, age, BMI, eGFR, Troponin T, and hs-CRP were not significantly associated with the levels of arginine metabolites (Figure 7.3).

Figure 7.2: Association between arginine metabolites and patient baseline characteristics: Gender, Diabetes mellitus, Hypertension and Dialysis

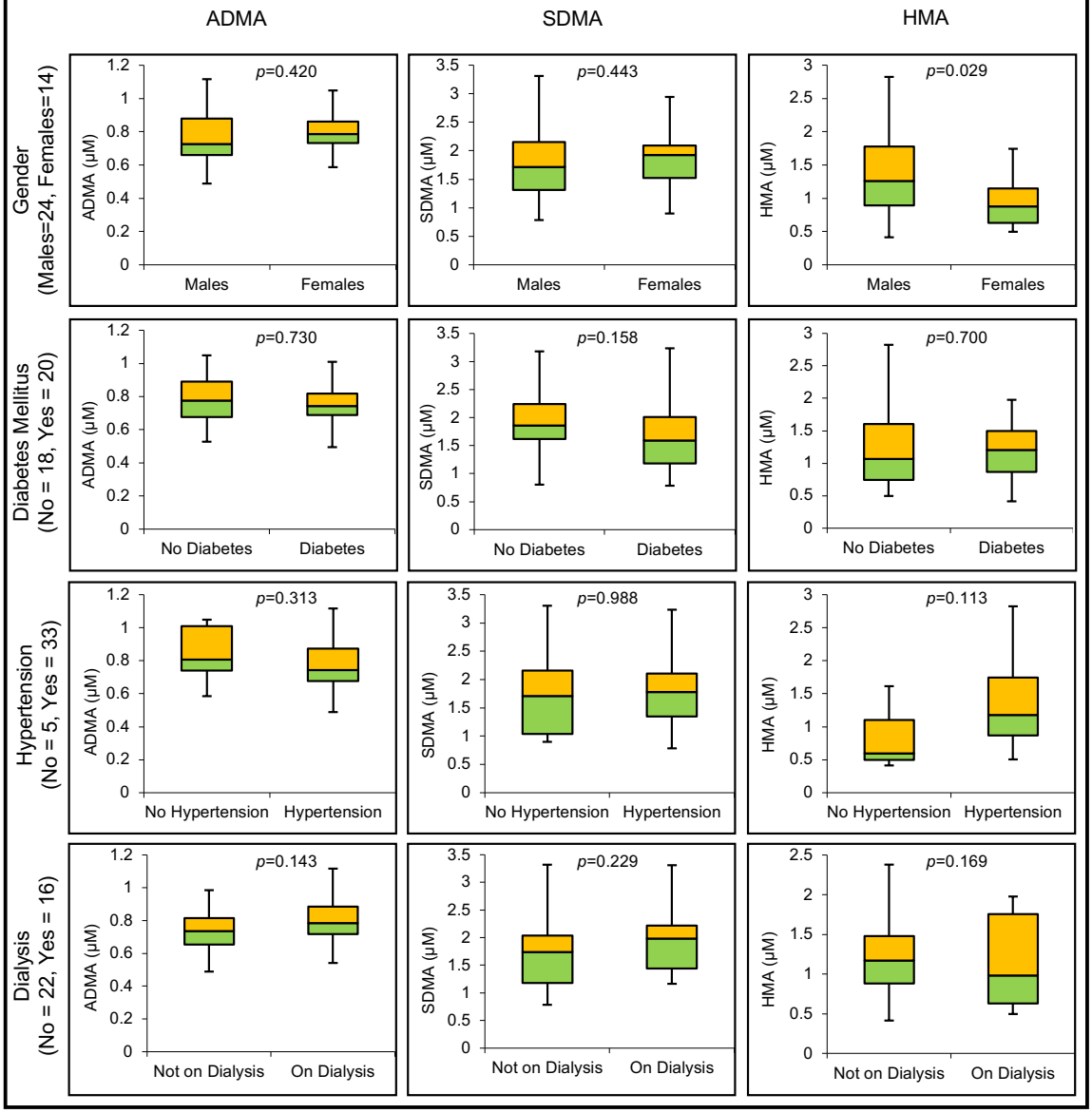

Figure 7.3: Association between arginine metabolites and patient baseline characteristics: Age, BMI, eGFR, Troponin T and hs-CRP.

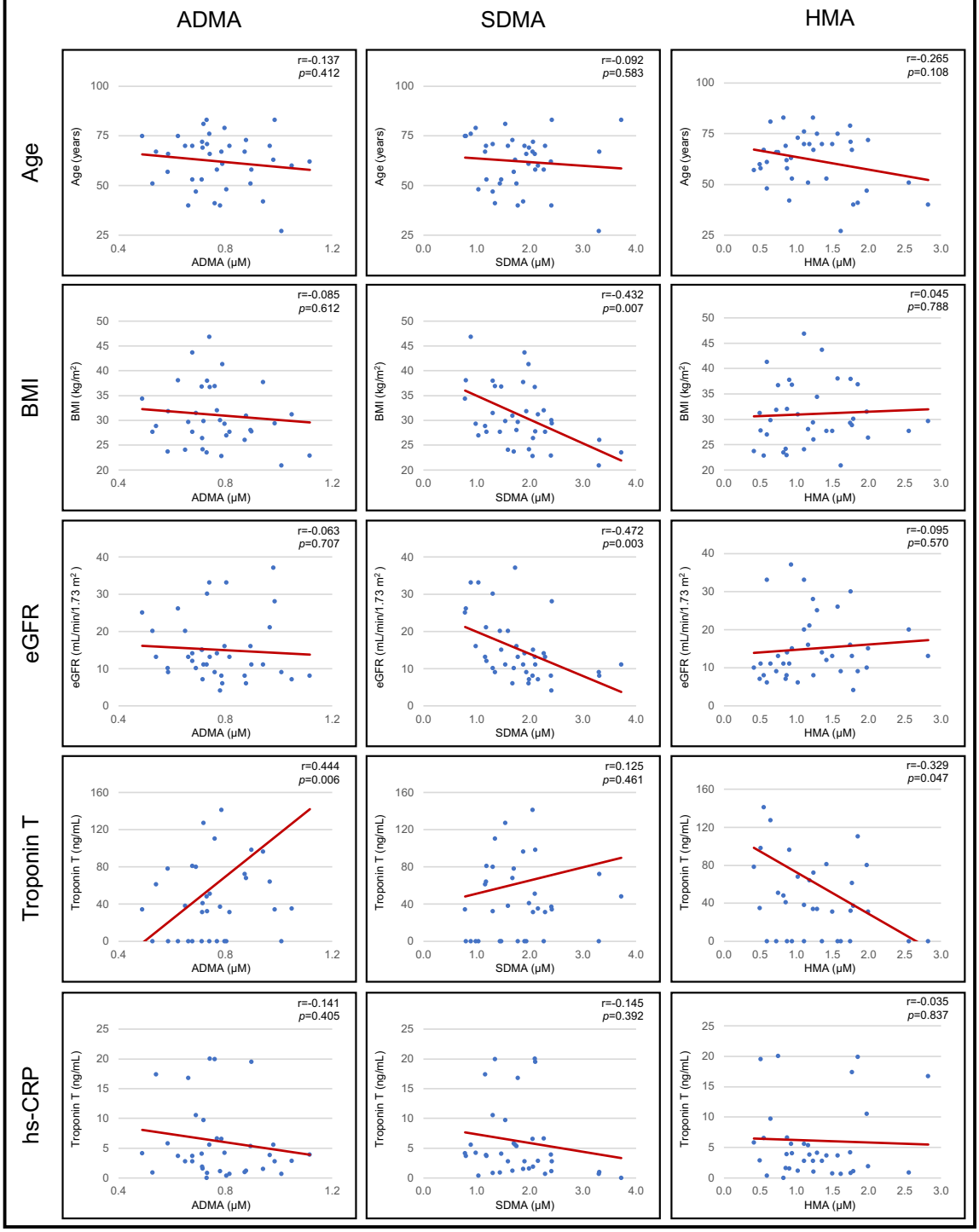

7.4.5 Association between Peri-Ventricular Adipose Tissue (PVAT) volume in the CKD Cohort and CMR derived parameters: Left Ventricular Ejection Fraction (LVEF), Indexed Left Ventricular Mass (LVMi), Stress OS-CMR and Stress T1 Mapping.

Figure 7.4: Association between arginine metabolites and CMR derived parameters: LVEF, LVMi, stress OSCMR and stress T1.

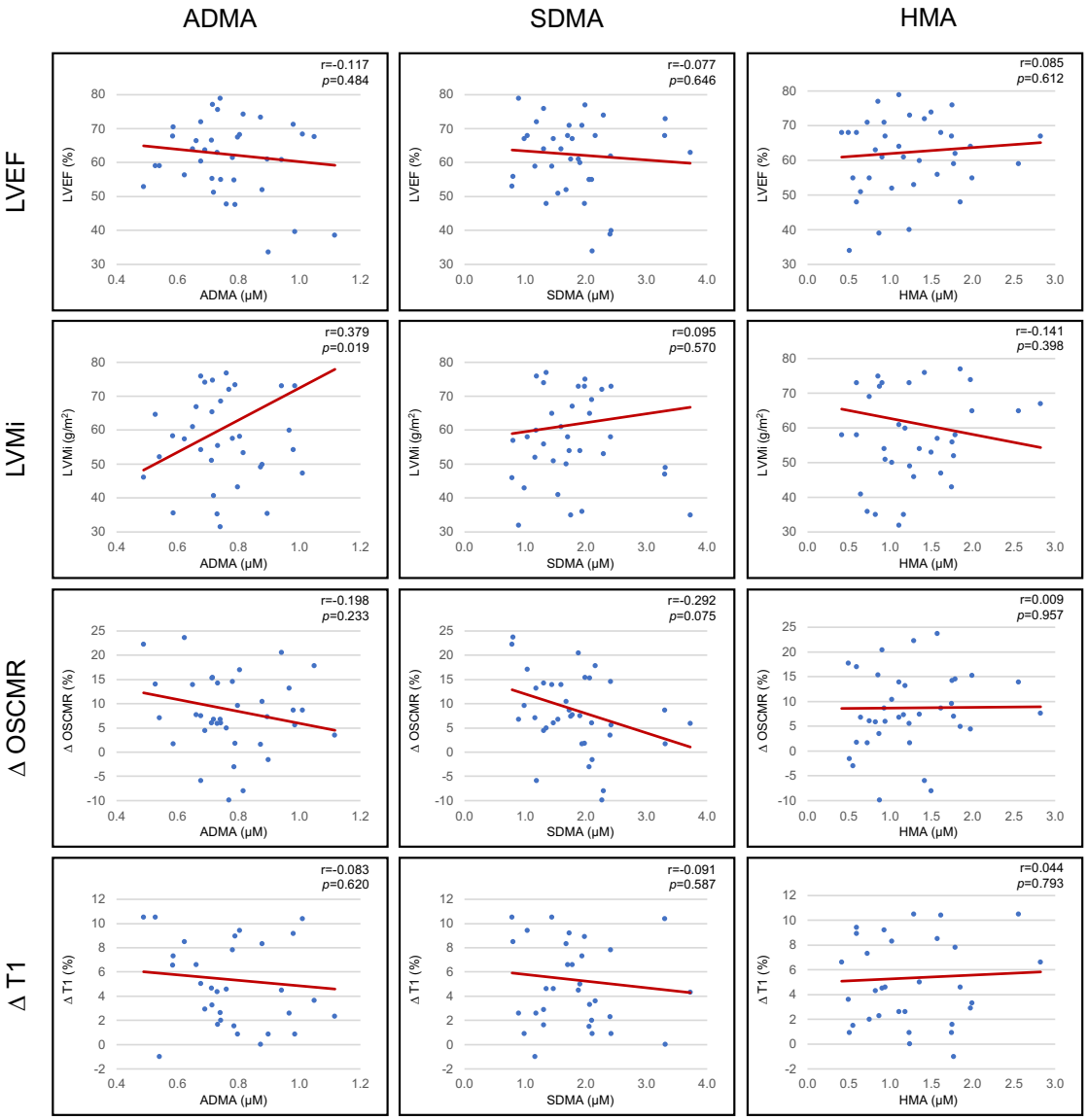

ADMA levels significantly increased with increasing indexed left ventricular mass (r = 0.379, p = 0.019). There was a trend for SDMA levels to increase with reducing Δ

OS-CMR SI (r = -0.292, *p* = 0.075). Apart from these, LVEF, LVMi, stress OSCMR and stress T1 mapping were not significantly associated with the levels of arginine metabolites (Figure 7.4).

7.4.6 Adjusted partial correlations of biochemical markers of endothelial dysfunction (arginine metabolites) with myocardial oxygenation (Δ OS-CMR SI) and perfusion response to stress (Δ T1).

Table 7.4 shows the partial correlation values between the arginine metabolites and OS-CMR and T1 mapping after adjusting for age, gender, body mass index, C-reactive protein and troponin T. There was no significant correlation between Δ OS-CMR SI and any of the metabolites.

Table 7.4: Partial correlation values between the arginine metabolites and OS-CMR and T1 mapping after adjusting for age, gender, body mass index, C-reactive protein and troponin T.

Analyte	OS-CMR (n=38)		T1 Mapping (n=30)	
	r-value	p-value	r-value	p-value
ADMA (μM)	-0.106	0.558	-0.419	0.037
L-ARG (μM)	-0.183	0.308	-0.338	0.098
CIT (μM)	-0.102	0.573	-0.444	0.026
HMA (μM)	-0.164	0.362	0.000	0.999
L-NMMA (μM)	0.078	0.666	-0.002	0.992
ORN (μM)	-0.156	0.387	-0.460	0.021
SDMA (μM)	-0.226	0.206	-0.080	0.702

Legend: ADMA, asymmetric dimethylarginine; L-ARG, L-arginine; CIT, L-citrulline; HMA, L-homoarginine; L-NMMA, N^G –monomethyl-L-arginine; ORN, L-ornithine; SDMA, symmetric dimethylarginine

Interestingly, there were significant negative correlations seen between Δ T1 and ADMA (r = -0.419, *p* = 0.037, n = 30), L-citrulline (r = -0.444, *p* = 0.026, n = 30) and Ornithine (r = -0.460, *p* = 0.021, n = 30). There was a negative trend observed for the

adjusted partial correlation between ∆ T1 and L-arginine (r = -0.338, *p* = 0.098, n=30) but no correlation between ∆ T1 and SDMA, HMA or L-NMMA.

7.5 Discussion

This is the first study to assess the relationship between biochemical markers of endothelial dysfunction and novel Gadolinium-free CMR methods of assessment of myocardial ischaemia. There are a few important findings in this study which are discussed below.

Most importantly, there was a significant negative association between ∆ T1 response and ADMA and Ornithine levels in CKD patients. In contrast, ∆ OS-CMR SI was not significantly associated with circulating levels of arginine metabolites. It was found that reduced myocardial perfusion reserve (as denoted by the ∆ T1 response) was associated with some biochemical markers of endothelial dysfunction in the CKD population, but reduced myocardial oxygenation (as denoted by stress ∆ OS-CMR SI response) was not. The presence of diffuse interstitial fibrosis in CKD patients would have resulted in higher resting T1 values (335, 336) and concomitant lower Δ T1 values. At the same time, CKD may be associated with metabolic changes to avert ischaemia in the face of hypoperfusion resulting in a down-regulation of energy requiring processes, such as that thought to occur in hibernating myocardium. This may result in a degree of physiological reserve that results in decreased tissue deoxygenation during hypoperfusion and therefore apparent higher Δ OS-CMR SI values in the patient group with advanced CKD than what would be expected. Above discussed factors may explain the poor correlation seen between resting OS-CMR and markers of endothelial dysfunction in these patients.

Another important finding in this study was that ADMA and SDMA levels were higher and HMA levels lower in patients with CKD when compared to the normal volunteers. This can be regarded as indirect evidence for endothelial dysfunction in the CKD cohort. These findings are in line with previous studies where patients with mild-moderate CKD have elevated plasma levels of ADMA and SDMA compared to normal controls (223-226). This increase is more pronounced in ESKD (227, 228).

Furthermore, ADMA, SDMA and HMA were not significantly different in the CKD patients with CAD when compared to CKD patients without CAD. Similar to CAD, CKD too is associated with higher levels of ADMA and SDMA and lower levels of HMA. This might have made the difference between the 2 groups (CKD without CAD versus CKD with CAD) less significant. Furthermore, when compared to the general population, the pathogenesis of CAD is more complex in the CKD population. In addition to traditional risk factors, several uraemia-related risk factors such as inflammation, oxidative stress, endothelial dysfunction, coronary artery calcification, hyperhomocysteinemia, and immunosuppressants have been associated with accelerated atherosclerosis. Thus, the pathogenesis of CAD in this group of patients is diverse and without any single common pathway, which makes the detection of CAD by any one test very difficult in this group.

Endothelial function (as indirectly assessed by measuring levels of ADMA and HMA) was noted to be worse in females, older age and those with increased LVMi and troponin T levels. These findings are not surprising and have been described previously.

In CKD, endothelial dysfunction and atherosclerosis are almost universal, as well as cardiovascular complications. Endothelial cell damage or injury is invariably

associated with such clinical conditions as thrombosis, hypertension, renal failure and atherosclerosis and may be also responsible for accelerated atherosclerosis in patients with chronic renal failure. Although traditional risk factors are common among CKD patients, they can only in part explain the increased susceptibility to CVD (201). Non-traditional cardiovascular risk factors are important in the pathogenesis of CVD in CKD. These non-traditional risk factors result in endothelial dysfunction which has a central role in the pathogenesis of CVD together with inflammation and atherosclerosis. Considering that CKD patients are more likely to die of CVD than to progress to End-Stage Renal Disease (ESRD), the search for novel CVD risk factors in this population may yield novel therapeutic targets.

7.5.1 Limitations

Due to the small sample size, these results are hypothesis-generating and therefore need to be confirmed with larger studies. Secondly, CTCA or invasive coronary angiogram was not performed (due to advanced renal failure) in this patient cohort and therefore it may be possible that some patients might have had significant undiagnosed CAD. Thirdly, the CKD patients were unable to have gadolinium contrast due to the risk of nephrogenic systemic fibrosis, therefore late gadolinium enhancement could not be performed. Fourthly, endothelial function was not directly assessed. Lastly, although image quality was generally good, artefacts could not always be resolved with frequency and shim adjustments and this could lead to reduced specificity.

7.6 Conclusion

This study demonstrates that there is a significant association between ADMA levels and Stress T1 response in CKD patients. However, Δ OS-CMR SI was not significantly associated with circulating ADMA or HMA levels.

7.7 Future Directions

This pilot study needs to be confirmed with larger, multi-centre studies to investigate the prognostic role of ADMA in CKD patients with CMR-documented CAD. Further studies may allow inclusion of patients with less severe kidney disease into the study.

CHAPTER 8: SUMMARY AND CONCLUSIONS

8.1 Summary of findings in the thesis and conclusions

With significant medical advancements made in the past few decades the number of patients with severe kidney disease requiring renal replacement therapy (RRT) is rising (Figure 1.1). Patients with End Stage Kidney Disease (ESKD) carry a 5-10-fold higher risk for developing cardiovascular disease (CVD) compared to age-matched controls. According to the Australia and New Zealand Dialysis and Transplant Registry, the median expected remaining lifespan of patients while on maintenance dialysis (between 2008 to 2017) was approximately 6.4 years for those aged 45-64 years and 4.7 years for those aged 65-74 years suggesting that survival, especially in older patients, is comparable to that of lung cancer.

Cardiovascular disease (CVD) is the leading cause of mortality in patients with CKD, of which coronary artery disease (CAD) is the most common. CKD is an independent risk factor for the development of CAD (8) and it is present even in early renal disease (13, 17). Decreasing renal function has been shown to be associated with increased risk of death (7, 12) and increased severity of cardiac disease (13-15).

With the above problem in mind, it becomes important that CAD be diagnosed early and accurately in the CKD population. CAD often causes silent or asymptomatic myocardial ischaemia in CKD patients (5, 6) and atypical presentation of CAD in patients with CKD often leads to delay in diagnosis and treatment (337). Current functional cardiac investigations are neither sensitive nor specific for assessment of myocardial ischaemia in CKD patients (338). Exercise tests have limited diagnostic ability in the CKD patients due to reduced exercise capacity, resting ECG changes and ‘balanced ischaemia’. Use of gadolinium-based (as in perfusion CMR) or iodine-

based (as in invasive coronary angiography) contrast agents should best be avoided in advanced CKD due to nephrogenic systemic sclerosis (NSF) and possibility of worsening the renal function. Therefore, there is an unmet need for a functional stress test that is non-invasive, safe and relatively accurate in this very high-risk CKD population. Two novel gadolinium-free stress CMR techniques for the assessment of myocardial ischaemia in CKD have been described here. These are Oxygen Sensitive CMR (OS-CMR) and stress T1 mapping.

OS-CMR uses the paramagnetic properties of deoxygenated haemoglobin as an intrinsic contrast so that the transverse magnetisation or T2 time is increased when there is a drop in the proportion of deoxyhaemoglobin and decreased when there is a rise in the proportion of deoxyhaemoglobin. It detects both epicardial and microvascular CAD without the use of potentially toxic contrast agents. OS-CMR has been validated in human and animal models with promising results (107-117). OS-CMR has been utilised in several human studies to assess myocardial oxygenation as a measure of ischaemia (107, 108, 118-122) including Syndrome X, hypertensive patients, patients with CAD, hypertrophic cardiomyopathy and aortic stenosis. The diagnostic ability of stress OS-CMR in the CKD population has been previously studied in smaller number of CKD patients (127). In this study, OS-CMR stress response was significantly blunted in CKD patients with no known cardiac disease when compared to healthy and hypertensive controls. No previous study has investigated the prognostic utility of OS-CMR in any group (CKD or non-CKD) of patients. An important finding from this thesis study was that impaired OS-CMR response may have prognostic value in its capacity to predict CKD patients at higher risk of death, non-fatal myocardial infarction, heart failure and ventricular arrhythmias

in the future. This can help in targeting specific therapies to specific groups of patients.

T1 relaxation time, spin-lattice relaxation time, or simply T1, describes the exponential recovery of the longitudinal component of magnetization back towards its thermal equilibrium. T1 is prolonged by increased water content and, importantly, depends on blood T1 through its partial volume. Recent studies have shown that T1 mapping, when used with a vasodilator stress, can distinguish between normal, ischaemic, infarcted and remote (i.e. segments without ischaemia or infarction) myocardium without the need for gadolinium contrast agents (144). This method has subsequently been validated against invasive coronary measures for the accurate detection and differentiation between epicardial coronary artery disease and microvascular dysfunction (145). T1 mapping technique may have a few advantages over OS-CMR. Firstly, the method of stress T1 mapping described in the studies above used measurements in three myocardial slices whereas OS-CMR measurements (described in chapter 3) were performed on one slice only. Secondly, T1 mapping can be performed on both 1.5T and 3T magnets and therefore can be widely available to all centres whereas OS-CMR measurements require a 3T magnet which has limited availability. Stress T1 mapping has not been studied in the CKD population previously. This thesis study demonstrates that not only is stress T1 mapping feasible in CKD patients, it is impaired in these patients even when they do not have symptoms suggestive of CAD. In those with known CAD, adenosine stress and rest T1 mapping was also able to differentiate between normal, infarcted, ischemic, and remote myocardial tissue classes with distinctive T1 profiles, but OS-CMR was not significantly different between these groups. This technique may also be of specific use in the chronic kidney disease population where both epicardial

coronary artery disease and microvascular dysfunction are common and use of gadolinium-based contrast agents is not preferred.

Increased epicardial fat is associated with the more traditional metabolic risk factors such as BMI, dyslipidemia, impaired fasting glucose, Type 2 Diabetes Mellitus (T2DM) and hypertension. CKD is often the result of one or more of the above risk factors (188). Obesity is common amongst patients with moderate-severe CKD (189, 190). Echocardiographically assessed epicardial fat thickness is significantly greater in patients on hemodialysis compared with healthy controls and positively correlated with hemodialysis duration (191, 192). Furthermore, echocardiographically assessed epicardial fat tissue thickness has been shown to correlate with oxidant biomarkers in CKD and CKD disease progression (193). However, echocardiographic assessment of epicardial fat was limited in these studies as only 2 dimensional assessments were made. CMR has an advantage in this regard as it can measure fat volumes. CMR assessed PVAT volumes have not previously been studied in the CKD population. In this thesis study, PVAT volume was increased in patients with CKD compared to normal individuals. This finding is similar to previous studies described above using echocardiography. However, the increased PVAT volume in this study was not a predictor of future events.

Reduced nitric oxide (NO) bioavailability is a major risk factor for cardiovascular disease and progression to kidney failure in patients with chronic kidney disease (CKD) (310-312). Endothelial nitric oxide synthase (eNOS) catalyzes the conversion of L-arginine (ARG) and L-homoarginine (HMA) to NO (314). LNMMA, ADMA and SDMA are inhibitors of eNOS activity. This thesis is the first study to assess the relationship between the above biochemical markers of endothelial dysfunction and

novel Gadolinium-free CMR methods of assessment of myocardial ischaemia. ADMA and SDMA levels were higher and HMA levels lower in patients with CKD when compared to the normal volunteers. However, these biomarkers were not significantly different in the CKD patients with CAD when compared to CKD patients without CAD. Importantly, there was a significant negative association between stress T1 response and ADMA and Ornithine levels in CKD patients. However, Δ OS-CMR SI was not significantly associated with circulating levels of arginine metabolites. In other words, reduced myocardial perfusion (as denoted by the stress T1 response) was associated with some biochemical markers of endothelial dysfunction in the CKD population, but reduced myocardial oxygenation (as denoted by stress OS-CMR response) was not. These are novel findings and in future studies may help further understand the complex pathophysiological processes involved in CAD in the CKD population.

To summarize, this thesis study provided a better understanding of the complex relationships between CKD and CAD using non-invasive CMR methods. The thesis proposed two important CMR diagnostic stress imaging methods that are safe, non-invasive and without the risks of radiation exposure or contrast agents. Moreover, one of these methods may potentially predict adverse events in these patients with CKD. Furthermore, it may be possible to differentiate between normal, infarcted, ischemic, and remote myocardial tissue utilizing their distinctive tissue characteristics and stress responses.

8.2 Future Directions

The studies in this thesis were done in relatively small number of patients and need to be confirmed with larger, multi-centre studies to determine the wider diagnostic

and prognostic value of stress OS-CMR and T1 mapping in the CKD population in guiding clinical decision-making and predicting long-term prognosis. The hypothesis should further be extended to patients with less severe CKD which form the larger CKD community with a higher life expectancy and therefore potentially to benefit more from therapeutic interventions. These patients could then have CTCA or invasive coronary angiography and this could avoid one of the big limitations in the studies presented in this thesis which was that CTCA or invasive coronary angiography was not performed (due to advanced renal failure) and therefore it may have been possible that some of these patients might have had significant undiagnosed CAD. These studies will help in further understanding of the complex mechanisms that lead to the higher CVD risk in CKD patients, decide treatment interventions and improve long term outcomes.

References

1. ANZDATA Registry. 40th Report, Chapter 1: Incidence of End Stage Kidney Disease. Australia and New Zealand Dialysis and Transplant Registry, Adelaide, Australia. 2018. Available at: http://www.anzdata.org.au.

2. Iimori S, Naito S, Noda Y, Nishida H, Kihira H, Yui N, et al. Anaemia management and mortality risk in newly visiting patients with chronic kidney disease in Japan: The CKD-ROUTE study. Nephrology (Carlton). 2015;20(9):601-8.

3. Ritchie J, Rainone F, Green D, Alderson H, Chiu D, Middleton R, et al. Extreme Elevations in Blood Pressure and All-Cause Mortality in a Referred CKD Population: Results from the CRISIS Study. Int J Hypertens. 2013;2013:597906.

4. Shah R, Matthews GJ, Shah RY, McLaughlin C, Chen J, Wolman M, et al. Serum Fractalkine (CX3CL1) and Cardiovascular Outcomes and Diabetes: Findings From the Chronic Renal Insufficiency Cohort (CRIC) Study. Am J Kidney Dis. 2015;66(2):266-73.

5. Ohtake T, Kobayashi S, Moriya H, Negishi K, Okamoto K, Maesato K, et al. High prevalence of occult coronary artery stenosis in patients with chronic kidney disease at the initiation of renal replacement therapy: an angiographic examination. J Am Soc Nephrol. 2005;16(4):1141-8.

6. Hase H, Tsunoda T, Tanaka Y, Takahashi Y, Imamura Y, Ishikawa H, et al. Risk factors for de novo acute cardiac events in patients initiating hemodialysis with no previous cardiac symptom. Kidney Int. 2006;70(6):1142-8.

7. Tonelli M, Wiebe N, Culleton B, House A, Rabbat C, Fok M, et al. Chronic kidney disease and mortality risk: a systematic review. J Am Soc Nephrol. 2006;17(7):2034-47.

8. Sarnak MJ, Levey AS, Schoolwerth AC, Coresh J, Culleton B, Hamm LL, et al. Kidney disease as a risk factor for development of cardiovascular disease: a statement from the American Heart Association Councils on Kidney in Cardiovascular Disease, High Blood Pressure Research, Clinical Cardiology, and Epidemiology and Prevention. Circulation. 2003;108(17):2154-69.

9. Foley RN, Parfrey PS, Sarnak MJ. Clinical epidemiology of cardiovascular disease in chronic renal disease. Am J Kidney Dis. 1998;32(5 Suppl 3):S112-9.

10. Gansevoort RT, Correa-Rotter R, Hemmelgarn BR, Jafar TH, Heerspink HJ, Mann JF, et al. Chronic kidney disease and cardiovascular risk: epidemiology, mechanisms, and prevention. Lancet. 2013;382(9889):339-52.

11. National Kidney F. K/DOQI clinical practice guidelines for chronic kidney disease: evaluation, classification, and stratification. Am J Kidney Dis. 2002;39(2 Suppl 1):S1-266.

12. Sharples EJ, Pereira D, Summers S, Cunningham J, Rubens M, Goldsmith D, et al. Coronary artery calcification measured with electron-beam computerized tomography correlates poorly with coronary artery angiography in dialysis patients. Am J Kidney Dis. 2004;43(2):313-9.

13. Joosen IA, Schiphof F, Versteylen MO, Laufer EM, Winkens MH, Nelemans PJ, et al. Relation between mild to moderate chronic kidney disease and coronary artery disease determined with coronary CT angiography. PLoS One. 2012;7(10):e47267.

14. Chronic Kidney Disease Prognosis C, Matsushita K, van der Velde M, Astor BC, Woodward M, Levey AS, et al. Association of estimated glomerular filtration rate and albuminuria with all-cause and cardiovascular mortality in general population cohorts: a collaborative meta-analysis. Lancet. 2010;375(9731):2073-81.

15. Manjunath G, Tighiouart H, Ibrahim H, MacLeod B, Salem DN, Griffith JL, et al. Level of kidney function as a risk factor for atherosclerotic cardiovascular outcomes in the community. J Am Coll Cardiol. 2003;41(1):47-55.

16. Stack AG, Bloembergen WE. Prevalence and clinical correlates of coronary artery disease among new dialysis patients in the United States: a cross-sectional study. J Am Soc Nephrol. 2001;12(7):1516-23.

17. Henry RM, Kostense PJ, Bos G, Dekker JM, Nijpels G, Heine RJ, et al. Mild renal insufficiency is associated with increased cardiovascular mortality: The Hoorn Study. Kidney Int. 2002;62(4):1402-7.

18. Goodman WG, Goldin J, Kuizon BD, Yoon C, Gales B, Sider D, et al. Coronary-artery calcification in young adults with end-stage renal disease who are undergoing dialysis. N Engl J Med. 2000;342(20):1478-83.

19. Wetmore JB, Broce M, Malas A, Almehmi A. Painless myocardial ischemia is associated with mortality in patients with chronic kidney disease. Nephron Clin Pract. 2012;122(1-2):9-16.

20. Kawai H, Sarai M, Motoyama S, Harigaya H, Ito H, Sanda Y, et al. Coronary plaque characteristics in patients with mild chronic kidney disease. Analysis by 320-row area detector computed tomography. Circ J. 2012;76(6):1436-41.

21. Charytan DM, Shelbert HR, Di Carli MF. Coronary microvascular function in early chronic kidney disease. Circ Cardiovasc Imaging. 2010;3(6):663-71.

22. Lin T, Rechenmacher S, Rasool S, Varadarajan P, Pai RG. Reduced survival in patients with "coronary microvascular disease". Int J Angiol. 2012;21(2):89-94.

23. Cho I, Min HS, Chun EJ, Park SK, Choi Y, Blumenthal RS, et al. Coronary atherosclerosis detected by coronary CT angiography in asymptomatic subjects with early chronic kidney disease. Atherosclerosis. 2010;208(2):406-11.

24. Amann K, Wiest G, Zimmer G, Gretz N, Ritz E, Mall G. Reduced capillary density in the myocardium of uremic rats--a stereological study. Kidney Int. 1992;42(5):1079-85.

25. Jacobi J, Porst M, Cordasic N, Namer B, Schmieder RE, Eckardt KU, et al. Subtotal nephrectomy impairs ischemia-induced angiogenesis and hindlimb re-perfusion in rats. Kidney Int. 2006;69(11):2013-21.

26. Amann K, Breitbach M, Ritz E, Mall G. Myocyte/capillary mismatch in the heart of uremic patients. J Am Soc Nephrol. 1998;9(6):1018-22.

27. Charytan DM, Padera R, Helfand AM, Zeisberg M, Xu X, Liu X, et al. Increased concentration of circulating angiogenesis and nitric oxide inhibitors induces endothelial to mesenchymal transition and myocardial fibrosis in patients with chronic kidney disease. Int J Cardiol. 2014;176(1):99-109.

28. Chade AR, Brosh D, Higano ST, Lennon RJ, Lerman LO, Lerman A. Mild renal insufficiency is associated with reduced coronary flow in patients with non-obstructive coronary artery disease. Kidney Int. 2006;69(2):266-71.

29. Charytan DM, Skali H, Shah NR, Veeranna V, Cheezum MK, Taqueti VR, et al. Coronary flow reserve is predictive of the risk of cardiovascular death regardless of chronic kidney disease stage. Kidney Int. 2018;93(2):501-9.

30. Joki N, Hase H, Kawano Y, Nakamura S, Nakajima K, Hatta T, et al. Myocardial perfusion imaging for predicting cardiac events in Japanese patients with advanced chronic kidney disease: 1-year interim report of the J-ACCESS 3 investigation. Eur J Nucl Med Mol Imaging. 2014;41(9):1701-9.

31. Bhatti S, Hakeem A, Dhanalakota S, Palani G, Husain Z, Jacobsen G, et al. Prognostic value of regadenoson myocardial single-photon emission computed

tomography in patients with different degrees of renal dysfunction. Eur Heart J Cardiovasc Imaging. 2014;15(8):933-40.

32. Yoda S, Nakanishi K, Tano A, Kasamaki Y, Kunimoto S, Matsumoto N, et al. Risk stratification of cardiovascular events in patients at all stages of chronic kidney disease using myocardial perfusion SPECT. J Cardiol. 2012;60(5):377-82.

33. Okuyama C, Nakajima K, Hatta T, Nishimura S, Kusuoka H, Yamashina A, et al. Incremental prognostic value of myocardial perfusion single photon emission computed tomography for patients with diabetes and chronic kidney disease. Nucl Med Commun. 2011;32(10):913-9.

34. Al-Mallah MH, Hachamovitch R, Dorbala S, Di Carli MF. Incremental prognostic value of myocardial perfusion imaging in patients referred to stress single-photon emission computed tomography with renal dysfunction. Circ Cardiovasc Imaging. 2009;2(6):429-36.

35. Hatta T, Nishimura S, Nishimura T. Prognostic risk stratification of myocardial ischaemia evaluated by gated myocardial perfusion SPECT in patients with chronic kidney disease. Eur J Nucl Med Mol Imaging. 2009;36(11):1835-41.

36. Momose M, Babazono T, Kondo C, Kobayashi H, Nakajima T, Kusakabe K. Prognostic significance of stress myocardial ECG-gated perfusion imaging in asymptomatic patients with diabetic chronic kidney disease on initiation of haemodialysis. Eur J Nucl Med Mol Imaging. 2009;36(8):1315-21.

37. Foley RN, Parfrey PS, Sarnak MJ. Epidemiology of cardiovascular disease in chronic renal disease. J Am Soc Nephrol. 1998;9(12 Suppl):S16-23.

38. Levin A, Singer J, Thompson CR, Ross H, Lewis M. Prevalent left ventricular hypertrophy in the predialysis population: identifying opportunities for intervention. Am J Kidney Dis. 1996;27(3):347-54.

39. Zoccali C, Benedetto FA, Mallamaci F, Tripepi G, Giacone G, Cataliotti A, et al. Prognostic impact of the indexation of left ventricular mass in patients undergoing dialysis. J Am Soc Nephrol. 2001;12(12):2768-74.

40. Dimeny EM. Cardiovascular disease after renal transplantation. Kidney Int Suppl. 2002(80):78-84.

41. Ojo AO. Cardiovascular complications after renal transplantation and their prevention. Transplantation. 2006;82(5):603-11.

42. ANZDATA Registry. 40th Report, Chapter 3: Mortality in End Stage Kidney Disease. Australia and New Zealand Dialysis and Transplant Registry, Adelaide, Australia. 2018. Available at: http://www.anzdata.org.au.

43. Nanmoku K, Matsuda Y, Yamamoto T, Tsujita M, Hiramitsu T, Goto N, et al. Clinical characteristics and outcomes of renal transplantation in elderly recipients. Transplant Proc. 2012;44(1):281-3.

44. Rigatto C, Parfrey P, Foley R, Negrijn C, Tribula C, Jeffery J. Congestive heart failure in renal transplant recipients: risk factors, outcomes, and relationship with ischemic heart disease. J Am Soc Nephrol. 2002;13(4):1084-90.

45. Marcassi AP, Yasbek DC, Pestana JO, Fachini FC, De Lira Filho EB, Cassiolato JL, et al. Ventricular arrhythmia in incident kidney transplant recipients: prevalence and associated factors. Transpl Int. 2011;24(1):67-72.

46. Boots JM, Christiaans MH, van Hooff JP. Effect of immunosuppressive agents on long-term survival of renal transplant recipients: focus on the cardiovascular risk. Drugs. 2004;64(18):2047-73.

47. Lang P, Pardon A, Audard V. Long-term benefit of mycophenolate mofetil in renal transplantation. Transplantation. 2005;79(3 Suppl):S47-8.

48. Borrows R, Loucaidou M, Chusney G, Borrows S, Tromp JV, Cairns T, et al. Anaemia and congestive heart failure early post-renal transplantation. Nephrol Dial Transplant. 2008;23(5):1728-34.

49. Chueh SC, Kahan BD. Dyslipidemia in renal transplant recipients treated with a sirolimus and cyclosporine-based immunosuppressive regimen: incidence, risk factors, progression, and prognosis. Transplantation. 2003;76(2):375-82.

50. First MR, Neylan JF, Rocher LL, Tejani A. Hypertension after renal transplantation. J Am Soc Nephrol. 1994;4(8 Suppl):S30-6.

51. Burdmann EA, Andoh TF, Yu L, Bennett WM. Cyclosporine nephrotoxicity. Semin Nephrol. 2003;23(5):465-76.

52. Ruggenenti P, Perico N, Mosconi L, Gaspari F, Benigni A, Amuchastegui CS, et al. Calcium channel blockers protect transplant patients from cyclosporine-induced daily renal hypoperfusion. Kidney Int. 1993;43(3):706-11.

53. Lipkin GW, Tucker B, Giles M, Raine AE. Ambulatory blood pressure and left ventricular mass in cyclosporin- and non-cyclosporin-treated renal transplant recipients. J Hypertens. 1993;11(4):439-42.

54. Pirsch JD, Miller J, Deierhoi MH, Vincenti F, Filo RS. A comparison of tacrolimus (FK506) and cyclosporine for immunosuppression after cadaveric renal transplantation. FK506 Kidney Transplant Study Group. Transplantation. 1997;63(7):977-83.

55. Ekberg H, Tedesco-Silva H, Demirbas A, Vitko S, Nashan B, Gurkan A, et al. Reduced exposure to calcineurin inhibitors in renal transplantation. N Engl J Med. 2007;357(25):2562-75.

56. Margreiter R, European Tacrolimus vs Ciclosporin Microemulsion Renal Transplantation Study G. Efficacy and safety of tacrolimus compared with ciclosporin

microemulsion in renal transplantation: a randomised multicentre study. Lancet. 2002;359(9308):741-6.

57. Ahsan N, Johnson C, Gonwa T, Halloran P, Stegall M, Hardy M, et al. Randomized trial of tacrolimus plus mycophenolate mofetil or azathioprine versus cyclosporine oral solution (modified) plus mycophenolate mofetil after cadaveric kidney transplantation: results at 2 years. Transplantation. 2001;72(2):245-50.

58. Johnson C, Ahsan N, Gonwa T, Halloran P, Stegall M, Hardy M, et al. Randomized trial of tacrolimus (Prograf) in combination with azathioprine or mycophenolate mofetil versus cyclosporine (Neoral) with mycophenolate mofetil after cadaveric kidney transplantation. Transplantation. 2000;69(5):834-41.

59. Tory R, Sachs-Barrable K, Goshko CB, Hill JS, Wasan KM. Tacrolimus-induced elevation in plasma triglyceride concentrations after administration to renal transplant patients is partially due to a decrease in lipoprotein lipase activity and plasma concentrations. Transplantation. 2009;88(1):62-8.

60. Chang RK, Alzona M, Alejos J, Jue K, McDiarmid SV. Marked left ventricular hypertrophy in children on tacrolimus (FK506) after orthotopic liver transplantation. Am J Cardiol. 1998;81(10):1277-80.

61. Euvrard S, Morelon E, Rostaing L, Goffin E, Brocard A, Tromme I, et al. Sirolimus and secondary skin-cancer prevention in kidney transplantation. N Engl J Med. 2012;367(4):329-39.

62. Morice MC, Serruys PW, Sousa JE, Fajadet J, Ban Hayashi E, Perin M, et al. A randomized comparison of a sirolimus-eluting stent with a standard stent for coronary revascularization. N Engl J Med. 2002;346(23):1773-80.

63. Serruys PW, Degertekin M, Tanabe K, Abizaid A, Sousa JE, Colombo A, et al. Intravascular ultrasound findings in the multicenter, randomized, double-blind

RAVEL (RAndomized study with the sirolimus-eluting VElocity balloon-expandable stent in the treatment of patients with de novo native coronary artery Lesions) trial. Circulation. 2002;106(7):798-803.

64. Webster AC, Lee VW, Chapman JR, Craig JC. Target of rapamycin inhibitors (TOR-I; sirolimus and everolimus) for primary immunosuppression in kidney transplant recipients. Cochrane Database Syst Rev. 2006(2):CD004290.

65. Levy G, Schmidli H, Punch J, Tuttle-Newhall E, Mayer D, Neuhaus P, et al. Safety, tolerability, and efficacy of everolimus in de novo liver transplant recipients: 12- and 36-month results. Liver Transpl. 2006;12(11):1640-8.

66. Gurk-Turner C, Manitpisitkul W, Cooper M. A comprehensive review of everolimus clinical reports: a new mammalian target of rapamycin inhibitor. Transplantation. 2012;94(7):659-68.

67. Gianrossi R, Detrano R, Mulvihill D, Lehmann K, Dubach P, Colombo A, et al. Exercise-induced ST depression in the diagnosis of coronary artery disease. A meta-analysis. Circulation. 1989;80(1):87-98.

68. Sharma R, Pellerin D, Gaze DC, Gregson H, Streather CP, Collinson PO, et al. Dobutamine stress echocardiography and the resting but not exercise electrocardiograph predict severe coronary artery disease in renal transplant candidates. Nephrol Dial Transplant. 2005;20(10):2207-14.

69. Schmidt A, Stefenelli T, Schuster E, Mayer G. Informational contribution of noninvasive screening tests for coronary artery disease in patients on chronic renal replacement therapy. Am J Kidney Dis. 2001;37(1):56-63.

70. Howden EJ, Weston K, Leano R, Sharman JE, Marwick TH, Isbel NM, et al. Cardiorespiratory fitness and cardiovascular burden in chronic kidney disease. J Sci Med Sport. 2015;18(4):492-7.

71. Armstrong WF, Zoghbi WA. Stress echocardiography: current methodology and clinical applications. J Am Coll Cardiol. 2005;45(11):1739-47.

72. Banerjee A, Newman DR, Van den Bruel A, Heneghan C. Diagnostic accuracy of exercise stress testing for coronary artery disease: a systematic review and meta-analysis of prospective studies. Int J Clin Pract. 2012;66(5):477-92.

73. Wang LW, Fahim MA, Hayen A, Mitchell RL, Lord SW, Baines LA, et al. Cardiac testing for coronary artery disease in potential kidney transplant recipients: a systematic review of test accuracy studies. Am J Kidney Dis. 2011;57(3):476-87.

74. Tita C, Karthikeyan V, Stroe A, Jacobsen G, Ananthasubramaniam K. Stress echocardiography for risk stratification in patients with end-stage renal disease undergoing renal transplantation. J Am Soc Echocardiogr. 2008;21(4):321-6.

75. Bergeron S, Hillis GS, Haugen EN, Oh JK, Bailey KR, Pellikka PA. Prognostic value of dobutamine stress echocardiography in patients with chronic kidney disease. Am Heart J. 2007;153(3):385-91.

76. Herzog CA, Marwick TH, Pheley AM, White CW, Rao VK, Dick CD. Dobutamine stress echocardiography for the detection of significant coronary artery disease in renal transplant candidates. Am J Kidney Dis. 1999;33(6):1080-90.

77. Marwick TH, Lauer MS, Lobo A, Nally J, Braun W. Use of dobutamine echocardiography for cardiac risk stratification of patients with chronic renal failure. J Intern Med. 1998;244(2):155-61.

78. Makani H, Bangalore S, Halpern D, Makwana HG, Chaudhry FA. Cardiac outcomes with submaximal normal stress echocardiography: a meta-analysis. J Am Coll Cardiol. 2012;60(15):1393-401.

79. Salerno M, Beller GA. Noninvasive assessment of myocardial perfusion. Circ Cardiovasc Imaging. 2009;2(5):412-24.

80. De Vriese AS, Vandecasteele SJ, Van den Bergh B, De Geeter FW. Should we screen for coronary artery disease in asymptomatic chronic dialysis patients? Kidney Int. 2012;81(2):143-51.

81. Bourque JM, Beller GA. Stress myocardial perfusion imaging for assessing prognosis: an update. JACC Cardiovasc Imaging. 2011;4(12):1305-19.

82. Lima RS, Watson DD, Goode AR, Siadaty MS, Ragosta M, Beller GA, et al. Incremental value of combined perfusion and function over perfusion alone by gated SPECT myocardial perfusion imaging for detection of severe three-vessel coronary artery disease. J Am Coll Cardiol. 2003;42(1):64-70.

83. Furuhashi T, Moroi M, Joki N, Hase H, Minakawa M, Masai H, et al. Prediction of cardiovascular events in pre-dialysis chronic kidney disease patients with normal SPECT myocardial perfusion imaging. J Cardiol. 2014;63(2):154-8.

84. Hakeem A, Bhatti S, Dillie KS, Cook JR, Samad Z, Roth-Cline MD, et al. Predictive value of myocardial perfusion single-photon emission computed tomography and the impact of renal function on cardiac death. Circulation. 2008;118(24):2540-9.

85. Wang LW, Masson P, Turner RM, Lord SW, Baines LA, Craig JC, et al. Prognostic value of cardiac tests in potential kidney transplant recipients: a systematic review. Transplantation. 2015;99(4):731-45.

86. Fukushima K, Javadi MS, Higuchi T, Bravo PE, Chien D, Lautamaki R, et al. Impaired global myocardial flow dynamics despite normal left ventricular function and regional perfusion in chronic kidney disease: a quantitative analysis of clinical 82Rb PET/CT studies. J Nucl Med. 2012;53(6):887-93.

87. Koivuviita N, Tertti R, Jarvisalo M, Pietila M, Hannukainen J, Sundell J, et al. Increased basal myocardial perfusion in patients with chronic kidney disease without symptomatic coronary artery disease. Nephrol Dial Transplant. 2009;24(9):2773-9.

88. Rabbat CG, Treleaven DJ, Russell JD, Ludwin D, Cook DJ. Prognostic value of myocardial perfusion studies in patients with end-stage renal disease assessed for kidney or kidney-pancreas transplantation: a meta-analysis. J Am Soc Nephrol. 2003;14(2):431-9.

89. Hage FG, Dean P, Bhatia V, Iqbal F, Heo J, Iskandrian AE. The prognostic value of the heart rate response to adenosine in relation to diabetes mellitus and chronic kidney disease. Am Heart J. 2011;162(2):356-62.

90. Hage FG, Dean P, Iqbal F, Heo J, Iskandrian AE. A blunted heart rate response to regadenoson is an independent prognostic indicator in patients undergoing myocardial perfusion imaging. J Nucl Cardiol. 2011;18(6):1086-94.

91. Venkataraman R, Hage FG, Dorfman TA, Heo J, Aqel RA, de Mattos AM, et al. Relation between heart rate response to adenosine and mortality in patients with end-stage renal disease. Am J Cardiol. 2009;103(8):1159-64.

92. Wilson RF, Wyche K, Christensen BV, Zimmer S, Laxson DD. Effects of adenosine on human coronary arterial circulation. Circulation. 1990;82(5):1595-606.

93. Karamitsos TD, Dall'Armellina E, Choudhury RP, Neubauer S. Ischemic heart disease: comprehensive evaluation by cardiovascular magnetic resonance. Am Heart J. 2011;162(1):16-30.

94. Gerber BL, Raman SV, Nayak K, Epstein FH, Ferreira P, Axel L, et al. Myocardial first-pass perfusion cardiovascular magnetic resonance: history, theory, and current state of the art. J Cardiovasc Magn Reson. 2008;10:18.

95. Hamon M, Fau G, Nee G, Ehtisham J, Morello R, Hamon M. Meta-analysis of the diagnostic performance of stress perfusion cardiovascular magnetic resonance for detection of coronary artery disease. J Cardiovasc Magn Reson. 2010;12:29.

96. Nandalur KR, Dwamena BA, Choudhri AF, Nandalur MR, Carlos RC. Diagnostic performance of stress cardiac magnetic resonance imaging in the detection of coronary artery disease: a meta-analysis. J Am Coll Cardiol. 2007;50(14):1343-53.

97. Mandapaka S, D'Agostino R, Jr., Hundley WG. Does late gadolinium enhancement predict cardiac events in patients with ischemic cardiomyopathy? Circulation. 2006;113(23):2676-8.

98. Vogel-Claussen J, Rochitte CE, Wu KC, Kamel IR, Foo TK, Lima JA, et al. Delayed enhancement MR imaging: utility in myocardial assessment. Radiographics. 2006;26(3):795-810.

99. Saeed M, Wagner S, Wendland MF, Derugin N, Finkbeiner WE, Higgins CB. Occlusive and reperfused myocardial infarcts: differentiation with Mn-DPDP--enhanced MR imaging. Radiology. 1989;172(1):59-64.

100. Sueyoshi E, Sakamoto I, Uetani M. Myocardial delayed contrast-enhanced MRI: relationships between various enhancing patterns and myocardial diseases. Br J Radiol. 2009;82(980):691-7.

101. Wagner A, Mahrholdt H, Holly TA, Elliott MD, Regenfus M, Parker M, et al. Contrast-enhanced MRI and routine single photon emission computed tomography (SPECT) perfusion imaging for detection of subendocardial myocardial infarcts: an imaging study. Lancet. 2003;361(9355):374-9.

102. Dewey M, Kaufels N, Laule M, Schnorr J, Wagner S, Kivelitz D, et al. Assessment of myocardial infarction in pigs using a rapid clearance blood pool contrast medium. Magn Reson Med. 2004;51(4):703-9.

103. Ganesan AN, Gunton J, Nucifora G, McGavigan AD, Selvanayagam JB. Impact of Late Gadolinium Enhancement on mortality, sudden death and major adverse cardiovascular events in ischemic and nonischemic cardiomyopathy: A systematic review and meta-analysis. Int J Cardiol. 2018;254:230-7.

104. Prince MR, Zhang H, Morris M, MacGregor JL, Grossman ME, Silberzweig J, et al. Incidence of nephrogenic systemic fibrosis at two large medical centers. Radiology. 2008;248(3):807-16.

105. Golding LP, Provenzale JM. Nephrogenic systemic fibrosis: possible association with a predisposing infection. AJR Am J Roentgenol. 2008;190(4):1069-75.

106. Bose C, Megyesi JK, Shah SV, Hiatt KM, Hall KA, Karaduta O, et al. Evidence Suggesting a Role of Iron in a Mouse Model of Nephrogenic Systemic Fibrosis. PLoS One. 2015;10(8):e0136563.

107. Karamitsos TD, Dass S, Suttie J, Sever E, Birks J, Holloway CJ, et al. Blunted myocardial oxygenation response during vasodilator stress in patients with hypertrophic cardiomyopathy. J Am Coll Cardiol. 2013;61(11):1169-76.

108. Mahmod M, Francis JM, Pal N, Lewis A, Dass S, De Silva R, et al. Myocardial perfusion and oxygenation are impaired during stress in severe aortic stenosis and correlate with impaired energetics and subclinical left ventricular dysfunction. J Cardiovasc Magn Reson. 2014;16:29.

109. Zheng J, Wang J, Nolte M, Li D, Gropler RJ, Woodard PK. Dynamic estimation of the myocardial oxygen extraction ratio during dipyridamole stress by MRI: a preliminary study in canines. Magn Reson Med. 2004;51(4):718-26.

110. Vohringer M, Flewitt JA, Green JD, Dharmakumar R, Wang J, Jr., Tyberg JV, et al. Oxygenation-sensitive CMR for assessing vasodilator-induced changes of myocardial oxygenation. J Cardiovasc Magn Reson. 2010;12:20.

111. McCommis KS, Zhang H, Goldstein TA, Misselwitz B, Abendschein DR, Gropler RJ, et al. Myocardial blood volume is associated with myocardial oxygen consumption: an experimental study with cardiac magnetic resonance in a canine model. JACC Cardiovasc Imaging. 2009;2(11):1313-20.

112. McCommis KS, Goldstein TA, Abendschein DR, Herrero P, Misselwitz B, Gropler RJ, et al. Quantification of regional myocardial oxygenation by magnetic resonance imaging: validation with positron emission tomography. Circ Cardiovasc Imaging. 2010;3(1):41-6.

113. Reeder SB, Holmes AA, McVeigh ER, Forder JR. Simultaneous noninvasive determination of regional myocardial perfusion and oxygen content in rabbits: toward direct measurement of myocardial oxygen consumption at MR imaging. Radiology. 1999;212(3):739-47.

114. Shea SM, Fieno DS, Schirf BE, Bi X, Huang J, Omary RA, et al. T2-prepared steady-state free precession blood oxygen level-dependent MR imaging of myocardial perfusion in a dog stenosis model. Radiology. 2005;236(2):503-9.

115. Foltz WD, Huang H, Fort S, Wright GA. Vasodilator response assessment in porcine myocardium with magnetic resonance relaxometry. Circulation. 2002;106(21):2714-9.

116. Fieno DS, Shea SM, Li Y, Harris KR, Finn JP, Li D. Myocardial perfusion imaging based on the blood oxygen level-dependent effect using T2-prepared steady-state free-precession magnetic resonance imaging. Circulation. 2004;110(10):1284-90.

117. Dharmakumar R, Arumana JM, Tang R, Harris K, Zhang Z, Li D. Assessment of regional myocardial oxygenation changes in the presence of coronary artery stenosis with balanced SSFP imaging at 3.0 T: theory and experimental evaluation in canines. J Magn Reson Imaging. 2008;27(5):1037-45.

118. Karamitsos TD, Arnold JR, Pegg TJ, Francis JM, Birks J, Jerosch-Herold M, et al. Patients with syndrome X have normal transmural myocardial perfusion and oxygenation: a 3-T cardiovascular magnetic resonance imaging study. Circ Cardiovasc Imaging. 2012;5(2):194-200.

119. Karamitsos TD, Leccisotti L, Arnold JR, Recio-Mayoral A, Bhamra-Ariza P, Howells RK, et al. Relationship between regional myocardial oxygenation and perfusion in patients with coronary artery disease: insights from cardiovascular magnetic resonance and positron emission tomography. Circ Cardiovasc Imaging. 2010;3(1):32-40.

120. Wacker CM, Hartlep AW, Pfleger S, Schad LR, Ertl G, Bauer WR. Susceptibility-sensitive magnetic resonance imaging detects human myocardium supplied by a stenotic coronary artery without a contrast agent. J Am Coll Cardiol. 2003;41(5):834-40.

121. Friedrich MG, Niendorf T, Schulz-Menger J, Gross CM, Dietz R. Blood oxygen level-dependent magnetic resonance imaging in patients with stress-induced angina. Circulation. 2003;108(18):2219-23.

122. Beache GM, Herzka DA, Boxerman JL, Post WS, Gupta SN, Faranesh AZ, et al. Attenuated myocardial vasodilator response in patients with hypertensive hypertrophy revealed by oxygenation-dependent magnetic resonance imaging. Circulation. 2001;104(11):1214-7.

123. Wacker CM, Bock M, Hartlep AW, Bauer WR, van Kaick G, Pfleger S, et al. BOLD-MRI in ten patients with coronary artery disease: evidence for imaging of capillary recruitment in myocardium supplied by the stenotic artery. MAGMA. 1999;8(1):48-54.

124. Manka R, Paetsch I, Schnackenburg B, Gebker R, Fleck E, Jahnke C. BOLD cardiovascular magnetic resonance at 3.0 tesla in myocardial ischemia. J Cardiovasc Magn Reson. 2010;12:54.

125. Arnold JR, Karamitsos TD, Bhamra-Ariza P, Francis JM, Searle N, Robson MD, et al. Myocardial oxygenation in coronary artery disease: insights from blood oxygen level-dependent magnetic resonance imaging at 3 tesla. J Am Coll Cardiol. 2012;59(22):1954-64.

126. Walcher T, Manzke R, Hombach V, Rottbauer W, Wohrle J, Bernhardt P. Myocardial perfusion reserve assessed by T2-prepared steady-state free precession blood oxygen level-dependent magnetic resonance imaging in comparison to fractional flow reserve. Circ Cardiovasc Imaging. 2012;5(5):580-6.

127. Parnham S, Gleadle JM, Bangalore S, Grover S, Perry R, Woodman RJ, et al. Impaired Myocardial Oxygenation Response to Stress in Patients With Chronic Kidney Disease. J Am Heart Assoc. 2015;4(8):e002249.

128. Messroghli DR, Radjenovic A, Kozerke S, Higgins DM, Sivananthan MU, Ridgway JP. Modified Look-Locker inversion recovery (MOLLI) for high-resolution T1 mapping of the heart. Magn Reson Med. 2004;52(1):141-6.

129. Piechnik SK, Ferreira VM, Dall'Armellina E, Cochlin LE, Greiser A, Neubauer S, et al. Shortened Modified Look-Locker Inversion recovery (ShMOLLI) for clinical myocardial T1-mapping at 1.5 and 3 T within a 9 heartbeat breathhold. J Cardiovasc Magn Reson. 2010;12:69.

130. Lee JJ, Liu S, Nacif MS, Ugander M, Han J, Kawel N, et al. Myocardial T1 and extracellular volume fraction mapping at 3 tesla. J Cardiovasc Magn Reson. 2011;13:75.

131. Weingartner S, Roujol S, Akcakaya M, Basha TA, Nezafat R. Free-breathing multislice native myocardial T1 mapping using the slice-interleaved T1 (STONE) sequence. Magn Reson Med. 2015;74(1):115-24.

132. Chow K, Flewitt JA, Green JD, Pagano JJ, Friedrich MG, Thompson RB. Saturation recovery single-shot acquisition (SASHA) for myocardial T(1) mapping. Magn Reson Med. 2014;71(6):2082-95.

133. Weingartner S, Akcakaya M, Basha T, Kissinger KV, Goddu B, Berg S, et al. Combined saturation/inversion recovery sequences for improved evaluation of scar and diffuse fibrosis in patients with arrhythmia or heart rate variability. Magn Reson Med. 2014;71(3):1024-34.

134. Piechnik SK, Ferreira VM, Lewandowski AJ, Ntusi NA, Banerjee R, Holloway C, et al. Normal variation of magnetic resonance T1 relaxation times in the human population at 1.5 T using ShMOLLI. J Cardiovasc Magn Reson. 2013;15:13.

135. Dall'Armellina E, Piechnik SK, Ferreira VM, Si QL, Robson MD, Francis JM, et al. Cardiovascular magnetic resonance by non contrast T1-mapping allows assessment of severity of injury in acute myocardial infarction. J Cardiovasc Magn Reson. 2012;14:15.

136. Bull S, White SK, Piechnik SK, Flett AS, Ferreira VM, Loudon M, et al. Human non-contrast T1 values and correlation with histology in diffuse fibrosis. Heart. 2013;99(13):932-7.

137. Ferreira VM, Piechnik SK, Dall'Armellina E, Karamitsos TD, Francis JM, Choudhury RP, et al. Non-contrast T1-mapping detects acute myocardial edema with high diagnostic accuracy: a comparison to T2-weighted cardiovascular magnetic resonance. J Cardiovasc Magn Reson. 2012;14:42.

138. Ferreira VM, Piechnik SK, Dall'Armellina E, Karamitsos TD, Francis JM, Ntusi N, et al. T(1) mapping for the diagnosis of acute myocarditis using CMR: comparison to T2-weighted and late gadolinium enhanced imaging. JACC Cardiovasc Imaging. 2013;6(10):1048-58.

139. Karamitsos TD, Piechnik SK, Banypersad SM, Fontana M, Ntusi NB, Ferreira VM, et al. Noncontrast T1 mapping for the diagnosis of cardiac amyloidosis. JACC Cardiovasc Imaging. 2013;6(4):488-97.

140. Ferreira VM, Piechnik SK, Dall'Armellina E, Karamitsos TD, Francis JM, Ntusi N, et al. Native T1-mapping detects the location, extent and patterns of acute myocarditis without the need for gadolinium contrast agents. J Cardiovasc Magn Reson. 2014;16:36.

141. Sado DM, Maestrini V, Piechnik SK, Banypersad SM, White SK, Flett AS, et al. Noncontrast myocardial T1 mapping using cardiovascular magnetic resonance for iron overload. J Magn Reson Imaging. 2015;41(6):1505-11.

142. Judd RM, Levy BI. Effects of barium-induced cardiac contraction on large- and small-vessel intramyocardial blood volume. Circ Res. 1991;68(1):217-25.

143. Crystal GJ, Downey HF, Bashour FA. Small vessel and total coronary blood volume during intracoronary adenosine. Am J Physiol. 1981;241(2):H194-201.

144. Liu A, Wijesurendra RS, Francis JM, Robson MD, Neubauer S, Piechnik SK, et al. Adenosine Stress and Rest T1 Mapping Can Differentiate Between Ischemic, Infarcted, Remote, and Normal Myocardium Without the Need for Gadolinium Contrast Agents. JACC Cardiovasc Imaging. 2016;9(1):27-36.

145. Liu A, Wijesurendra RS, Liu JM, Greiser A, Jerosch-Herold M, Forfar JC, et al. Gadolinium-Free Cardiac MR Stress T1-Mapping to Distinguish Epicardial From Microvascular Coronary Disease. J Am Coll Cardiol. 2018;71(9):957-68.

146. Calle EE, Thun MJ, Petrelli JM, Rodriguez C, Heath CW, Jr. Body-mass index and mortality in a prospective cohort of U.S. adults. N Engl J Med. 1999;341(15):1097-105.

147. Van Gaal LF, Mertens IL, De Block CE. Mechanisms linking obesity with cardiovascular disease. Nature. 2006;444(7121):875-80.

148. Fantuzzi G, Mazzone T. Adipose tissue and atherosclerosis: exploring the connection. Arterioscler Thromb Vasc Biol. 2007;27(5):996-1003.

149. Okura T, Nakata Y, Yamabuki K, Tanaka K. Regional body composition changes exhibit opposing effects on coronary heart disease risk factors. Arterioscler Thromb Vasc Biol. 2004;24(5):923-9.

150. Larsson B, Svardsudd K, Welin L, Wilhelmsen L, Bjorntorp P, Tibblin G. Abdominal adipose tissue distribution, obesity, and risk of cardiovascular disease and death: 13 year follow up of participants in the study of men born in 1913. Br Med J (Clin Res Ed). 1984;288(6428):1401-4.

151. Wildman RP, Muntner P, Reynolds K, McGinn AP, Rajpathak S, Wylie-Rosett J, et al. The obese without cardiometabolic risk factor clustering and the normal weight with cardiometabolic risk factor clustering: prevalence and correlates of 2

phenotypes among the US population (NHANES 1999-2004). Arch Intern Med. 2008;168(15):1617-24.

152. Iacobellis G. Epicardial and pericardial fat: close, but very different. Obesity (Silver Spring). 2009;17(4):625; author reply 6-7.

153. Marchington JM, Mattacks CA, Pond CM. Adipose tissue in the mammalian heart and pericardium: structure, foetal development and biochemical properties. Comp Biochem Physiol B. 1989;94(2):225-32.

154. Fluchter S, Haghi D, Dinter D, Heberlein W, Kuhl HP, Neff W, et al. Volumetric assessment of epicardial adipose tissue with cardiovascular magnetic resonance imaging. Obesity (Silver Spring). 2007;15(4):870-8.

155. Nelson AJ, Worthley MI, Psaltis PJ, Carbone A, Dundon BK, Duncan RF, et al. Validation of cardiovascular magnetic resonance assessment of pericardial adipose tissue volume. J Cardiovasc Magn Reson. 2009;11:15.

156. Turer AT, Scherer PE. Adiponectin: mechanistic insights and clinical implications. Diabetologia. 2012;55(9):2319-26.

157. Fang X, Palanivel R, Cresser J, Schram K, Ganguly R, Thong FS, et al. An APPL1-AMPK signaling axis mediates beneficial metabolic effects of adiponectin in the heart. Am J Physiol Endocrinol Metab. 2010;299(5):E721-9.

158. Wong HK, Cheung TT, Cheung BM. Adrenomedullin and cardiovascular diseases. JRSM Cardiovasc Dis. 2012;1(5).

159. Greenstein AS, Khavandi K, Withers SB, Sonoyama K, Clancy O, Jeziorska M, et al. Local inflammation and hypoxia abolish the protective anticontractile properties of perivascular fat in obese patients. Circulation. 2009;119(12):1661-70.

160. Libby P, Ridker PM, Maseri A. Inflammation and atherosclerosis. Circulation. 2002;105(9):1135-43.

161. Iacobellis G, Ribaudo MC, Zappaterreno A, Iannucci CV, Leonetti F. Relation between epicardial adipose tissue and left ventricular mass. Am J Cardiol. 2004;94(8):1084-7.

162. Malavazos AE, Di Leo G, Secchi F, Lupo EN, Dogliotti G, Coman C, et al. Relation of echocardiographic epicardial fat thickness and myocardial fat. Am J Cardiol. 2010;105(12):1831-5.

163. Berg AH, Scherer PE. Adipose tissue, inflammation, and cardiovascular disease. Circ Res. 2005;96(9):939-49.

164. Iacobellis G, Bianco AC. Epicardial adipose tissue: emerging physiological, pathophysiological and clinical features. Trends Endocrinol Metab. 2011;22(11):450-7.

165. Iacobellis G, Pistilli D, Gucciardo M, Leonetti F, Miraldi F, Brancaccio G, et al. Adiponectin expression in human epicardial adipose tissue in vivo is lower in patients with coronary artery disease. Cytokine. 2005;29(6):251-5.

166. Baker AR, Silva NF, Quinn DW, Harte AL, Pagano D, Bonser RS, et al. Human epicardial adipose tissue expresses a pathogenic profile of adipocytokines in patients with cardiovascular disease. Cardiovasc Diabetol. 2006;5:1.

167. Otsuka F, Sugiyama S, Kojima S, Maruyoshi H, Funahashi T, Matsui K, et al. Plasma adiponectin levels are associated with coronary lesion complexity in men with coronary artery disease. J Am Coll Cardiol. 2006;48(6):1155-62.

168. Iwayama T, Nitobe J, Watanabe T, Ishino M, Tamura H, Nishiyama S, et al. Role of epicardial adipose tissue in coronary artery disease in non-obese patients. J Cardiol. 2014;63(5):344-9.

169. Ishii T, Asuwa N, Masuda S, Ishikawa Y, Kiguchi H, Shimada K. Atherosclerosis suppression in the left anterior descending coronary artery by the

presence of a myocardial bridge: an ultrastructural study. Mod Pathol. 1991;4(4):424-31.

170. Ishii T, Asuwa N, Masuda S, Ishikawa Y. The effects of a myocardial bridge on coronary atherosclerosis and ischaemia. J Pathol. 1998;185(1):4-9.

171. Robicsek F, Thubrikar MJ. The freedom from atherosclerosis of intramyocardial coronary arteries: reduction of mural stress--a key factor. Eur J Cardiothorac Surg. 1994;8(5):228-35.

172. Rosito GA, Massaro JM, Hoffmann U, Ruberg FL, Mahabadi AA, Vasan RS, et al. Pericardial fat, visceral abdominal fat, cardiovascular disease risk factors, and vascular calcification in a community-based sample: the Framingham Heart Study. Circulation. 2008;117(5):605-13.

173. Iwasaki K, Matsumoto T, Aono H, Furukawa H, Samukawa M. Relationship between epicardial fat measured by 64-multidetector computed tomography and coronary artery disease. Clin Cardiol. 2011;34(3):166-71.

174. Ding J, Kritchevsky SB, Harris TB, Burke GL, Detrano RC, Szklo M, et al. The association of pericardial fat with calcified coronary plaque. Obesity (Silver Spring). 2008;16(8):1914-9.

175. Gorter PM, van Lindert AS, de Vos AM, Meijs MF, van der Graaf Y, Doevendans PA, et al. Quantification of epicardial and peri-coronary fat using cardiac computed tomography; reproducibility and relation with obesity and metabolic syndrome in patients suspected of coronary artery disease. Atherosclerosis. 2008;197(2):896-903.

176. Dey D, Wong ND, Tamarappoo B, Nakazato R, Gransar H, Cheng VY, et al. Computer-aided non-contrast CT-based quantification of pericardial and thoracic fat

and their associations with coronary calcium and Metabolic Syndrome. Atherosclerosis. 2010;209(1):136-41.

177. Yerramasu A, Dey D, Venuraju S, Anand DV, Atwal S, Corder R, et al. Increased volume of epicardial fat is an independent risk factor for accelerated progression of sub-clinical coronary atherosclerosis. Atherosclerosis. 2012;220(1):223-30.

178. Ito T, Suzuki Y, Ehara M, Matsuo H, Teramoto T, Terashima M, et al. Impact of epicardial fat volume on coronary artery disease in symptomatic patients with a zero calcium score. Int J Cardiol. 2013;167(6):2852-8.

179. Konishi M, Sugiyama S, Sugamura K, Nozaki T, Ohba K, Matsubara J, et al. Association of pericardial fat accumulation rather than abdominal obesity with coronary atherosclerotic plaque formation in patients with suspected coronary artery disease. Atherosclerosis. 2010;209(2):573-8.

180. Schlett CL, Ferencik M, Kriegel MF, Bamberg F, Ghoshhajra BB, Joshi SB, et al. Association of pericardial fat and coronary high-risk lesions as determined by cardiac CT. Atherosclerosis. 2012;222(1):129-34.

181. Rajani R, Shmilovich H, Nakazato R, Nakanishi R, Otaki Y, Cheng VY, et al. Relationship of epicardial fat volume to coronary plaque, severe coronary stenosis, and high-risk coronary plaque features assessed by coronary CT angiography. J Cardiovasc Comput Tomogr. 2013;7(2):125-32.

182. Kim TH, Yu SH, Choi SH, Yoon JW, Kang SM, Chun EJ, et al. Pericardial fat amount is an independent risk factor of coronary artery stenosis assessed by multidetector-row computed tomography: the Korean Atherosclerosis Study 2. Obesity (Silver Spring). 2011;19(5):1028-34.

183. Wong CX, Abed HS, Molaee P, Nelson AJ, Brooks AG, Sharma G, et al. Pericardial fat is associated with atrial fibrillation severity and ablation outcome. J Am Coll Cardiol. 2011;57(17):1745-51.

184. Wong CX, Ganesan AN, Selvanayagam JB. Epicardial fat and atrial fibrillation: current evidence, potential mechanisms, clinical implications, and future directions. Eur Heart J. 2017;38(17):1294-302.

185. Cheng VY, Dey D, Tamarappoo B, Nakazato R, Gransar H, Miranda-Peats R, et al. Pericardial fat burden on ECG-gated noncontrast CT in asymptomatic patients who subsequently experience adverse cardiovascular events. JACC Cardiovasc Imaging. 2010;3(4):352-60.

186. Harada K, Amano T, Uetani T, Tokuda Y, Kitagawa K, Shimbo Y, et al. Cardiac 64-multislice computed tomography reveals increased epicardial fat volume in patients with acute coronary syndrome. Am J Cardiol. 2011;108(8):1119-23.

187. Mahabadi AA, Berg MH, Lehmann N, Kalsch H, Bauer M, Kara K, et al. Association of epicardial fat with cardiovascular risk factors and incident myocardial infarction in the general population: the Heinz Nixdorf Recall Study. J Am Coll Cardiol. 2013;61(13):1388-95.

188. Saran R, Robinson B, Abbott KC, Agodoa LY, Albertus P, Ayanian J, et al. US Renal Data System 2016 Annual Data Report: Epidemiology of Kidney Disease in the United States. Am J Kidney Dis. 2017;69(3 Suppl 1):A7-A8.

189. Carrero JJ, Avesani CM. Pros and cons of body mass index as a nutritional and risk assessment tool in dialysis patients. Semin Dial. 2015;28(1):48-58.

190. Stenvinkel P, Zoccali C, Ikizler TA. Obesity in CKD--what should nephrologists know? J Am Soc Nephrol. 2013;24(11):1727-36.

191. Altun B, Tasolar H, Eren N, Binnetoglu E, Altun M, Temiz A, et al. Epicardial adipose tissue thickness in hemodialysis patients. Echocardiography. 2014;31(8):941-6.

192. Atakan A, Macunluoglu B, Kaya Y, Ari E, Demir H, Asicioglu E, et al. Epicardial fat thickness is associated with impaired coronary flow reserve in hemodialysis patients. Hemodial Int. 2014;18(1):62-9.

193. Karatas A, Canakci E, Bektas O, Bayrak T, Bayrak A, Altinbas A, et al. Relationship of epicardial fat tissue thickness with oxidant biomarkers in chronic kidney disease. Bratisl Lek Listy. 2018;119(9):566-71.

194. Kerr JD, Holden RM, Morton AR, Nolan RL, Hopman WM, Pruss CM, et al. Associations of epicardial fat with coronary calcification, insulin resistance, inflammation, and fibroblast growth factor-23 in stage 3-5 chronic kidney disease. BMC Nephrol. 2013;14:26.

195. Cordeiro AC, Amparo FC, Oliveira MA, Amodeo C, Smanio P, Pinto IM, et al. Epicardial fat accumulation, cardiometabolic profile and cardiovascular events in patients with stages 3-5 chronic kidney disease. J Intern Med. 2015;278(1):77-87.

196. Fleischmann E, Teal N, Dudley J, May W, Bower JD, Salahudeen AK. Influence of excess weight on mortality and hospital stay in 1346 hemodialysis patients. Kidney Int. 1999;55(4):1560-7.

197. Port FK, Ashby VB, Dhingra RK, Roys EC, Wolfe RA. Dialysis dose and body mass index are strongly associated with survival in hemodialysis patients. J Am Soc Nephrol. 2002;13(4):1061-6.

198. Hall YN, Xu P, Chertow GM. Relationship of body size and mortality among US Asians and Pacific Islanders on dialysis. Ethn Dis. 2011;21(1):40-6.

199. Hoogeveen EK, Halbesma N, Rothman KJ, Stijnen T, van Dijk S, Dekker FW, et al. Obesity and mortality risk among younger dialysis patients. Clin J Am Soc Nephrol. 2012;7(2):280-8.

200. Ladhani M, Craig JC, Irving M, Clayton PA, Wong G. Obesity and the risk of cardiovascular and all-cause mortality in chronic kidney disease: a systematic review and meta-analysis. Nephrol Dial Transplant. 2017;32(3):439-49.

201. Sarnak MJ, Levey AS, Schoolwerth AC, Coresh J, Culleton B, Hamm LL, et al. Kidney disease as a risk factor for development of cardiovascular disease: a statement from the American Heart Association Councils on Kidney in Cardiovascular Disease, High Blood Pressure Research, Clinical Cardiology, and Epidemiology and Prevention. Hypertension. 2003;42(5):1050-65.

202. Moncada S, Palmer RM, Higgs EA. Nitric oxide: physiology, pathophysiology, and pharmacology. Pharmacol Rev. 1991;43(2):109-42.

203. Vallance P, Leone A, Calver A, Collier J, Moncada S. Accumulation of an endogenous inhibitor of nitric oxide synthesis in chronic renal failure. Lancet. 1992;339(8793):572-5.

204. Bode-Boger SM, Scalera F, Kielstein JT, Martens-Lobenhoffer J, Breithardt G, Fobker M, et al. Symmetrical dimethylarginine: a new combined parameter for renal function and extent of coronary artery disease. J Am Soc Nephrol. 2006;17(4):1128-34.

205. Kielstein JT, Bode-Boger SM, Frolich JC, Ritz E, Haller H, Fliser D. Asymmetric dimethylarginine, blood pressure, and renal perfusion in elderly subjects. Circulation. 2003;107(14):1891-5.

206. Hrabak A, Bajor T, Temesi A. Comparison of substrate and inhibitor specificity of arginase and nitric oxide (NO) synthase for arginine analogues and related

compounds in murine and rat macrophages. Biochem Biophys Res Commun. 1994;198(1):206-12.

207. Knowles RG, Palacios M, Palmer RM, Moncada S. Formation of nitric oxide from L-arginine in the central nervous system: a transduction mechanism for stimulation of the soluble guanylate cyclase. Proc Natl Acad Sci U S A. 1989;86(13):5159-62.

208. Valtonen P, Laitinen T, Lyyra-Laitinen T, Raitakari OT, Juonala M, Viikari JS, et al. Serum L-homoarginine concentration is elevated during normal pregnancy and is related to flow-mediated vasodilatation. Circ J. 2008;72(11):1879-84.

209. Yang Z, Ming XF. Endothelial arginase: a new target in atherosclerosis. Curr Hypertens Rep. 2006;8(1):54-9.

210. Henningsson R, Lundquist I. Arginine-induced insulin release is decreased and glucagon increased in parallel with islet NO production. Am J Physiol. 1998;275(3):E500-6.

211. Radomski MW, Palmer RM, Moncada S. An L-arginine/nitric oxide pathway present in human platelets regulates aggregation. Proc Natl Acad Sci U S A. 1990;87(13):5193-7.

212. van der Zwan LP, Davids M, Scheffer PG, Dekker JM, Stehouwer CD, Teerlink T. L-Homoarginine and L-arginine are antagonistically related to blood pressure in an elderly population: the Hoorn study. J Hypertens. 2013;31(6):1114-23.

213. Marz W, Meinitzer A, Drechsler C, Pilz S, Krane V, Kleber ME, et al. Homoarginine, cardiovascular risk, and mortality. Circulation. 2010;122(10):967-75.

214. Pilz S, Meinitzer A, Tomaschitz A, Drechsler C, Ritz E, Krane V, et al. Low homoarginine concentration is a novel risk factor for heart disease. Heart. 2011;97(15):1222-7.

215. Pilz S, Tomaschitz A, Meinitzer A, Drechsler C, Ritz E, Krane V, et al. Low serum homoarginine is a novel risk factor for fatal strokes in patients undergoing coronary angiography. Stroke. 2011;42(4):1132-4.

216. Ravani P, Maas R, Malberti F, Pecchini P, Mieth M, Quinn R, et al. Homoarginine and mortality in pre-dialysis chronic kidney disease (CKD) patients. PLoS One. 2013;8(9):e72694.

217. Drechsler C, Meinitzer A, Pilz S, Krane V, Tomaschitz A, Ritz E, et al. Homoarginine, heart failure, and sudden cardiac death in haemodialysis patients. Eur J Heart Fail. 2011;13(8):852-9.

218. Kielstein JT, Zoccali C. Asymmetric dimethylarginine: a cardiovascular risk factor and a uremic toxin coming of age? Am J Kidney Dis. 2005;46(2):186-202.

219. Mendes Ribeiro AC, Roberts NB, Lane C, Yaqoob M, Ellory JC. Accumulation of the endogenous L-arginine analogue NG-monomethyl-L-arginine in human end-stage renal failure patients on regular haemodialysis. Exp Physiol. 1996;81(3):475-81.

220. Torremans A, Marescau B, Vanholder R, De Smet R, Billiouw JM, De Deyn PP. The low nanomolar levels of N G-monomethylarginine in serum and urine of patients with chronic renal insufficiency are not significantly different from control levels. Amino Acids. 2003;24(4):375-81.

221. Martens-Lobenhoffer J, Bode-Boger SM. Amino acid N-acetylation: metabolic elimination of symmetric dimethylarginine as symmetric N(alpha)-acetyldimethylarginine, determined in human plasma and urine by LC-MS/MS. J Chromatogr B Analyt Technol Biomed Life Sci. 2015;975:59-64.

222. Martens-Lobenhoffer J, Rodionov RN, Bode-Boger SM. Determination of asymmetric Nalpha-acetyldimethylarginine in humans: a phase II metabolite of asymmetric dimethylarginine. Anal Biochem. 2014;452:25-30.

223. Fliser D, Kronenberg F, Kielstein JT, Morath C, Bode-Boger SM, Haller H, et al. Asymmetric dimethylarginine and progression of chronic kidney disease: the mild to moderate kidney disease study. J Am Soc Nephrol. 2005;16(8):2456-61.

224. Ravani P, Tripepi G, Malberti F, Testa S, Mallamaci F, Zoccali C. Asymmetrical dimethylarginine predicts progression to dialysis and death in patients with chronic kidney disease: a competing risks modeling approach. J Am Soc Nephrol. 2005;16(8):2449-55.

225. Hanai K, Babazono T, Nyumura I, Toya K, Tanaka N, Tanaka M, et al. Asymmetric dimethylarginine is closely associated with the development and progression of nephropathy in patients with type 2 diabetes. Nephrol Dial Transplant. 2009;24(6):1884-8.

226. Kielstein JT, Boger RH, Bode-Boger SM, Frolich JC, Haller H, Ritz E, et al. Marked increase of asymmetric dimethylarginine in patients with incipient primary chronic renal disease. J Am Soc Nephrol. 2002;13(1):170-6.

227. Zoccali C, Bode-Boger S, Mallamaci F, Benedetto F, Tripepi G, Malatino L, et al. Plasma concentration of asymmetrical dimethylarginine and mortality in patients with end-stage renal disease: a prospective study. Lancet. 2001;358(9299):2113-7.

228. Shafi T, Hostetter TH, Meyer TW, Hwang S, Hai X, Melamed ML, et al. Serum Asymmetric and Symmetric Dimethylarginine and Morbidity and Mortality in Hemodialysis Patients. Am J Kidney Dis. 2017;70(1):48-58.

229. Schlesinger S, Sonntag SR, Lieb W, Maas R. Asymmetric and Symmetric Dimethylarginine as Risk Markers for Total Mortality and Cardiovascular Outcomes:

A Systematic Review and Meta-Analysis of Prospective Studies. PLoS One. 2016;11(11):e0165811.

230. Willeit P, Freitag DF, Laukkanen JA, Chowdhury S, Gobin R, Mayr M, et al. Asymmetric dimethylarginine and cardiovascular risk: systematic review and meta-analysis of 22 prospective studies. J Am Heart Assoc. 2015;4(6):e001833.

231. Busch M, Fleck C, Wolf G, Stein G. Asymmetrical (ADMA) and symmetrical dimethylarginine (SDMA) as potential risk factors for cardiovascular and renal outcome in chronic kidney disease - possible candidates for paradoxical epidemiology? Amino Acids. 2006;30(3):225-32.

232. Kalousova M, Kielstein JT, Hodkova M, Zima T, Dusilova-Sulkova S, Martens-Lobenhoffer J, et al. No benefit of hemodiafiltration over hemodialysis in lowering elevated levels of asymmetric dimethylarginine in ESRD patients. Blood Purif. 2006;24(5-6):439-44.

233. Kielstein JT, Boger RH, Bode-Boger SM, Martens-Lobenhoffer J, Lonnemann G, Frolich JC, et al. Low dialysance of asymmetric dimethylarginine (ADMA)--in vivo and in vitro evidence of significant protein binding. Clin Nephrol. 2004;62(4):295-300.

234. Kato S, Chmielewski M, Honda H, Pecoits-Filho R, Matsuo S, Yuzawa Y, et al. Aspects of immune dysfunction in end-stage renal disease. Clin J Am Soc Nephrol. 2008;3(5):1526-33.

235. Vanholder R, Glorieux G, Lameire N. New insights in uremic toxicity. Contrib Nephrol. 2005;149:315-24.

236. Vanholder R, De Smet R, Glorieux G, Argiles A, Baurmeister U, Brunet P, et al. Review on uremic toxins: classification, concentration, and interindividual variability. Kidney Int. 2003;63(5):1934-43.

237. Devaki R, Basavana Gowdappa H, Nataraj S, Prashanth V, Akila P, Anjali Devi BD, et al. A study of C- Reactive protein and its relationship with CHD and lipid metabolism. International Journal of Pharmaceutical Sciences Review and Research. 2011;6:125-7.

238. Paffen E, DeMaat MP. C-reactive protein in atherosclerosis: A causal factor? Cardiovasc Res. 2006;71(1):30-9.

239. Mehta JL, Sukhija R, Romeo F, Sepulveda JL. Value of CRP in coronary risk determination. Indian Heart J. 2007;59(2):173-7.

240. Parikh NI, Hwang SJ, Larson MG, Levy D, Fox CS. Chronic kidney disease as a predictor of cardiovascular disease (from the Framingham Heart Study). Am J Cardiol. 2008;102(1):47-53.

241. Wang TJ, Larson MG, Levy D, Benjamin EJ, Kupka MJ, Manning WJ, et al. C-reactive protein is associated with subclinical epicardial coronary calcification in men and women: the Framingham Heart Study. Circulation. 2002;106(10):1189-91.

242. Koenig W, Khuseyinova N, Baumert J, Meisinger C. Prospective study of high-sensitivity C-reactive protein as a determinant of mortality: results from the MONICA/KORA Augsburg Cohort Study, 1984-1998. Clin Chem. 2008;54(2):335-42.

243. Pearson TA, Mensah GA, Alexander RW, Anderson JL, Cannon RO, 3rd, Criqui M, et al. Markers of inflammation and cardiovascular disease: application to clinical and public health practice: A statement for healthcare professionals from the Centers for Disease Control and Prevention and the American Heart Association. Circulation. 2003;107(3):499-511.

244. Strandberg TE, Tilvis RS. C-reactive protein, cardiovascular risk factors, and mortality in a prospective study in the elderly. Arterioscler Thromb Vasc Biol. 2000;20(4):1057-60.

245. Bansal S, Ridker PM. Comparison of characteristics of future myocardial infarctions in women with baseline high versus baseline low levels of high-sensitivity C-reactive protein. Am J Cardiol. 2007;99(11):1500-3.

246. Cao JJ, Arnold AM, Manolio TA, Polak JF, Psaty BM, Hirsch CH, et al. Association of carotid artery intima-media thickness, plaques, and C-reactive protein with future cardiovascular disease and all-cause mortality: the Cardiovascular Health Study. Circulation. 2007;116(1):32-8.

247. Wanner C, Zimmermann J, Schwedler S, Metzger T. Inflammation and cardiovascular risk in dialysis patients. Kidney Int Suppl. 2002(80):99-102.

248. Bayes B, Pastor MC, Bonal J, Junca J, Hernandez JM, Riutort N, et al. Homocysteine, C-reactive protein, lipid peroxidation and mortality in haemodialysis patients. Nephrol Dial Transplant. 2003;18(1):106-12.

249. Chung SH, Heimburger O, Stenvinkel P, Qureshi AR, Lindholm B. Association between residual renal function, inflammation and patient survival in new peritoneal dialysis patients. Nephrol Dial Transplant. 2003;18(3):590-7.

250. Mallamaci F, Tripepi G, Cutrupi S, Malatino LS, Zoccali C. Prognostic value of combined use of biomarkers of inflammation, endothelial dysfunction, and myocardiopathy in patients with ESRD. Kidney Int. 2005;67(6):2330-7.

251. deFilippi C, Wasserman S, Rosanio S, Tiblier E, Sperger H, Tocchi M, et al. Cardiac troponin T and C-reactive protein for predicting prognosis, coronary atherosclerosis, and cardiomyopathy in patients undergoing long-term hemodialysis. JAMA. 2003;290(3):353-9.

252. Wang AY, Woo J, Lam CW, Wang M, Sea MM, Lui SF, et al. Is a single time point C-reactive protein predictive of outcome in peritoneal dialysis patients? J Am Soc Nephrol. 2003;14(7):1871-9.

253. Herzig KA, Purdie DM, Chang W, Brown AM, Hawley CM, Campbell SB, et al. Is C-reactive protein a useful predictor of outcome in peritoneal dialysis patients? J Am Soc Nephrol. 2001;12(4):814-21.

254. Tong J, Liu M, Li H, Luo Z, Zhong X, Huang J, et al. Mortality and Associated Risk Factors in Dialysis Patients with Cardiovascular Disease. Kidney Blood Press Res. 2016;41(4):479-87.

255. Menon V, Greene T, Wang X, Pereira AA, Marcovina SM, Beck GJ, et al. C-reactive protein and albumin as predictors of all-cause and cardiovascular mortality in chronic kidney disease. Kidney Int. 2005;68(2):766-72.

256. Zimmermann J, Herrlinger S, Pruy A, Metzger T, Wanner C. Inflammation enhances cardiovascular risk and mortality in hemodialysis patients. Kidney Int. 1999;55(2):648-58.

257. Yeun JY, Levine RA, Mantadilok V, Kaysen GA. C-Reactive protein predicts all-cause and cardiovascular mortality in hemodialysis patients. Am J Kidney Dis. 2000;35(3):469-76.

258. Ikizler TA, Wingard RL, Harvell J, Shyr Y, Hakim RM. Association of morbidity with markers of nutrition and inflammation in chronic hemodialysis patients: a prospective study. Kidney Int. 1999;55(5):1945-51.

259. Noh H, Lee SW, Kang SW, Shin SK, Choi KH, Lee HY, et al. Serum C-reactive protein: a predictor of mortality in continuous ambulatory peritoneal dialysis patients. Perit Dial Int. 1998;18(4):387-94.

260. Iseki K, Tozawa M, Yoshi S, Fukiyama K. Serum C-reactive protein (CRP) and risk of death in chronic dialysis patients. Nephrol Dial Transplant. 1999;14(8):1956-60.

261. Nicholls SJ, Hazen SL. Myeloperoxidase and cardiovascular disease. Arterioscler Thromb Vasc Biol. 2005;25(6):1102-11.

262. Carr AC, McCall MR, Frei B. Oxidation of LDL by myeloperoxidase and reactive nitrogen species: reaction pathways and antioxidant protection. Arterioscler Thromb Vasc Biol. 2000;20(7):1716-23.

263. Cayley WE, Jr. Prognostic value of myeloperoxidase in patients with chest pain. N Engl J Med. 2004;350(5):516-8; author reply -8.

264. Scharnagl H, Kleber ME, Genser B, Kickmaier S, Renner W, Weihrauch G, et al. Association of myeloperoxidase with total and cardiovascular mortality in individuals undergoing coronary angiography--the LURIC study. Int J Cardiol. 2014;174(1):96-105.

265. Pirillo A, Norata GD, Catapano AL. LOX-1, OxLDL, and atherosclerosis. Mediators Inflamm. 2013;2013:152786.

266. Meuwese MC, Stroes ES, Hazen SL, van Miert JN, Kuivenhoven JA, Schaub RG, et al. Serum myeloperoxidase levels are associated with the future risk of coronary artery disease in apparently healthy individuals: the EPIC-Norfolk Prospective Population Study. J Am Coll Cardiol. 2007;50(2):159-65.

267. Zhang R, Brennan ML, Fu X, Aviles RJ, Pearce GL, Penn MS, et al. Association between myeloperoxidase levels and risk of coronary artery disease. JAMA. 2001;286(17):2136-42.

268. Baldus S, Heeschen C, Meinertz T, Zeiher AM, Eiserich JP, Munzel T, et al. Myeloperoxidase serum levels predict risk in patients with acute coronary syndromes. Circulation. 2003;108(12):1440-5.

269. Brennan ML, Penn MS, Van Lente F, Nambi V, Shishehbor MH, Aviles RJ, et al. Prognostic value of myeloperoxidase in patients with chest pain. N Engl J Med. 2003;349(17):1595-604.

270. Mocatta TJ, Pilbrow AP, Cameron VA, Senthilmohan R, Frampton CM, Richards AM, et al. Plasma concentrations of myeloperoxidase predict mortality after myocardial infarction. J Am Coll Cardiol. 2007;49(20):1993-2000.

271. Rudolph V, Keller T, Schulz A, Ojeda F, Rudolph TK, Tzikas S, et al. Diagnostic and prognostic performance of myeloperoxidase plasma levels compared with sensitive troponins in patients admitted with acute onset chest pain. Circ Cardiovasc Genet. 2012;5(5):561-8.

272. Ndrepepa G, Braun S, Mehilli J, von Beckerath N, Schomig A, Kastrati A. Myeloperoxidase level in patients with stable coronary artery disease and acute coronary syndromes. Eur J Clin Invest. 2008;38(2):90-6.

273. Naruko T, Furukawa A, Yunoki K, Komatsu R, Nakagawa M, Matsumura Y, et al. Increased expression and plasma levels of myeloperoxidase are closely related to the presence of angiographically-detected complex lesion morphology in unstable angina. Heart. 2010;96(21):1716-22.

274. Borissoff JI, Joosen IA, Versteylen MO, Brill A, Fuchs TA, Savchenko AS, et al. Elevated levels of circulating DNA and chromatin are independently associated with severe coronary atherosclerosis and a prothrombotic state. Arterioscler Thromb Vasc Biol. 2013;33(8):2032-40.

275. Sugiyama S, Kugiyama K, Aikawa M, Nakamura S, Ogawa H, Libby P. Hypochlorous acid, a macrophage product, induces endothelial apoptosis and tissue factor expression: involvement of myeloperoxidase-mediated oxidant in plaque erosion and thrombogenesis. Arterioscler Thromb Vasc Biol. 2004;24(7):1309-14.

276. Kalantar-Zadeh K, Brennan ML, Hazen SL. Serum myeloperoxidase and mortality in maintenance hemodialysis patients. Am J Kidney Dis. 2006;48(1):59-68.

277. Kitabayashi C, Naruko T, Sugioka K, Yunoki K, Nakagawa M, Inaba M, et al. Positive association between plasma levels of oxidized low-density lipoprotein and myeloperoxidase after hemodialysis in patients with diabetic end-stage renal disease. Hemodial Int. 2013;17(4):557-67.

278. Shiu SW, Xiao SM, Wong Y, Chow WS, Lam KS, Tan KC. Carbamylation of LDL and its relationship with myeloperoxidase in type 2 diabetes mellitus. Clin Sci (Lond). 2014;126(2):175-81.

279. Wada S, Sugioka K, Naruko T, Kato Y, Shibata T, Inoue T, et al. Myeloperoxidase and progression of aortic valve stenosis in patients undergoing hemodialysis. J Heart Valve Dis. 2013;22(5):640-7.

280. Grover S, Leong DP, Selvanayagam JB. Evaluation of left ventricular function using cardiac magnetic resonance imaging. J Nucl Cardiol. 2011;18(2):351-65.

281. Sanderson JE. Heart failure with a normal ejection fraction. Heart. 2007;93(2):155-8.

282. Tseng WY, Dou J, Reese TG, Wedeen VJ. Imaging myocardial fiber disarray and intramural strain hypokinesis in hypertrophic cardiomyopathy with MRI. J Magn Reson Imaging. 2006;23(1):1-8.

283. Jurcut R, Wildiers H, Ganame J, D'Hooge J, De Backer J, Denys H, et al. Strain rate imaging detects early cardiac effects of pegylated liposomal Doxorubicin as adjuvant therapy in elderly patients with breast cancer. J Am Soc Echocardiogr. 2008;21(12):1283-9.

284. Maceira AM, Tuset-Sanchis L, Lopez-Garrido M, San Andres M, Lopez-Lereu MP, Monmeneu JV, et al. Feasibility and reproducibility of feature-tracking-based

strain and strain rate measures of the left ventricle in different diseases and genders. J Magn Reson Imaging. 2018;47(5):1415-25.

285. Hor KN, Gottliebson WM, Carson C, Wash E, Cnota J, Fleck R, et al. Comparison of magnetic resonance feature tracking for strain calculation with harmonic phase imaging analysis. JACC Cardiovasc Imaging. 2010;3(2):144-51.

286. Moody WE, Taylor RJ, Edwards NC, Chue CD, Umar F, Taylor TJ, et al. Comparison of magnetic resonance feature tracking for systolic and diastolic strain and strain rate calculation with spatial modulation of magnetization imaging analysis. J Magn Reson Imaging. 2015;41(4):1000-12.

287. Nucifora G, Muser D, Tioni C, Shah R, Selvanayagam JB. Prognostic value of myocardial deformation imaging by cardiac magnetic resonance feature-tracking in patients with a first ST-segment elevation myocardial infarction. Int J Cardiol. 2018.

288. Muser D, Tioni C, Shah R, Selvanayagam JB, Nucifora G. Prevalence, Correlates, and Prognostic Relevance of Myocardial Mechanical Dispersion as Assessed by Feature-Tracking Cardiac Magnetic Resonance After a First ST-Segment Elevation Myocardial Infarction. Am J Cardiol. 2017;120(4):527-33.

289. Eitel I, Stiermaier T, Lange T, Rommel KP, Koschalka A, Kowallick JT, et al. Cardiac Magnetic Resonance Myocardial Feature Tracking for Optimized Prediction of Cardiovascular Events Following Myocardial Infarction. JACC Cardiovasc Imaging. 2018.

290. Romano S, Judd RM, Kim RJ, Kim HW, Klem I, Heitner JF, et al. Feature-Tracking Global Longitudinal Strain Predicts Death in a Multicenter Population of Patients with Ischemic and Nonischemic Dilated Cardiomyopathy Incremental to Ejection Fraction and Late Gadolinium Enhancement. JACC Cardiovasc Imaging. 2018.

291. Illman JE, Arunachalam SP, Arani A, Chang IC, Glockner JF, Dispenzieri A, et al. MRI feature tracking strain is prognostic for all-cause mortality in AL amyloidosis. Amyloid. 2018:1-8.

292. Romano S, Judd RM, Kim RJ, Kim HW, Klem I, Heitner J, et al. Association of Feature-Tracking Cardiac Magnetic Resonance Imaging Left Ventricular Global Longitudinal Strain With All-Cause Mortality in Patients With Reduced Left Ventricular Ejection Fraction. Circulation. 2017;135(23):2313-5.

293. Akinboboye OO, Idris O, Chou RL, Sciacca RR, Cannon PJ, Bergmann SR. Absolute quantitation of coronary steal induced by intravenous dipyridamole. J Am Coll Cardiol. 2001;37(1):109-16.

294. Levelt E, Rodgers CT, Clarke WT, Mahmod M, Ariga R, Francis JM, et al. Cardiac energetics, oxygenation, and perfusion during increased workload in patients with type 2 diabetes mellitus. Eur Heart J. 2016;37(46):3461-9.

295. Goicoechea M, de Vinuesa SG, Gomez-Campdera F, Luno J. Predictive cardiovascular risk factors in patients with chronic kidney disease (CKD). Kidney Int Suppl. 2005(93):S35-8.

296. Foley RN, Parfrey PS, Harnett JD, Kent GM, Martin CJ, Murray DC, et al. Clinical and echocardiographic disease in patients starting end-stage renal disease therapy. Kidney Int. 1995;47(1):186-92.

297. Edwards NC, Hirth A, Ferro CJ, Townend JN, Steeds RP. Subclinical abnormalities of left ventricular myocardial deformation in early-stage chronic kidney disease: the precursor of uremic cardiomyopathy? J Am Soc Echocardiogr. 2008;21(12):1293-8.

298. Liu YW, Su CT, Huang YY, Yang CS, Huang JW, Yang MT, et al. Left ventricular systolic strain in chronic kidney disease and hemodialysis patients. Am J Nephrol. 2011;33(1):84-90.

299. Egred M, Al-Mohammad A, Waiter GD, Redpath TW, Semple SK, Norton M, et al. Detection of scarred and viable myocardium using a new magnetic resonance imaging technique: blood oxygen level dependent (BOLD) MRI. Heart. 2003;89(7):738-44.

300. Dass S, Suttie JJ, Piechnik SK, Ferreira VM, Holloway CJ, Banerjee R, et al. Myocardial tissue characterization using magnetic resonance noncontrast t1 mapping in hypertrophic and dilated cardiomyopathy. Circ Cardiovasc Imaging. 2012;5(6):726-33.

301. Puntmann VO, Arroyo Ucar E, Hinojar Baydes R, Ngah NB, Kuo YS, Dabir D, et al. Aortic stiffness and interstitial myocardial fibrosis by native T1 are independently associated with left ventricular remodeling in patients with dilated cardiomyopathy. Hypertension. 2014;64(4):762-8.

302. Le DE, Jayaweera AR, Wei K, Coggins MP, Lindner JR, Kaul S. Changes in myocardial blood volume over a wide range of coronary driving pressures: role of capillaries beyond the autoregulatory range. Heart. 2004;90(10):1199-205.

303. Lindner JR, Skyba DM, Goodman NC, Jayaweera AR, Kaul S. Changes in myocardial blood volume with graded coronary stenosis. Am J Physiol. 1997;272(1 Pt 2):H567-75.

304. Shah R, Parnham S, Liang Z, Perry R, Bradbrook C, Smith E, et al. Prognostic Utility of Oxygen-Sensitive Cardiac Magnetic Resonance Imaging in Diabetic and Nondiabetic Chronic Kidney Disease Patients With No Known Coronary Artery Disease. JACC Cardiovasc Imaging. 2019;12(6):1107-9.

305. Hayes AJ, Lung TW, Bauman A, Howard K. Modelling obesity trends in Australia: unravelling the past and predicting the future. Int J Obes (Lond). 2017;41(1):178-85.

306. Wang Y, Chen X, Song Y, Caballero B, Cheskin LJ. Association between obesity and kidney disease: a systematic review and meta-analysis. Kidney Int. 2008;73(1):19-33.

307. Kalantar-Zadeh K, Block G, Humphreys MH, Kopple JD. Reverse epidemiology of cardiovascular risk factors in maintenance dialysis patients. Kidney Int. 2003;63(3):793-808.

308. Park J, Ahmadi SF, Streja E, Molnar MZ, Flegal KM, Gillen D, et al. Obesity paradox in end-stage kidney disease patients. Prog Cardiovasc Dis. 2014;56(4):415-25.

309. Paradoxical association between body mass index and mortality in men with CKD not yet on dialysis. 2007;49(5):581-91.

310. Kielstein JT, Zoccali C. Asymmetric dimethylarginine: a novel marker of risk and a potential target for therapy in chronic kidney disease. Curr Opin Nephrol Hypertens. 2008;17(6):609-15.

311. Schwedhelm E, Boger RH. The role of asymmetric and symmetric dimethylarginines in renal disease. Nat Rev Nephrol. 2011;7(5):275-85.

312. Baylis C. Nitric oxide deficiency in chronic kidney disease. Am J Physiol Renal Physiol. 2008;294(1):F1-9.

313. Furchgott RF, Zawadzki JV. The obligatory role of endothelial cells in the relaxation of arterial smooth muscle by acetylcholine. Nature. 1980;288(5789):373-6.

314. Forstermann U, Closs EI, Pollock JS, Nakane M, Schwarz P, Gath I, et al. Nitric oxide synthase isozymes. Characterization, purification, molecular cloning, and functions. Hypertension. 1994;23(6 Pt 2):1121-31.

315. Cooke JP, Rossitch E, Jr., Andon NA, Loscalzo J, Dzau VJ. Flow activates an endothelial potassium channel to release an endogenous nitrovasodilator. J Clin Invest. 1991;88(5):1663-71.

316. Hogg N, Kalyanaraman B, Joseph J, Struck A, Parthasarathy S. Inhibition of low-density lipoprotein oxidation by nitric oxide. Potential role in atherogenesis. FEBS Lett. 1993;334(2):170-4.

317. Wolf A, Zalpour C, Theilmeier G, Wang BY, Ma A, Anderson B, et al. Dietary L-arginine supplementation normalizes platelet aggregation in hypercholesterolemic humans. J Am Coll Cardiol. 1997;29(3):479-85.

318. Kubes P, Suzuki M, Granger DN. Nitric oxide: an endogenous modulator of leukocyte adhesion. Proc Natl Acad Sci U S A. 1991;88(11):4651-5.

319. Boger RH, Bode-Boger SM, Kienke S, Stan AC, Nafe R, Frolich JC. Dietary L-arginine decreases myointimal cell proliferation and vascular monocyte accumulation in cholesterol-fed rabbits. Atherosclerosis. 1998;136(1):67-77.

320. Stuhlinger MC, Oka RK, Graf EE, Schmolzer I, Upson BM, Kapoor O, et al. Endothelial dysfunction induced by hyperhomocyst(e)inemia: role of asymmetric dimethylarginine. Circulation. 2003;108(8):933-8.

321. Calver A, Collier J, Leone A, Moncada S, Vallance P. Effect of local intra-arterial asymmetric dimethylarginine (ADMA) on the forearm arteriolar bed of healthy volunteers. J Hum Hypertens. 1993;7(2):193-4.

322. Boger RH, Bode-Boger SM, Szuba A, Tsao PS, Chan JR, Tangphao O, et al. Asymmetric dimethylarginine (ADMA): a novel risk factor for endothelial dysfunction: its role in hypercholesterolemia. Circulation. 1998;98(18):1842-7.

323. Miyazaki H, Matsuoka H, Cooke JP, Usui M, Ueda S, Okuda S, et al. Endogenous nitric oxide synthase inhibitor: a novel marker of atherosclerosis. Circulation. 1999;99(9):1141-6.

324. Surdacki A, Nowicki M, Sandmann J, Tsikas D, Boeger RH, Bode-Boeger SM, et al. Reduced urinary excretion of nitric oxide metabolites and increased plasma levels of asymmetric dimethylarginine in men with essential hypertension. J Cardiovasc Pharmacol. 1999;33(4):652-8.

325. Abbasi F, Asagmi T, Cooke JP, Lamendola C, McLaughlin T, Reaven GM, et al. Plasma concentrations of asymmetric dimethylarginine are increased in patients with type 2 diabetes mellitus. Am J Cardiol. 2001;88(10):1201-3.

326. Lundman P, Eriksson MJ, Stuhlinger M, Cooke JP, Hamsten A, Tornvall P. Mild-to-moderate hypertriglyceridemia in young men is associated with endothelial dysfunction and increased plasma concentrations of asymmetric dimethylarginine. J Am Coll Cardiol. 2001;38(1):111-6.

327. Stuhlinger MC, Abbasi F, Chu JW, Lamendola C, McLaughlin TL, Cooke JP, et al. Relationship between insulin resistance and an endogenous nitric oxide synthase inhibitor. JAMA. 2002;287(11):1420-6.

328. Boger RH, Zoccali C. ADMA: a novel risk factor that explains excess cardiovascular event rate in patients with end-stage renal disease. Atheroscler Suppl. 2003;4(4):23-8.

329. Lu TM, Ding YA, Lin SJ, Lee WS, Tai HC. Plasma levels of asymmetrical dimethylarginine and adverse cardiovascular events after percutaneous coronary intervention. Eur Heart J. 2003;24(21):1912-9.

330. Valkonen VP, Paiva H, Salonen JT, Lakka TA, Lehtimaki T, Laakso J, et al. Risk of acute coronary events and serum concentration of asymmetrical dimethylarginine. Lancet. 2001;358(9299):2127-8.

331. Meinitzer A, Seelhorst U, Wellnitz B, Halwachs-Baumann G, Boehm BO, Winkelmann BR, et al. Asymmetrical dimethylarginine independently predicts total and cardiovascular mortality in individuals with angiographic coronary artery disease (the Ludwigshafen Risk and Cardiovascular Health study). Clin Chem. 2007;53(2):273-83.

332. Pernow J, Jung C. Arginase as a potential target in the treatment of cardiovascular disease: reversal of arginine steal? Cardiovasc Res. 2013;98(3):334-43.

333. Durante W, Johnson FK, Johnson RA. Arginase: a critical regulator of nitric oxide synthesis and vascular function. Clin Exp Pharmacol Physiol. 2007;34(9):906-11.

334. Caldwell RB, Toque HA, Narayanan SP, Caldwell RW. Arginase: an old enzyme with new tricks. Trends Pharmacol Sci. 2015;36(6):395-405.

335. Graham-Brown MP, March DS, Churchward DR, Stensel DJ, Singh A, Arnold R, et al. Novel cardiac nuclear magnetic resonance method for noninvasive assessment of myocardial fibrosis in hemodialysis patients. Kidney Int. 2016;90(4):835-44.

336. Rutherford E, Talle MA, Mangion K, Bell E, Rauhalammi SM, Roditi G, et al. Defining myocardial tissue abnormalities in end-stage renal failure with cardiac

magnetic resonance imaging using native T1 mapping. Kidney Int. 2016;90(4):845-52.

337. Sosnov J, Lessard D, Goldberg RJ, Yarzebski J, Gore JM. Differential symptoms of acute myocardial infarction in patients with kidney disease: a community-wide perspective. Am J Kidney Dis. 2006;47(3):378-84.

338. Parnham SF, Gleadle JM, De Pasquale CG, Selvanayagam JB. Myocardial Ischemia Assessment in Chronic Kidney Disease: Challenges and Pitfalls. Front Cardiovasc Med. 2014;1:13.